

Weak chaos in the disordered nonlinear Schrödinger chain: destruction of Anderson localization by Arnold diffusion

D. M. Basko

*UJF-Grenoble 1/CNRS, Laboratoire de Physique et Modélisation des Milieux Condensés UMR 5493,
BP166, 38042 Grenoble, France*

Abstract

The subject of this study is the long-time equilibration dynamics of a strongly disordered one-dimensional chain of coupled weakly anharmonic classical oscillators. It is shown that chaos in this system has a very particular spatial structure: it can be viewed as a dilute gas of chaotic spots. Each chaotic spot corresponds to a stochastic pump which drives the Arnold diffusion of the oscillators surrounding it, thus leading to their relaxation and thermalization. The most important mechanism of relaxation at long distances is provided by random migration of the chaotic spots along the chain, which bears analogy with variable-range hopping of electrons in strongly disordered solids. The corresponding macroscopic transport equations are obtained.

Keywords: Anderson localization, Arnold diffusion, weak chaos, nonlinear Schrödinger equation

1. Introduction

Anderson localization [1] is a general phenomenon occurring in many linear wave-like systems subject to a disordered background (see Ref. [2] for a recent review). It is especially pronounced in one-dimensional systems, where even an arbitrarily weak disorder localizes all normal modes of the system [3, 4]. Anderson localization in linear systems (single-particle problems in quantum mechanics) has been thoroughly studied over the last 50 years; its physical picture is quite clear by now (although some open questions still remain), and even rigorous mathematical results have been established. The situation is much less clear in the presence of nonlinearities/interactions.

One of the simplest systems where the effect of a classical nonlinearity on the Anderson localization can be studied, is the disordered nonlinear Schrödinger equation (DNLSE) in one dimension, discrete or continuous. It has attracted a lot of interest in

Email address: denis.basko@grenoble.cnrs.fr (D. M. Basko)

Preprint submitted to Elsevier

October 22, 2018

the last few years, including both stationary and non-stationary problems, as well as the problem of the dynamic stability of stationary solutions [5, 6, 7, 8, 9, 10, 11, 12, 13, 14, 15, 16, 17, 18, 19, 20, 21, 22, 23, 24, 25, 26, 27, 28, 29, 30, 31, 32, 33, 34, 35, 36, 37]. This interest was especially motivated by the experimental observation of the Anderson localization of light in disordered photonic lattices [38, 39, 40], where DNLSE describes light propagation in the paraxial approximation, and of cold atoms in disordered optical lattices [41, 42, 43], for which DNLSE provides the mean-field description. Other systems have also been studied, such as a chain of anharmonic oscillators [5, 15, 44, 45, 20, 21, 32, 33, 35, 46], a chain of classical spins [5, 47], a nonlinear Stark ladder [48, 49].

In contrast to linear problems which can always be reduced to finding the normal modes and the corresponding eigenvalues, the problem of localization in a nonlinear system can be stated in different inequivalent ways. For example, one can study solutions of the stationary nonlinear Schrödinger equation with disorder [12, 14, 28]; however, in a nonlinear system they are not directly related to the dynamics. Another possible setting is the system subject to an external perturbation or probe; studies of the transmission of a finite-length sample where an external flow is imposed [6, 8, 9, 10, 11, 19, 25, 27], or dipolar oscillations in an external trap potential [18], fall into this category. Most attention has been paid to the problem of spreading of an initially localized wave packet of a finite norm [7, 8, 9, 13, 15, 16, 17, 50, 20, 21, 22, 23, 48, 49, 24, 29, 30, 31, 32, 33, 34] (in linear systems it remains exponentially suppressed at long distances for all times). This setting corresponds directly to experiments [38, 39, 40, 41, 42]. A closely related but not equivalent problem is that of thermalization of an initially out-of-equilibrium system (in a linear localized system thermalization does not occur). The difference between these two settings is that in the latter the total energy stored in the system is proportional to its (infinite) size, while in the former the infinite system initially receives a finite amount of energy. The problem of thermalization has also received attention [44, 45, 47, 26], and it is the main subject of the present work (although the problem of wave packet spreading will also be briefly discussed). Still, despite a large body of work, detailed understanding of the equilibration dynamics in one-dimensional disordered nonlinear systems is still lacking.

On the one hand, the direct numerical integration of the differential equation shows that an initially localized wave packet of a finite norm does spread indefinitely, its size growing with time as a sub-diffusive power law [7, 9, 15, 16, 20, 21, 32, 33, 35]. Existence of different regimes of spreading, depending on whether the system is in the regime of strong or weak chaos, has been discussed [33, 35]. Several authors suggested a macroscopic description of the long-time dynamics in terms of a nonlinear diffusion-type equation resulting in sub-diffusive spreading of the wave packet [33, 31, 34]; however, arguments used to justify this equations are based on an *a priori* assumption of spatially uniform chaos.

On the other hand, it was argued that among different initial conditions with a finite

norm, at least some should exhibit regular quasi-periodic dynamics, and thus would not spread indefinitely [5, 13, 37]. For finite-size systems, scaling of the probability for the system to be in the chaotic or regular regime has been studied numerically [36]. When scaling arguments are applied to the results of the numerical integration of the equation of motion, they indicate slowing down of the power-law spreading [34]. Rigorous mathematical arguments support the conclusion that at long times the wave packet should spread (if spread at all) slower than any power law [50].

The aim of the present work is the analysis of statistical properties of weak chaos in the discrete one-dimensional disordered nonlinear Schrödinger equation with the initial conditions corresponding to finite norm and energy *densities*. The main focus is on long-time dynamics and relaxation at large distances, when no stationary superfluid flow can exist in the system [11, 27] and the dynamics is chaotic. It is often assumed that upon thermalization chaos has no spatial structure, and all sites of the chain are more or less equally chaotic; here it is argued not to be the case.¹ Namely, in the regime of strong disorder and weak nonlinearity chaos is concentrated on a small number of rare chaotic spots (essentially the same picture was also proposed in Ref. [47] for a disordered chain of coupled classical spins, but it was not put on a quantitative basis). A chaotic spot is a collection of resonantly coupled oscillators, in which one can separate a collective degree of freedom (namely, their relative phase whose dynamics is slow because of the resonance), which performs chaotic motion. Under the conditions of weak coupling between neighboring oscillators and weak nonlinearity (i. e., Anderson localization being the strongest effect), the distance between different chaotic spots is much greater than the typical size of the spot. The stochastic motion of the collective degree of freedom of each chaotic spot acts as a stochastic pump, i. e. drives the exchange of energy between other oscillators, non-resonantly coupled to the spot, which corresponds to the Arnold diffusion. This represents the main mechanism for relaxation and thermalization of the oscillators, as well as for the transport of conserved quantities (energy and norm). An important role is played by the fact that chaotic spots can migrate along the chain, as the collective degree of freedom may get in and out of the chaotic region of its phase space. A similar phenomenon has recently been proven to exist in a chain of weakly coupled pendula [51]. This migration also bears analogy with the variable-range hopping of electrons in strongly disordered solids [52, 53]. Still, there is an important difference that the chaotic spot does not carry any energy or norm; it only drives relaxation of oscillators surrounding it.

The main technical challenge in this work is the analysis of high orders of the perturbation theory, which is necessary both to separate the collective degree of freedom performing the chaotic motion, and to couple other oscillators to this degree of freedom. The perturbation theory is divergent, as chaos is a non-perturbative phenomenon. The divergence occurs because of overlapping resonances, according to Chirikov's criterion

¹ We will call the motion of an oscillator the more chaotic the faster it loses the phase memory.

of chaos. In this work, the probability for resonances to occur is estimated in each order of perturbation theory. The subsequent treatment of each resonance and description of the associated chaotic motion is based on the stochastic pump model of the Arnold diffusion, which was proposed for systems with few degrees of freedom [54, 55]. Thus, the present work is not more rigorous than the stochastic pump model; it does not add anything new to the current understanding of how chaos is generated in nonlinear systems; it rather deals with the statistics of chaos in a spatially extended system with an infinite number of degrees of freedom and local coupling between them.

The main quantitative result of the present work is the system of macroscopic equations which describe transport of the conserved quantities (energy and norm) along the chain. Such transport determines equilibration of the chain at large distances, which occurs at long time scales. These equations are of nonlinear-diffusion type, and explicit expressions for the transport coefficients are derived. The macroscopic equations are valid at distances exceeding a certain length scale, which is also explicitly estimated.

The paper is organized as follows. In Sec. 2 the model is formulated and the main assumptions are discussed. Sec. 3 summarizes the main results. In Sec. 4 we qualitatively describe the physical picture and the main ingredients of the solution; various implications and some related issues are discussed. In Sec. 5 we analyze the chaotic phase space in few-oscillator configurations. In Sec. 6 perturbation theory is developed and statistics of different terms is analyzed. In Sec. 7 this perturbation theory is used to study the statistics of the chaotic phase volume for an arbitrary number of oscillators. Sec. 8 is dedicated to the analysis of the coupling between chaotic spots and other oscillators, and to the description of Arnold diffusion. In Sec. 9 the macroscopic transport coefficients are found.

2. Model and assumptions

The main subject of this study is the one-dimensional discrete nonlinear Schrödinger equation with diagonal disorder:

$$i \frac{d\psi_n}{dt} = \omega_n \psi_n - \tau \Delta (\psi_{n-1} + \psi_{n+1}) + g \psi_n^* \psi_n^2. \quad (2.1)$$

Here the integer n runs from $-\infty$ to $+\infty$ and labels sites of a one-dimensional lattice. To each site a pair of complex conjugate variables ψ_n, ψ_n^* is associated.

Eq. (2.1) together with its complex conjugate are the Hamilton equations,

$$\frac{d\psi_n}{dt} = \frac{\partial H}{\partial(i\psi_n^*)}, \quad \frac{d(i\psi_n^*)}{dt} = -\frac{\partial H}{\partial\psi_n}, \quad (2.2)$$

corresponding to the classical Hamiltonian

$$H(\{i\psi_n^*\}, \{\psi_n\}) = \sum_n \left[\omega_n \psi_n^* \psi_n - \tau \Delta (\psi_n^* \psi_{n+1} + \psi_{n+1}^* \psi_n) + \frac{g}{2} (\psi_n^*)^2 \psi_n^2 \right], \quad (2.3)$$

where $i\psi_n^*$ is the canonical momentum conjugate to the coordinate ψ_n . For this ψ_n must have a dimensionality of (action)^{1/2}. One can pass to another set of canonical variables, the actions I_n and the phases ϕ_n , as

$$\psi_n = \sqrt{I_n} e^{-i\phi_n}, \quad (2.4)$$

so that the Hamiltonian becomes

$$H(\{I_n\}, \{\phi_n\}) = \sum_n \left[\omega_n I_n - 2\tau\Delta \sqrt{I_n I_{n+1}} \cos(\phi_n - \phi_{n+1}) + \frac{g}{2} I_n^2 \right], \quad (2.5)$$

and the equations of motion are

$$\frac{d\phi_n}{dt} = \frac{\partial H}{\partial I_n}, \quad \frac{dI_n}{dt} = -\frac{\partial H}{\partial \phi_n}. \quad (2.6)$$

It is convenient to introduce the action-dependent frequency of each oscillator,

$$\tilde{\omega}_n(I_n) = \omega_n + gI_n, \quad (2.7)$$

to be distinguished from the bare frequencies ω_n .

The first term on the right-hand side of Eq. (2.1) represents the diagonal disorder. The bare frequencies ω_n are assumed to be independent random variables uniformly distributed over the interval

$$-\frac{\Delta}{2} \leq \omega_n \leq \frac{\Delta}{2}. \quad (2.8)$$

The second term on the right-hand side of Eq. (2.1) will be referred to as tunneling.² It is convenient to measure its strength with respect to the disorder, so the dimensionless parameter τ is introduced. Together with the disorder term, the tunneling term constitutes the linear part of the problem, whose normal modes are determined from the eigenvalue equation

$$(\omega - \omega_n)\psi_n + \tau\Delta(\psi_{n-1} + \psi_{n+1}) = 0. \quad (2.9)$$

As we are dealing with a one-dimensional system, any eigenfunction has an envelope, exponentially localized around some site \bar{n} , $\psi_n \sim e^{-\kappa|n-\bar{n}|/2}$. The smaller τ , the stronger the localization. We assume

$$\tau \ll 1. \quad (2.10)$$

In this case $\kappa \approx \ln(1/2e\tau) \gg 1$,³ so each eigenstate is essentially localized on a single site, with weak perturbative tails on the neighboring sites.

²May the reader not be confused by this ‘‘quantum-mechanical’’ term: here we are always dealing with a classical Hamiltonian system. This term is the standard one in studies of Anderson localization on a lattice.

³This estimate can be obtained, e. g. from the Thouless relation between the localization length and the density of states [56], approximating the latter by the box of the width Δ .

The third term on the right-hand side of Eq. (2.1) represents the nonlinearity whose strength is governed by the coupling constant $g > 0$.⁴ As mentioned above, we are interested in the case when the nonlinearity is weak. However, it would be meaningless to simply say that g is small. Indeed, Eq. (2.1) is invariant under the change

$$\psi_n \rightarrow C\psi_n, \quad g \rightarrow \frac{g}{C^2}, \quad (2.11)$$

where C is an arbitrary constant. Thus, it is the product $g|\psi_n|^2$, the nonlinear frequency shift of the n th oscillator, which can be compared to other frequency scales. This nonlinear shift is determined by g , as well as by the initial conditions for Eq. (2.1). We will assume that it is much smaller than the disorder and denote the corresponding dimensionless small parameter by ρ :

$$\frac{g|\psi_n|^2}{\Delta} \sim \rho \ll 1. \quad (2.12)$$

Eq. (2.12) also expresses another assumption of the present work, that the typical scale of $|\psi_n|^2$ is about the same for all oscillators; in other words, there is no significant correlation between $|\psi_n|^2$ and ω_n . As an example of the opposite one could prepare an initial condition where most of the norm $|\psi_n|^2$ is put on the oscillators with ω_n 's near the bottom of the band. This case is more complicated (e. g., it includes all physics related to superfluidity, such as Bose condensate being the ground state of the classical Hamiltonian (2.3), as well as large localization length for low-frequency phonons [57]); it is beyond the scope of the present work. The criterion can be conveniently formulated in terms of the two integrals of motion of Eq. (2.1): the total energy, given by Eq. (2.3), and the total action (norm),

$$I_{tot} \equiv \sum_{n=-\infty}^{\infty} |\psi_n|^2. \quad (2.13)$$

In the situation favoring oscillators with frequencies near the bottom of the band one obtains $H \approx -(\Delta/2)I_{tot}$, since the dominant contribution to both H and I_{tot} comes from the oscillators with ω_n close to $-\Delta/2$ (the coupling and the nonlinear terms in H are assumed to be small). In the case with $|\psi_n|^2$ independent of ω_n there is a significant cancellation between contributions $\omega_n|\psi_n|^2$ to the Hamiltonian (2.3) with $\omega_n > 0$ and $\omega_n < 0$, so assuming all oscillators to be excited on the same scale is equivalent to assuming $|H|/I_{tot} \lesssim \Delta/2$. In the following, we will assume the strong inequality,

$$\frac{|H|}{I_{tot}} \ll \Delta, \quad (2.14)$$

⁴Generally speaking, the sign of g is not important for the dynamics, since the change $g \rightarrow -g$ is equivalent to $\psi_n \rightarrow (-1)^n \psi_n^*$, $\omega_n \rightarrow -\omega_n$; the latter has no effect since the disorder distribution is symmetric. However, later we will be interested in the thermodynamics of the chain, so it is convenient to have the Hamiltonian bounded from below.

which is made for pure technical convenience only. It does not affect the qualitative conclusions of the work, but simplifies the calculations since it effectively decouples different realizations of disorder and different initial conditions.

Finally, we will assume

$$H < 0. \quad (2.15)$$

It turns out that for certain values of H and I_{tot} the system cannot thermalize, which can be seen from very basic thermodynamic arguments (see Ref. [58] and Appendix A for details). Condition (2.15) in combination with Eqs. (2.12), (2.14) ensures that the system is not in that non-thermal region.

When all three terms on the right-hand side of Eq. (2.1) are present, the equation has only two integrals of motion: the total energy, H , and the total action, $I_{tot} = \sum_n I_n$. However, if $\tau = 0$ or $g = 0$, the system is integrable. Thus, one is free to choose any of the two as the perturbation destroying the integrability. The most natural choice is the tunneling. Then, each I_n being an integral of motion at $\tau = 0$, Hamiltonian (2.5) is already written in the correct variables. It may seem that this implies the condition $\tau \ll \rho$ (since ρ is the effective strength of the nonlinearity). Indeed, as will be seen below (Sec. 5), some elements of the physical picture admit a simpler quantitative description at $\tau \ll \rho$. However, the main results of this paper are obtained using the perturbation theory both in τ and g , and are valid for any relation between τ and ρ , as long as both are small (on the issue of smallness, see also Sec. 4.5.6).

3. Main results

The first statement is that for general initial conditions, satisfying the assumptions of the previous section, the system locally thermalizes with a finite relaxation time. Local thermalization means that on a finite, sufficiently long segment of the chain [the corresponding length scale L_* is given explicitly below, Eq. (3.7)], the actions and the phases are distributed according to the grand canonical distribution, $e^{-\beta(H-\mu I_{tot})}$. To respect the two conserved quantities, the total energy H and action I_{tot} of the chosen segment, two Lagrange multipliers are introduced: $\beta \equiv 1/T$ is the inverse temperature, and μ has the meaning of the chemical potential, although it has the dimensionality of a frequency. The issue of thermalization is discussed in more detail in Sec. 4.5.2.

The values of μ and T , which define the thermal distribution on each segment, are determined by the total norm and energy initially contained on this segment, that is, by the initial conditions. It turns out that for some values of energy and norm (namely, when the energy is too high for a given norm), the corresponding μ and T do not exist, as discussed in Ref. [58] and Appendix A, so the system may equilibrate in the micro-canonical sense, but still not be thermal. The assumption of negative total energy, made in the previous section [Eq. (2.15)], ensures that such problem does not arise, and the system indeed thermalizes. However, even when the local thermalization has occurred, generally speaking, μ and T still have different values for different segments, depending

on the initial conditions, so the system is still not in the global equilibrium. The results described in the following, concern precisely the global equilibration of the system.

To account for the dependence of μ and T on the position, we introduce a continuous variable, $n \rightarrow x$, and assume a dependence on the position, $T = T(x)$, $\mu = \mu(x)$, smooth on the scale L_* . Let us define the smoothed macroscopic energy and action densities,

$$\mathcal{I}(x) = \frac{1}{L_*} \sum_{n=x-L_*/2}^{x+L_*/2} |\psi_n|^2, \quad (3.1a)$$

$$\mathcal{H}(x) = \frac{1}{L_*} \sum_{n=x-L_*/2}^{x+L_*/2} \left[\omega_n |\psi_n|^2 - \tau \Delta (\psi_n^* \psi_{n+1} + \psi_{n+1}^* \psi_n) + \frac{g}{2} |\psi_n|^4 \right]. \quad (3.1b)$$

At each point x they are related to the local values of $T(x)$, $\mu(x)$ by the standard thermodynamics (see Appendix A). It is convenient to define dimensionless variables

$$\rho \equiv \frac{g\mathcal{I}}{\Delta}, \quad h \equiv \frac{g\mathcal{H}}{\Delta^2}. \quad (3.2)$$

Under the assumptions of the previous section, namely, $\tau \ll 1$, $\rho \ll 1$, $|h| \ll \rho$, the thermodynamic relations take a very simple form (the condition $|h| \ll \rho$ turns out to be equivalent to $\mu < 0$, $|\mu| \gg \Delta$):

$$\rho = \frac{gT}{|\mu|\Delta}, \quad h = \left(\frac{gT}{|\mu|\Delta} \right)^2 - \frac{1}{12} \frac{gT}{\mu^2}. \quad (3.3)$$

In the global equilibrium, T and μ must be constant over the entire chain. As the values of $\mu(x)$ and $T(x)$ are determined by the densities $\mathcal{I}(x)$ and $\mathcal{H}(x)$, during the global equilibration norm and energy must be transported along the chain. Thus, the corresponding currents, $J^{\mathcal{I}}$ and $J^{\mathcal{H}}$, must be flowing during the equilibration. The conservation laws for the total energy and norm impose the corresponding continuity equations:

$$\frac{\partial}{\partial t} \begin{bmatrix} \mathcal{I} \\ \mathcal{H} \end{bmatrix} = -\frac{\partial}{\partial x} \begin{bmatrix} J^{\mathcal{I}} \\ J^{\mathcal{H}} \end{bmatrix}. \quad (3.4)$$

The currents must vanish for $T(x), \mu(x) = \text{const}$. Thus, they can be expanded in the gradients, and only the first term is retained:

$$\begin{bmatrix} J^{\mathcal{I}} \\ J^{\mathcal{H}} \end{bmatrix} = -\sigma(T, \mu) \frac{\partial}{\partial x} \begin{bmatrix} \mu/T \\ -1/T \end{bmatrix}. \quad (3.5)$$

$\sigma(T, \mu)$ is a 2×2 matrix of the transport coefficients which will be called conductivity. Since $-\mu/T$ and $1/T$ are thermodynamically conjugate to \mathcal{I} and \mathcal{H} , the matrix σ is symmetric by virtue of the Onsager relations. The statement about the finiteness of σ , equivalent to the validity of the gradient expansion, and to the normal character of diffusion in the system, is already not trivial. Indeed, σ could be zero or infinite, leading to

anomalous diffusion; in Ref. [31] $\sigma = 0$ was suggested. Our result is that σ is finite, and given by

$$\sigma(T, \mu) \sim \frac{\Delta^3}{g^2} \begin{bmatrix} 1 & O(\rho\Delta) \\ O(\rho\Delta) & O(\Delta^2) \end{bmatrix} \exp \left\{ -C' \left(\frac{\ln(1/\rho)}{\ln(1/\tau)} \right) \ln^2 \frac{1}{\tau^p \rho} \ln \frac{1}{\rho} \right\}. \quad (3.6a)$$

It depends on T and μ only through the combination $\rho = gT/(|\mu|\Delta)$, which is the consequence of the condition $|\mu| \gg \Delta$, or, equivalently, of Eq. (2.14). The argument of the exponential is written with the logarithmic accuracy. The function $C'(\ln(1/\rho)/\ln(1/\tau))$ is bounded from above and below,

$$\frac{1/3}{[1 + \ln(1+x)]^2} \leq C'(x) \leq \frac{8}{[1 + \ln(1+x)]^2}. \quad (3.6b)$$

Finally, the power p is bounded by

$$\frac{1}{2} \leq p \leq 3. \quad (3.6c)$$

The author has not been able to calculate $C'(x)$ and p explicitly. Given this uncertainty, it would make little sense to calculate slow prefactors. The prefactor Δ^3/g^2 is put to keep the correct dimensionality. Also, an order-of-magnitude estimate for the relative magnitude of different matrix elements of σ could be established.

Equations (3.2)–(3.6c) form a closed system of macroscopic equations describing action and energy transport along the chain and constitute the main quantitative result of the present work. Eq. (3.6a) is already sufficient to conclude that the dependence of σ on the integrability-breaking parameters τ and ρ is stronger than any power law, but weaker than a stretched exponential which would be the expected dependence of the Arnold diffusion rate on the integrability-breaking perturbation [54, 55, 59]. This phenomenon is known as fast Arnold diffusion [60], and arises because of a large number of degrees of freedom in the system.

The above expression for $\sigma(T, \mu)$, Eq. (3.6a), does not imply averaging over many disorder realizations. In fact, its inverse, σ^{-1} , is a self-averaging quantity. The length scale L_* at which this self-averaging occurs can be viewed as boundary separating macroscopic and microscopic distances. It can be estimated as

$$\ln L_* \sim C' \ln^2 \frac{1}{\tau^p \rho}. \quad (3.7)$$

Segments much longer than L_* contain a sufficient number of sites to effectively replace the average over realizations. Transport properties of a segment shorter than L_* are strongly realization-dependent, and fluctuations are of the same order as the average. This situation is analogous to that with hopping conduction in one dimension [61].

The macroscopic transport equations given above describe equilibration of a chain whose average action \mathcal{I} and energy \mathcal{H} per oscillator are finite. Still, having written

these macroscopic equations, one can always prepare an initial condition $\mathcal{I}(x), \mathcal{H}(x)$ in the form of a finite-size packet, and see how it spreads according to the equations. In Appendix B the equations are shown to give the size of the packet, $L(t)$, to grow as

$$L(t) \sim e^{[(C')^{-1} \ln t]^{1/3}}. \quad (3.8)$$

This is slower than any power law, in agreement with Ref. [50], and in disagreement with Refs. [7, 9, 15, 16, 20, 21, 32, 33, 35]. Possible reasons for this disagreement will be discussed in Sec. 4.5.6. Note, however, that as the packet size $L(t)$ increases, the corresponding density inside the packet, $\rho \propto 1/L(t)$, decreases. Thus, the length scale L_* , given by Eq. (3.7), very quickly diverges so after some time we will inevitably have $L(t) < L_*$. Since the macroscopic equations are only valid at distances exceeding L_* , they lose their applicability as the packet spreads.

4. Qualitative picture

4.1. Search for chaos

Appearance of chaos in systems with a few degrees of freedom has been thoroughly studied in the past [54, 55, 59]; the main steps will be reviewed in Sec. 5. The essential ingredients are the following.

1. When an integer linear combination of several frequencies $\tilde{\omega}_n(I_n)$ of the integrable system vanishes for some values of I_n , that is $m_1 \tilde{\omega}_{n_1} + \dots + m_N \tilde{\omega}_{n_N} = 0$ (guiding resonance, in Chirikov's terminology [54]), one can separate a slow degree of freedom $\tilde{\phi}$, which is the corresponding linear combination of the phases: $\tilde{\phi} = m_1 \phi_{n_1} + \dots + m_N \phi_{n_N}$. Exactly at resonance this degree of freedom has no dynamics at all (in the unperturbed system).
2. If the perturbation has a term resonant with $\tilde{\phi}$, the latter acquires a non-trivial dynamics whose characteristic frequency Ω is proportional to the square root of the perturbation strength. The corresponding phase space has a separatrix.
3. Chaos arises upon destruction of this separatrix by another term of the perturbation which oscillates at some characteristic frequency ϖ . The volume of the resulting chaotic region around the separatrix in the phase space of the slow degree of freedom (the so-called stochastic layer) (i) is proportional to the strength of the separatrix-destroying perturbation (up to a logarithmic factor), and (ii) is exponentially small, $\sim e^{-\varpi/\Omega}$, when $\varpi \gg \Omega$ (which is typically the case). Destruction of the separatrix will be also reviewed in more detail in Sec. 5.2.

In the particular case of Eq. (2.1) the perturbation conserves the total action and energy, so the minimal number of oscillators, necessary to generate chaos, is three.

To determine the main contribution to the chaotic phase volume, we need (i) to identify the guiding resonances which have the largest resonant perturbation strength and

thus the highest frequency Ω ; (ii) to find the separatrix-destroying terms of the perturbation which oscillate at the smallest possible frequency ϖ and are not too weak (layer resonances, in Chirikov's terminology [54]). It is important that the mentioned perturbation terms include not only those directly appearing in the Hamiltonian (2.3) or (2.5), but also terms of the kind

$$\begin{aligned} V &= \mathcal{K} \left(\psi_{n_1}^* \dots \psi_{n_N}^* \psi_{\bar{n}_1} \dots \psi_{\bar{n}_N} + \psi_{\bar{n}_1}^* \dots \psi_{\bar{n}_N}^* \psi_{n_1} \dots \psi_{n_N} \right) \\ &= 2\mathcal{K} \sqrt{I_{n_1} \dots I_{n_N} I_{\bar{n}_1} \dots I_{\bar{n}_N}} \cos(\phi_{n_1} + \dots + \phi_{n_N} - \phi_{\bar{n}_1} - \dots - \phi_{\bar{n}_N}). \end{aligned} \quad (4.1)$$

Such “ N -particle” terms are effectively generated in high orders of the perturbation theory in τ and g , which is developed in Sec. 6. They oscillate at the frequency $\varpi = \tilde{\omega}_{n_1} + \dots + \tilde{\omega}_{n_N} - \tilde{\omega}_{\bar{n}_1} - \dots - \tilde{\omega}_{\bar{n}_N}$, which is easier to make small for larger N , as discussed in Sec. 6.6. However, the corresponding strength \mathcal{K} contains a high power of the coupling constants.

Consider the simplest resonance, that of two oscillators:

$$\omega_n + gI_n = \omega_{n'} + gI_{n'}. \quad (4.2)$$

Since the typical values of actions $I_n, I_{n'} \sim T/|\mu|$, this equation can be satisfied only if

$$|\omega_n - \omega_{n'}| \sim \frac{gT}{|\mu|}. \quad (4.3)$$

Two arbitrary sites have $|\omega_n - \omega_{n'}| \sim \Delta$, so for weak nonlinearity, $gT/|\mu| \ll \Delta$ [Eq. (2.12)], one has to look for special pairs. If we fix n , the appropriate partner n' will be found typically at distances $|n - n'| \sim |\mu|\Delta/(gT) \equiv 1/\rho$. This distance gives also the minimal order of the perturbation theory in the tunneling which couples two such oscillators and produces a separatrix, so that $\Omega \propto \sqrt{\tau^{1/\rho}}$. The thickness of the corresponding stochastic layer, $\propto e^{-\varpi/\Omega}$, will be very small. The same occurs if one tries an N -oscillator resonance: even though the equation

$$m_1(\omega_{n_1} + gI_{n_1}) + \dots + m_N(\omega_{n_N} + gI_{n_N}) = 0 \quad (4.4)$$

is easier to satisfy than Eq. (4.2), a high order of the perturbation theory is required to couple these oscillators altogether, and thus Ω is again proportional to a high power of τ , which then enters as $e^{-\varpi/\Omega}$.

The “cheapest” way to produce a moderately small Ω is to find a pair of nearest neighbors, $n' = n \pm 1$, such that $|\omega_n - \omega_{n+1}| \sim gT/|\mu|$. Such pairs are rare, they occur every $1/\rho$ sites on the average, but they have $\Omega \propto \sqrt{\tau}$. The low density of these pairs gives a small factor $\sim \rho$ in the total chaotic phase volume, but it is much less dramatic than $\tau^{1/\rho}$ exponentiated. It is here that the assumption $\tau \ll \rho$ is necessary. Indeed, in the opposite case one would have to solve the linear part of the problem first and find the two eigenfrequencies, whose difference cannot be smaller than $\tau\Delta$ (the so-called

level repulsion). These eigenfrequencies should then be substituted into Eq. (4.3) which cannot be satisfied if $\tau \gg \rho$. In this latter case the resonant pair should be made out of oscillators separated by some distance l , so that their effective coupling is $\sim \tau^l \lesssim \rho$, which can always be satisfied for a sufficiently large l (see also Sec. 6.7).

Next, one has to identify the separatrix-destroying perturbation which produces the thickest stochastic layer. If we simply consider coupling between one of the sites of the resonant pair $n, n + 1$ and another oscillator n' , the frequency of this perturbation is $\varpi = |\tilde{\omega}_n - \tilde{\omega}_{n'}|$. Typically, this frequency is $\sim \Delta$, so the effect of the perturbation is exponentially small. Still, out of many available oscillators, it is possible to find one with a sufficiently close frequency, so that ϖ is also small. However, this oscillator will be far away, so the stochastic layer thickness will be proportional to a high power of τ . In high orders of perturbation theory many-oscillators terms can also be generated. Thus, one has to find an optimum between decreasing ϖ in $e^{-\varpi/\Omega}$ and multiplying it by a large power of τ . An analogous optimization procedure has been considered by Chirikov and Vecheslavov [60]. For our problem the resulting width of the stochastic layer is proportional to $e^{-\ln^2(1/\tau)}$.

Again, the way to bypass this smallness is to notice that the above arguments concern a resonant pair in a typical surrounding. There is, however, a small fraction of pairs which have a neighbor with a close frequency, i. e. *resonant triples*. Clearly, it makes no sense to tune the frequency of the third oscillator more precisely than the frequency mismatch of the resonant pair, so the density of such resonant triples is $\sim \rho^2$. Moreover, when all three frequencies are close, the chaotic region of the phase space does not have to be just a thin layer around the destroyed separatrix, but can be of the size of the separatrix itself. Thus, the chaotic region of the $\{I_1, I_2, I_3\}$ space is concentrated around the straight line $\omega_1 + gI_1 = \omega_2 + gI_2 = \omega_3 + gI_3$. A resonant triple will be called a *chaotic spot* if its dynamical variables fall in the chaotic region. The probability of this latter event, which turns out to be $\sim \tau/\rho$ if $\tau \ll \rho$ and ~ 1 if $\tau \gg \rho$, multiplied by the density of resonant triples, $\sim \rho^2$, gives the density of the chaotic spots, $\bar{w} \sim \min\{\tau\rho, \rho^2\}$. This is discussed in detail for $\tau \ll \rho$ in Sec. 5.4.

4.2. Arnold diffusion

The key property of a chaotic spot is that the Fourier transform of $\psi_n(t)$ has a continuous frequency spectrum, as discussed in Sec. 8.1 (see also Sec. 4.5.1). When the stochastic layer around the separatrix is thin, the spectrum can be evaluated explicitly via Melnikov-Arnold integral [62, 63, 54]. The spectrum is peaked around $\tilde{\omega}_n$ with the characteristic width Ω , and has an exponential tail, $e^{-|\omega - \tilde{\omega}_n|/\Omega}$ away from $\tilde{\omega}_n$. This should be contrasted with the case of an integrable system where the Fourier spectrum of the motion is made of δ -peaks with zero width.

The chaotic spot exerts a random force on other oscillators, thereby allowing them to exchange action and energy with the spot and among themselves. This exchange occurs by small random increments, so the relevant picture is that of random diffusion

in the multi-dimensional space of actions $\{I_n\}$. This corresponds to the standard picture of stochastic pump driving Arnold diffusion [54, 55]. This diffusion (i) must respect the total action and energy conservation laws, and (ii) cannot “turn off” the chaotic spot, since the dynamic variables of the spot oscillators cannot cross the stochastic layer boundary [54], so that the system stays on the guiding resonance $\sum_n m_n \tilde{\omega}_n = 0$. The corresponding diffusion equation is analyzed in Secs. 8.2 and 8.3.

To study the diffusion of an oscillator, located at large distance from the nearest chaotic spot, one should find a suitable perturbation term of the form (4.1) involving both this oscillator and an oscillator belonging to the spot (and, typically, many others). Again, one seeks (i) to be close to resonance with the spot oscillation frequency in order to avoid suppression $e^{-\varpi/\Omega}$, and (ii) to avoid too high orders of the perturbation theory, since the diffusion coefficient is proportional to the perturbation strength squared. Still, if the distance between the chaotic spot and the oscillator is L , the smallness τ^{2L} in the diffusion coefficient is already guaranteed. This is discussed in Sec. 8.4.

For a given number N of oscillators, the conditions

$$\sum_{n=1}^N I_n = NI, \quad \sum_{n=1}^N \left(\omega_n I_n + \frac{g}{2} I_n^2 \right) = N\mathcal{H}, \quad \sum_{n=1}^N m_n (\omega_n + gI_n) = 0, \quad I_1, \dots, I_N > 0, \quad (4.5)$$

define a region on an $(N - 3)$ -dimensional hypersurface whose $(N - 3)$ -dimensional volume is finite. Hence, it takes a finite time for the system to explore this region and to establish the micro-canonical distribution. This time, however, grows exponentially with N , as long as only one chaotic spot is present.

For a longer segment, such that it hosts two chaotic spots, the oscillators which are close to one spot equilibrate among themselves, and those close to the other spot – among themselves, much faster than equilibration between the two groups of oscillators occurs. Indeed, in order to transfer action and energy between the two groups, one has to find a perturbation term which couples oscillators from both groups to one of the spots. Since the coupling decays exponentially with distance, the best way to do this would be to couple oscillators which are near the boundary between the two groups, i. e., in the middle between the two spots. As mentioned in the previous subsection, the typical distance between chaotic spots is $\sim 1/\min\{\tau\rho, \rho^2\}$, so the characteristic time scale of equilibration is of the order of $(1/\tau)^{1/\min\{\tau\rho, \rho^2\}}$, which is enormously long. For the long chain with many spots it may become even worse if one considers anomalously long segments of the chain, not containing chaotic spots: even though such segments are rare, they efficiently block the transport along the chain.

The above picture assumes the positions of chaotic spots to be fixed. There is, however, a mechanism which provides a faster way of equilibration at long distances. Consider first a chaotic spot and the closest resonant triple which is not chaotic, assuming $\tau \ll \rho$. As discussed in Sec. 4.1, the typical distance to this triple, $\sim 1/\rho^2$, is smaller than the distance to the next chaotic spot, $\sim 1/(\tau\rho)$. Thus, the diffusion coefficient for

the actions of the triple is small as τ^{1/ρ^2} . As the triple explores its phase space in the course of Arnold diffusion, it may hit its own chaotic region. Importantly, this requires the same amount of time as the equilibration itself.⁵ Thus, a new chaotic spot is created, relatively close to the old one. However, now each of them can diffuse out of its stochastic layer, driven by the other one. If it happens to the old one, this means that the system has effectively switched from one guiding resonance to another one at the point of their intersection in the phase space. This switching is also accompanied by a jump of the chaotic spot in the real space.

It is important to realize that this jump does not correspond to a transfer of any action or energy: the chaotic spot does not carry any action or energy by itself; these are stored in the numerous oscillators surrounding the spot and transferred from one oscillator to another by Arnold diffusion, while the chaotic spot only drives this diffusion. Thus, to transfer action and energy between two groups of oscillators, which already have equilibrated among themselves, it is quicker to wait until the chaotic spot moves closer to the boundary between the two groups and drives the Arnold diffusion there, rather than doing it by diffusion driven from a remote spot.

If now the consideration is extended on triples which are not well in resonance, but have a noticeable frequency mismatch, this mismatch will translate into an activation barrier E , so the time required for a triple to reach its chaotic region will be longer than the equilibration time by a factor $e^{E/T}$. However, since the typical activation barrier of an arbitrary triple is $\sim |\mu|\Delta/g$, hopping to a typical nearest neighbor will only take the time $e^{1/\rho}$, much shorter than $(1/\tau)^{1/\rho^2}$. This means that resonant triples, on the one hand, host chaotic spots for most of the time, but on the other, are not the ones that determine the transport. Thus, one has to return to the beginning of Sec. 4.1 and look for guiding and layer resonances in a typical environment. For this, many-oscillator resonances have to be considered, and thus, high orders of the perturbation theory have to be analyzed.

4.3. Variable-range hopping of chaotic spots

Even when the guiding resonance involves several oscillators, it is still convenient to assign it to a single site of the chain (defined, e. g., as the leftmost site participating in the resonance). Then, each site n can be characterized by w_n , the chaotic fraction of the thermally-weighted phase volume, summed over all possible guiding resonances involving the site n and sites to the right of it (see Section 7.2 for details). It is determined by the configuration of the static disorder $\{\omega_{n'}\}$ around the site, but not by the values of

⁵ This is a property of the two-dimensional diffusion. Indeed, as the chaotic region of the three-dimensional action space of the triple is concentrated around the straight line $\omega_1 + gI_1 = \omega_2 + gI_2 = \omega_3 + gI_3$, it is sufficient to determine the time it takes for the system to touch the corresponding region in the two-dimensional section, perpendicular to this line. Consider diffusion with the coefficient D on a square $L \times L$, divided into small cells $a \times a$. It takes the time $\sim a^2/D$ to move to an adjacent cell, and the time $\sim L^2/D$ to cross the whole square. Thus, while crossing the square, the system visits $\sim L^2/a^2$ cells, i. e., a fraction of the order of unity. In dimensionality higher than two, only a small fraction of cells would be visited.

the dynamical variables (over the latter, the thermal average is performed). It represents the probability that at a given instant of time the site n is hosting a chaotic spot, and plays the same role in the migration of a chaotic spot as the thermal weight $e^{-E(x)/T}$ in the Brownian motion of a particle in an energy landscape $E(x)$.⁶ Let us estimate the typical value of w in the typical environment. Let N_g and N_ℓ be the number of oscillators involved in the guiding and layer resonances, respectively. Roughly,

$$w \sim \sum_{N_g, N_\ell=0}^{\infty} \exp\left(-\frac{e^{-N_g}}{\rho}\right) \exp\left(-\frac{e^{-N_\ell}}{(\tau^p \rho)^{N_g}}\right) (\tau^p \rho)^{N_\ell}. \quad (4.6)$$

The first exponential is just the thermal activation probability $e^{-(H-\mu I_{\text{tot}})/T}$ for a resonance like that in Eq. (4.4), where the smallest frequency mismatch that can be obtained out of $\sim e^{N_g}$ combinations of N_g frequencies (we do not distinguish between 2^{N_g} , e^{N_g} , or any other a^{N_g} with $a \sim 1$), is $\sim \Delta e^{-N_g}$. The characteristic frequency of the separatrix motion is then $\Omega \propto (\tau^p \rho)^{N_g}$, where $p N_g$ is the typical order in τ , needed to couple all the oscillators. The value of p is estimated in Sec. 7 as $1/2 \leq p \leq 3$. The second exponential corresponds to the exponential smallness of the Melnikov-Arnold integral $e^{-\varpi/\Omega}$, where the smallest frequency mismatch of the layer resonance is $\varpi \sim \Delta e^{-N_\ell}$. Finally, $(\tau^p \rho)^{N_\ell}$ is the strength of the layer resonance perturbation, determining the width of the stochastic layer. The leading exponential asymptotics of a sum of competing strong exponentials is determined by the largest term of the sum, or by the maximum of the exponent:

$$\ln \frac{1}{w} \sim \min_{N_g, N_\ell} \left(\frac{e^{-N_g}}{\rho} + \frac{e^{-N_\ell}}{(\tau^p \rho)^{N_g}} + N_\ell \ln \frac{1}{\tau^p \rho} \right) \sim \ln^2 \frac{1}{\tau^p \rho} \ln \frac{1}{\rho}, \quad (4.7)$$

the optimal values being $N_\ell \sim N_g \ln(1/\tau^p \rho) \sim \ln(1/\rho) \ln(1/\tau^p \rho)$. Note that this already reproduces the main exponential part of the τ, ρ -dependence of σ in Eq. (3.6a).

Thus, to each site is associated a random quantity w_n . For different sites, $n \neq n'$, w_n and $w_{n'}$ are assumed to be independent⁷. Then, it is natural to apply the variable-range hopping picture, proposed for electron transport in strongly disordered solids by Mott [52]: upon changing the guiding resonance, the chaotic spot typically shifts by a distance L which optimizes the compromise between the possibility to find a site with a large w_n (which is typically far away) and the exponential suppression of the hopping rate by the factor τ^L . It is also known that in one dimension the transport is determined not by typical hops, but by rare strong obstacles [53]. Such obstacles occur with a

⁶We emphasize again that the sum $\sum_n w_n$, equal to the average total number of chaotic spots on the chain, is dominated by rare “good” sites corresponding to resonant triples for $\tau \ll \rho$, as discussed in Sec. 4.1. Here we are interested in migration of chaotic spots between these triples.

⁷This is not obvious *a priori*, given the extended nature of the guiding and layer resonances. Note, however, that replacing ω_{n_1} by $\omega_{n_1 \pm 1}$ in Eq. (4.4) already changes the left-hand side by an amount $\sim \Delta$. Thus, the optimal guiding resonances corresponding to sites n and $n+1$ are likely to be completely different.

small probability, but in one dimension they block the transport efficiently as they cannot be bypassed, in contrast to higher dimensions. Following Ref. [61], we will use the term “breaks” to denote such obstacles.⁸ In the present problem, a break is a region of the chain where the chaotic fraction w assumes anomalously small values on many consecutive sites, i. e., a region of the chain rarely visited by chaotic spots.

To implement these arguments, one has to know the distribution of the random quantities w_n . The standard variable-range-hopping picture [52] assumes that $\ln(1/w) \equiv \lambda$ is uniformly distributed. Here it is definitely not the case, so the estimate of the typical value (4.7) is not sufficient; one has to calculate the whole distribution function $p(\lambda)$. This implies calculating the statistics of different terms of the perturbation theory of an arbitrarily large order. The structure of the perturbation theory for Eq. (2.1) is discussed in Sec. 6, and $p(\lambda)$ is calculated in Sec. 7. The result is given by the Gumbel distribution:

$$p(\lambda) = -\frac{d}{d\lambda} \exp\left(-C_1 \rho e^{[C \ln^2(1/\tau^p \rho)]^{-1} \lambda}\right). \quad (4.8)$$

Here C is again a bounded function of $\ln \rho / \ln \tau$. It differs from C' , which appears in Eq. (3.6a) for σ , by a factor of 2 at most. C_1 is another logarithmic function of τ and ρ ; it enters Eq. (3.6a) in the combination $\ln(1/C_1 \rho)$, so it is beyond the logarithmic accuracy and has been omitted from Eq. (3.6a). Eq. (4.8) is valid only for sufficiently large $\lambda \gg \ln^2(1/\tau^p \rho)$, so it cannot be used to find the average value of $w = e^{-\lambda}$. Indeed, the average is determined by smaller $\lambda \sim \ln(1/\tau \rho)$, corresponding to resonant triples, which should be treated separately. Given $p(\lambda)$ in the form (4.8), it is clear that the quantity which is uniformly distributed is the exponential under the derivative. Thus, λ_L^{typ} , the typical smallest value of λ which can be found within a segment of a length L , is found as

$$\frac{1}{L} \sim 1 - \exp\left[-C_1 \rho \left(e^{[C \ln^2(1/\tau^p \rho)]^{-1} \lambda_L^{\text{typ}}} - 1\right)\right], \quad \lambda_L^{\text{typ}} = C \ln^2(1/\tau^p \rho) \ln \frac{1}{C_1 \rho L}. \quad (4.9)$$

For $L \sim 1$ this agrees with the estimate (4.7).

It is crucial that all the discussion of this subsection is valid regardless of the relation between τ and ρ . Indeed, the typical order of the perturbation theory needed to form the guiding resonance is $N_g \sim \ln(1/\rho)$. Then the effective coupling between the oscillators of the guiding resonance, $\sim (\tau^p \rho)^{\ln(1/\rho)}$, is always smaller than ρ , regardless of τ .

4.4. Macroscopic transport coefficients

To relate the chaotic fraction w and the macroscopic conductivity σ , we use the fact that each segment between neighboring breaks contains many chaotic spots (this will be verified in the end of this subsection). Then, equilibration within each segment occurs

⁸ Other terms have also been used in the literature for these objects, such as “blockades” [64] or “weak links” [65]. The term “break” [61, 66] may not be the most precise, since the chain is not fully broken. Still, since the approach of the present work is analogous to that of Ref. [61], the same terminology is used.

much faster than between different segments, so each segment k of the length L_k can be characterized by its own values of the temperature and the chemical potential, μ_k, T_k , as well as the total action $I_{tot,k}$ and energy H_k . These latter ones slowly change due to the currents through the breaks J_k^I, J_k^H (which can be viewed as the definition of the currents). It is convenient to denote the corresponding 2-columns by

$$Q_k = \begin{bmatrix} I_{tot,k} \\ H_k \end{bmatrix}, \quad J_k = \begin{bmatrix} J_k^I \\ J_k^H \end{bmatrix}, \quad V_k = \begin{bmatrix} \mu_k/T_k \\ -1/T_k \end{bmatrix}, \quad (4.10)$$

where the k th break is assumed to separate the k th and the $(k+1)$ st segments. Then energy and action conservation can be written as

$$\frac{dQ_k}{dt} = J_{k-1} - J_k. \quad (4.11a)$$

The current through the k th break can be related to $\mu_k, T_k, \mu_{k+1}, T_{k+1}$ with the help of the diffusion equation in the space of actions $\{I_n\}$ (it is done in Sec. 9), and can be written as

$$J_k = R_k^{-1}(V_k - V_{k+1}), \quad (4.11b)$$

to the linear order in the potential difference $V_k - V_{k+1}$. The validity of the linear response theory follows quite generally from the diffusive character of the system dynamics in the space of actions. This is equivalent to finiteness of the coefficient R_k^{-1} , which is a symmetric 2×2 matrix and can be viewed as the conductance of the break. It is determined by the whole profile $\{\lambda_n\}$ of the break, $R_k = R(\{\lambda_n\})$, and is found in Sec. 9. Finally, we have a thermodynamic relation between $I_{tot,k}, H_k$ and T_k, μ_k , discussed in Sec. 3 and Appendix A [see Eqs. (A.1a), (A.1b)], which we write here as

$$Q_k = L_k Q(V_k). \quad (4.11c)$$

The explicit form of the function $Q(V)$ follows from the discussion of Sec. 3 and Appendix A, but is not important here.

Now we pass to macroscopic equations, valid at large distances $L \gg L_k$. Eqs. (4.11a) and (4.11c) lead to the continuity equation, $\partial Q(V)/\partial t = -\partial J/\partial x$. To relate the current J to the voltage gradient, we note that in a stationary situation, when a constant uniform current J flows through the chain, the potentials can be found from Eq. (4.11b) as $V_k = -\sum_{k' < k} R_{k'} J$. The potential drop over a distance L including many segments determines the macroscopic gradient:

$$\frac{\partial V}{\partial x} \approx \frac{V(x+L/2) - V(x-L/2)}{L} = -\frac{\sum_k R_k}{L} J = -\sigma^{-1} J. \quad (4.12)$$

Substituting the expression for the current in the continuity equation, we obtain the macroscopic transport equation:

$$\frac{dQ(V)}{dV} \frac{\partial V}{\partial t} = \frac{\partial}{\partial x} \sigma(V) \frac{\partial V}{\partial x}. \quad (4.13)$$

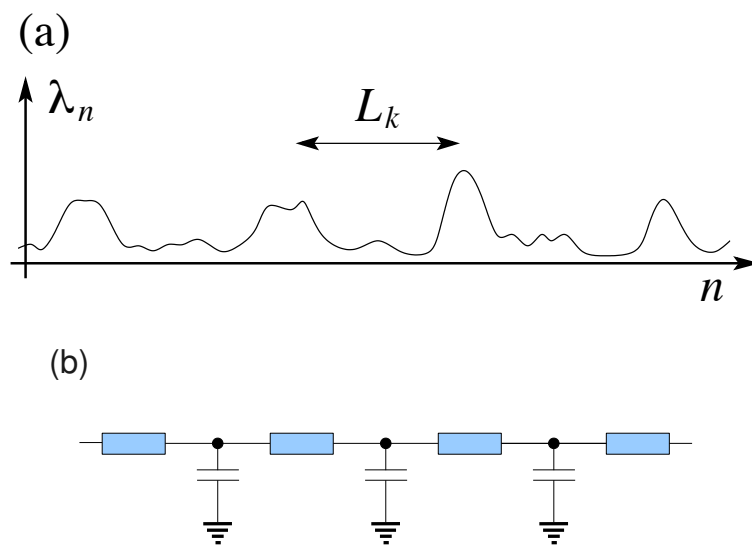


Figure 1: (a) A realization of $\lambda_n \equiv \ln(1/w_n)$, where w_n is the chaotic fraction of the thermally weighted phase volume, associated with the site n (see details in the text, Sec. 4.3). Four breaks are shown. (b) The equivalent electric circuit with resistors and nonlinear capacitors (the bottom plate of each capacitor is grounded).

Eqs. (4.11a)–(4.11c) are formally equivalent to those which describe an electric circuit, shown in Fig. 1(b). Namely, each segment corresponds to a capacitor, each break to a resistor, while Q_k and V_k correspond to electric charge and voltage. The only difference is that instead of the usual linear relation $Q_k = C_k V_k$, where C_k is the capacitance, we have a nonlinear relation (4.11c). In Eq. (4.13) dQ/dV plays the role of the macroscopic capacitance per unit length, and σ is the macroscopic conductivity. The physical reason for this analogy is that the theory of electric circuits describes nothing else but the transport of a conserved quantity (electric charge) driven by the gradient of the corresponding thermodynamically conjugate variable (voltage). In our problem the phenomenology is the same.

Eq. (4.12) expresses the usual addition rule for resistors in series. Since σ^{-1} is proportional to the sum of resistances of individual breaks R_k , and these resistances are independent due to large spatial separation between breaks, then by the law of large numbers σ^{-1} is self-averaging at long distances. Thus, we can write

$$\sigma^{-1} = \int R(\{\lambda_n\}) dP(\{\lambda_n\}), \quad (4.14)$$

where $dP(\{\lambda_n\})$ is the probability measure (per unit length) of the break configurations $\{\lambda_n\}$, determined by product of independent measures (4.8). The integral in Eq. (4.14) is mostly determined by the vicinity of a certain configuration which optimizes the strong competition between the exponentially growing $R(\{\lambda_n\})$ and quickly decreasing $dP(\{\lambda_n\})$ (Fig. 15). $R(\{\lambda_n\})$ is determined by the diffusion coefficient for oscillators in the break region. This diffusion coefficient contains the same small factors as the chaotic fraction w_n , so they are strongly correlated. We take this into account by assuming the diffusion coefficient to be proportional to $e^{-C_2 \lambda_L^{\text{sp}}}$, $1 \leq C_2 \leq 2$ (see Sec. 8.4). Calculation of the integral in Eq. (4.14) is performed in Sec. 9, and is quite analogous to the optimization procedure of Ref. [61]. The result is given by Eq. (3.6a). The self-averaging of σ^{-1} occurs at distances exceeding the typical distance between the optimal breaks, $L_* \sim e^{C \ln^2(1/\tau\rho)}$. Thus, it is L_* that determines the border between the microscopic and macroscopic scales, Eq. (3.7). Note that this distance is indeed much greater than the typical distance between chaotic spots (a power of $1/\tau$, $1/\rho$).

4.5. Various remarks

4.5.1. On the decay of correlations

Let us see how the difference between oscillators which belong to a chaotic spot and the rest of oscillators manifests itself in their dynamics. One can study the two-time correlator:

$$\tilde{A}_{nm}(t) = \lim_{t_0 \rightarrow \infty} \int_0^{t_0} \frac{dt'}{t_0} \psi_n(t' + t) \psi_n^*(t'), \quad (4.15)$$

or its Fourier transform, $A_{nm}(\omega)$, which can be called the spectral function. For uncoupled oscillators (at $\tau = 0$) the correlator simply oscillates as $\tilde{A}_{nn}(t) = I_n e^{-i(\omega_n + gI_n)t}$, without any decay, so $A_{nn}(\omega)$ is proportional to a δ -function.

For a chaotic spot residing on a resonant triple, the phase of each of its three oscillators is randomized on the time scale of the destroyed separatrix, $t_c \sim 1/\Omega$, which should give the time scale of decay of correlations (we neglect the small residual correlations found in Ref. [67] for the standard map). Let us now consider an oscillator which is far away from a chaotic spot. Its phase is randomized due to fluctuations of the action I_n , which translates into fluctuations of the frequency $\tilde{\omega}_n(I_n) = \omega_n + gI_n$. Namely,

$$\psi_n(t' + t) \psi_n^*(t') \propto \exp \left\{ -i \int_{t'}^{t'+t} [\omega_n + gI_n(t'') + g \delta I_n(t'')] dt'' \right\},$$

where $\delta I_n(t'') = I_n(t'') - I_n(t')$ is the random increment of the action. For the diffusive dynamics $\delta I_n(t'') \sim \sqrt{D_n |t'' - t'|}$, where D_n is the diffusion coefficient. The correlation is suppressed when the random part of the phase becomes ~ 1 , so it is natural to estimate the correlation time as $t_c \sim (g^2 D_n)^{-1/3}$. The diffusion coefficient is exponentially suppressed at least as τ^{2L} , where L is the distance to the nearest chaotic spot, so the correlation time is exponentially longer than the time $1/\Omega$ for the resonant triple.

However, it would be wrong to associate thus obtained t_c with the decay time of $\tilde{A}_{mn}(t)$ and $1/t_c$ with the width of the spectral peak in $A_{mn}(\omega)$. Indeed, the peak is supposed to be centered at the oscillator frequency; but as the latter depends on I_n , contributions from different times t' correspond to I_n 's differing on the thermal scale $T/|\mu|$, so the peak is smeared over $\sim gT/|\mu| = \rho\Delta$. This smearing is at least of the same order as $\Omega \sim \Delta \sqrt{\min\{\tau\rho, \rho^2\}}$. Thus, on the one hand, the spectrum of $A_{mn}(\omega)$ is broadened for all oscillators, and has no infinitely sharp δ -peaks, so the motion of all oscillators is chaotic. On the other hand, $A_{mn}(\omega)$ does not distinguish between oscillators belonging to chaotic spots and other oscillators.

To eliminate this ‘‘inhomogeneous broadening’’ effect, one can use the conditional average

$$\tilde{A}_{mn}(t|I) = \lim_{t_0 \rightarrow \infty} \frac{\int_0^{t_0} dt' \psi_n(t' + t) \psi_n^*(t') \delta(I_n(t') - I)}{\int_0^{t_0} dt' \delta(I_n(t') - I)}. \quad (4.16)$$

Then the main peak in $A_{mn}(\omega|I)$ would be positioned at $\omega = \omega_n + gI$, and broadened by $1/\Omega$ for oscillators belonging to resonant triples, or by an exponentially small value $(g^2 D_n)^{1/3}$ for other oscillators. Note that the spectrum $A_{mn}(\omega|I)$ also contains weak satellite peaks at different frequencies due to perturbative coupling to other oscillators.

Another way to eliminate the ‘‘inhomogeneous broadening’’ effect is to consider a four-time correlator,

$$\tilde{C}_{nnnn}(t) = \lim_{t_0 \rightarrow \infty} \int_0^{t_0} \frac{dt'}{t_0} \psi_n(t' + t) \psi_n^*(t') \psi_n^*(t') \psi_n(t' - t),$$

where the regular oscillation simply cancels out. For uncoupled oscillators this quantity is simply given by I_n^2 , while in the coupled system it decays on a time scale t_c which is

fast or slow for oscillators belonging or not to a chaotic spot, respectively, as discussed above. Accounting for the fact that a given oscillator can belong to a chaotic spot just for some intervals of time results in the correlator $\tilde{C}_{nmnn}(t)$ having both fast- and slow-decaying components with the corresponding weights.

4.5.2. On the thermalization of oscillators

Let us define thermalization of oscillators for a given trajectory of the system in the phase space $\{I_n(t), \phi_n(t)\}$. Let N oscillators n_1, \dots, n_N be called thermalized if the probability to find them in a given point of the phase space in the course of dynamics is given by the product of independent Gibbs distributions:

$$\lim_{\varepsilon \rightarrow 0} \lim_{t_0 \rightarrow \infty} \int_0^{t_0} \frac{dt}{t_0} \prod_{k=1}^N \delta_\varepsilon(I_{n_k}(t) - I_{n_k}) \delta_\varepsilon(\phi_{n_k}(t) - \phi_{n_k}) = \prod_{k=1}^N \frac{e^{-\beta(\omega_{n_k} - \mu)I_{n_k} - \beta g I_{n_k}^2 / 2}}{2\pi \int e^{-\beta(\omega_{n_k} - \mu)I - \beta g I^2 / 2} dI} + O(\tau). \quad (4.17)$$

Here δ_ε denotes the δ -function of a small but finite width ε .

Clearly, this must hold for oscillators which do not belong to a chaotic spot for most of the time, as their actions diffuse independently. However, this is not the case for oscillators which actually provide the main contribution to the chaotic fraction. Consider, for example, a resonant triple on the sites $n = 1, 2, 3$ at $\tau \ll \rho$. When it hosts a chaotic spot, the three actions stay close to the line $\omega_1 + gI_1 = \omega_2 + gI_2 = \omega_3 + gI_3$, so their joint probability distribution does not split into a product. Even though the chaotic spot eventually leaves the triple, and the three oscillators can diffuse independently for some time, the relative contribution of such “non-Gibbsian” time intervals to the integral in Eq. (4.17) may be significant.

Thus, the statement about thermalization of the chain is approximate. Namely, there is a small fraction of oscillators for which the Gibbs distribution is not valid. Nevertheless, it does not affect the conclusions of Sec. 3 and Appendix A. Indeed, when one calculates the total action and energy, their relative contribution is $\sim \min\{\tau\rho, \rho^2\}$, and thus is already beyond the precision of Eqs. (A.1a), (A.1b). Still, the situation is somewhat counter-intuitive: the “most chaotic” oscillators turn out to be the “least thermal”.

4.5.3. On the Kolmogorov-Arnold-Moser theorem

Thermalization of the oscillator chain for general initial conditions, discussed above, seems to contradict the Kolmogorov-Arnold-Moser (KAM) theorem [68, 69, 70]. According to the theorem, as the strength of the integrability-breaking perturbation $\tau \rightarrow 0$, the fraction of the chaotic part of the phase space must vanish. At sufficiently small τ most of the phase space must be occupied by the invariant tori, where no thermalization is possible, while here thermalization is argued to be the case for general initial conditions. There is, however, an essential difference between systems with finite and infinite number of degrees of freedom.

As discussed in the previous subsections, the typical spatial density of the chaotic spots is $\bar{w} \sim \min\{\tau\rho, \rho^2\}$. This means that the probability for a chain of length L to contain no chaotic spots at all, is given by $e^{-\bar{w}L}$. This is just the fraction of the total phase volume, occupied by the KAM tori. Even though it goes to unity as $\tau \rightarrow 0$ or $g \rightarrow 0$ for any fixed L , if one lets $L \rightarrow \infty$ first, it vanishes. Equivalently, even though one can prepare the initial conditions such that the chaotic dynamics is absent, they form a set of zero measure.

Infinite number of degrees of freedom by itself is not sufficient to destroy the regular regions of the phase space. There are two more conditions: (i) disorder and (ii) extensive norm, and both are crucial. Indeed, early studies on one-dimensional systems of interacting particles have shown that even though the proportion of the regular regions tended to decrease as the number of particles N increased [71], it remained finite even at $N \rightarrow \infty$ as energy per particle was kept finite, provided that interactions were sufficiently short-ranged [72, 73]. At the same time, for disordered systems invariant tori have been shown to exist [5, 74, 37], but they corresponded to a finite norm.

One can view the collective effect of the infinite length, randomness, and extensive norm in the following way. Let us consider finite segments of N neighboring oscillators: $n = n_0 + 1, \dots, n_0 + N$. Then, by simply varying n_0 one will always find a combination of frequencies $\omega_{n_0+1}, \dots, \omega_{n_0+N}$, arbitrarily close to some given one, and the norm density on that segment will not be vanishingly small (i. e., bounded from below with a bound independent of n_0).

4.5.4. On the effects of quantization

The most essential element of the picture developed in this work is the chaotic spot – a collection of a *finite* number of oscillators, whose frequency spectrum has a continuous component. Because of its the continuous spectrum, the chaotic spot can redistribute arbitrarily large amounts of energy between the oscillators (limited only by the total amount of the system’s energy, which is infinite for the infinite chain), given enough time. In quantum mechanics, the energy spectrum of a system of any finite number of oscillators is always discrete, so the amount of energy which oscillators can exchange is finite even for infinite time. In such a system, irreversibility can arise only when the system has a possibility to visit an infinite number of discrete quantum states in an infinite sequence of tunneling events. A necessary (but not sufficient) condition for this is that the coupling between different states should be strong enough as compared to the energy mismatch between these states (this mismatch is always finite when the levels are discrete). The appropriate physical picture is that of Anderson localization-delocalization transition [1]. However, now it should be considered not in the one-dimensional space of the chain, but in the space of excitations of the many-oscillator system.

The quantum version of Arnold diffusion for a few oscillators was considered in Refs. [75, 76]. The minimal number of oscillators giving the Arnold diffusion in each

model was taken, so the quantum system was effectively one-dimensional (moreover, of a finite length, since the number of oscillators was finite). Since in one-dimensional quantum problems with disorder all eigenstates are inevitably localized, the conclusion was that Arnold diffusion in a quantum system is always stopped by Anderson localization after a sufficiently long time.

In the present problem the Arnold diffusion occurs in a system with many degrees of freedom, so one may expect the effective dimensionality of the quantum localization problem to be very high. In this situation, Anderson transition can take place. The control parameter for this transition would be the measure of “quantumness” of the system, i. e. the Plank constant \hbar (of course, the measure of “quantumness” can also be expressed in terms of the physical parameters of the system at fixed \hbar , as discussed below). Namely, for \hbar not small enough thermalization and transport in the system can be completely blocked by Anderson localization. This transition would then be of the same nature as the many-body localization transition in a one-dimensional system of interacting bosons subject to disorder [77].

Indeed, quantization of the Hamiltonian (2.3) corresponds to replacing the canonical variables $\psi_n, i\psi_n^*$ by operators $\hat{\psi}_n, i\hat{\psi}_n^\dagger$ with the standard commutation relation, $[\hat{\psi}_n, i\hat{\psi}_n^\dagger] = i\hbar$. The resulting quantum Hamiltonian corresponds to the disordered Bose-Hubbard model. This model describes quantum bosonic particles, which interact with each other via contact potential, and whose motion is confined to an array of potential wells coupled by tunnelling. Then $\hat{\psi}_n^\dagger/\sqrt{\hbar}$ and $\hat{\psi}_n/\sqrt{\hbar}$ are creation and annihilation operators for the particle in the n th potential well, $\hbar\omega_n$ is the energy of the bound state in the n th well, $\hbar\tau\Delta$ is the tunnelling matrix element between bound states in the neighboring wells, and \hbar^2g corresponds to the Hubbard U , the interaction energy between two particles occupying the same potential well. The classical limit, formally corresponding to $\hbar \rightarrow 0$, can be also expressed in terms of physical quantities. If one starts from the Bose-Hubbard model with a given disorder energy bandwidth W (corresponding to $\hbar\Delta$) at a temperature T , the classical limit at fixed W corresponds to $T/W \rightarrow \infty$, $U/W \rightarrow 0$, $UT/W^2 = \text{const} \ll 1$.

The quantum bosonic system considered in Ref. [77] corresponded to the continuum limit of the Bose-Hubbard model: the lattice spacing $a \rightarrow 0$, the site number $|n| \rightarrow \infty$, maintaining $x = na = \text{const}$, and also $\tau \rightarrow \infty$, while keeping $\tau a^2 = \text{const}$. Thus, no direct correspondence between the systems studied in present work and that of Ref. [77] can be established.

4.5.5. On the Mott’s law for variable-range hopping

Taking the typical value, λ_L^{typ} , from Eq. (4.9), and maximizing $\tau^L e^{-(1+C_2)\lambda_L^{\text{typ}}}$ with respect to L gives the optimal distance for the hopping of the chaotic spot $L_{VRH} \sim \ln^2(1/\tau^p \rho)/\ln(1/\tau)$, and the variable-range-hopping (VRH) estimate for σ in the spirit of Mott [52]. This estimate is not supposed to be valid in one dimension because of rare breaks [53]. In our case, however, the only difference of this estimate from expres-

sion (3.6a) is in the factor C' , while the main functional form is the same (which still means that the resistance of a break is much greater than that of a long segment between breaks). This is due to the dramatic suppression (double exponential) of the probability $p(\lambda)$, Eq. (4.8), at very large λ , which makes too strong breaks very improbable (in the standard Mott's picture λ has a uniform distribution, corresponding to a constant density of states).

It may also seem surprising that the picture of hopping transport, which usually gives the temperature dependence in the form of a stretched exponential ($e^{-1/T^{d+1}}$ in the dimensionality $d > 1$ [52] and $e^{-1/T}$ in $d = 1$ [53]), translates here into $e^{-\ln^3(1/T)}$. The reason for this is that the hopping object, the chaotic spot, can be viewed as having many internal degrees of freedom. Indeed, on every site optimization is performed over a large number of available guiding resonances to minimize the frequency mismatch. As a result, the usual stretched exponential is stretched so much in this case, that its argument is logarithmic rather than power-law. This large number of internal degrees of freedom is also the reason for the strong suppression of $p(\lambda)$ at very large λ .

4.5.6. On the smallness of small parameters

As mentioned in Sec. 3, the results of the numerical integration of Eq. (2.1) [7, 9, 15, 16, 20, 21, 32, 33, 35] correspond to much faster dynamics than predicted in the present work. Moreover, the observed behavior could be understood assuming that upon thermalization of the expanding cloud, the chaos uniformly spreads over all oscillators of the cloud [21]. Again, this is quite different from the picture of rare chaotic spots. The average density of the chaotic spots was estimated in the present work as $\bar{w} \sim \min\{\tau\rho, \rho^2\}$, and the numerical coefficient was not obtained. Thus, the chaotic spot picture should be valid when τ and ρ are *sufficiently* small. The smallest values of τ and ρ , for which the direct numerical integration of Eq. (2.1) produced reliable results on the packet spreading, are $\tau = 1/40$ and ρ about 1 [78]. So the question arises, starting from which values of τ and ρ will the chaotic spot picture really work?

One of the main physical assumptions used in the present work is that most of the normal modes of the linear problem are localized on one site of the lattice. Numerical studies of the linear part of Eq. (2.1) have shown that at $\tau = 1$ the localization length is about 100, and it becomes ~ 1 only at $\tau \approx 0.1$ [79, 80]. This means that the disorder can be considered strong only for $\tau < 0.1$ at most.

In Ref. [36], chains of finite length L were considered, and the probability for the chain to be in the regular KAM regime was analyzed numerically. At low densities, this probability was found to scale as $\exp[-10^6(2\rho)^{9/4}(2\tau)^{35/16}(L/16)]$. In the present work, it is interpreted as the probability to have no chaotic spots on the segment, $e^{-\bar{w}L}$, as discussed in Sec. 4.5.3. Thus, the results of Ref. [36] approximately correspond to $\bar{w} \approx 10^6\tau^2\rho^2$. Apart from the difference from both $\bar{w} \propto \tau\rho$ and $\bar{w} \propto \rho^2$, obtained in the present work (the reasons for this discrepancy are unclear at the moment, so this issue deserves to be studied in the future), one should note the presence of the large

numerical coefficient 10^6 . This means that for the chaotic spots to be rare very small values $\tau\rho < 10^{-3}$ are needed.

These observations suggest that the transport regime, described in the present work, should set in at very small values of τ and ρ , which probably have not been accessed in the numerical works up to the present date.

5. Resonant triples

This section represents a detailed analysis of chaos in a system of three oscillators whose frequencies happen to be close to each other. Although such resonant triples do not contribute to the main result for the conductivity, Eq. (3.6a), they have the thickest stochastic layers. Estimation of their chaotic phase volume is the main task of the present section.

First, we discuss a resonant pair of oscillators where chaos is generated by an external perturbation, which can be studied by the standard methods [54, 55, 59]. Next, the closed system of three oscillators is considered, for which no analytical solution is available. Still, an estimate for the chaotic phase volume can be obtained by analyzing various limiting cases and using the results for a perturbed resonant pair.

The results of this section are relevant in the limit $\tau \ll \rho$. The opposite limiting case, $\tau \gg \rho$, requires analysis of high orders of perturbation theory, and will be discussed in Sec. 6.7.

5.1. Two oscillators: separatrix

The Hamiltonian of two oscillators has the form

$$H = \omega_1 I_1 + \frac{g}{2} I_1^2 + \omega_2 I_2 + \frac{g}{2} I_2^2 - 2\tau\Delta \sqrt{I_1 I_2} \cos(\phi_1 - \phi_2). \quad (5.1)$$

Let us perform a canonical change of variables:

$$\check{\phi} = \phi_1 - \phi_2, \quad \check{I} = \frac{I_1 - I_2}{2}, \quad \phi = \frac{\phi_1 + \phi_2}{2}, \quad I = I_1 + I_2, \quad (5.2a)$$

$$H = \frac{\omega_1 + \omega_2}{2} I + \frac{g}{4} I^2 + (\omega_1 - \omega_2)\check{I} + g\check{I}^2 - 2\tau\Delta \sqrt{I^2/4 - \check{I}^2} \cos \check{\phi}. \quad (5.2b)$$

The total action I is conserved, so only $\check{I}, \check{\phi}$ have a non-trivial dynamics:

$$\frac{d\check{\phi}}{dt} = \frac{\partial H}{\partial \check{I}} = \omega_1 - \omega_2 + 2g\check{I} + 2\tau\Delta \frac{\check{I} \cos \check{\phi}}{\sqrt{I^2/4 - \check{I}^2}}, \quad (5.3a)$$

$$\frac{d\check{I}}{dt} = -\frac{\partial H}{\partial \check{\phi}} = -2\tau\Delta \sqrt{I^2/4 - \check{I}^2} \sin \check{\phi}. \quad (5.3b)$$

A separatrix in the phase space $(\check{I}, \check{\phi})$ appears when these dynamical equations have a hyperbolic stationary point.

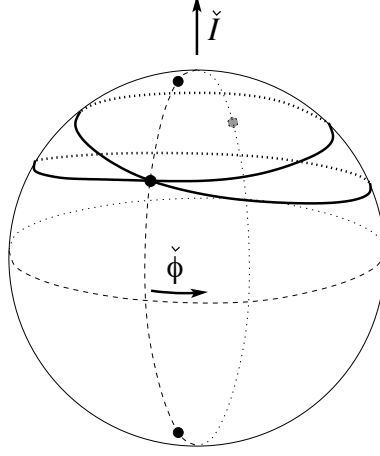


Figure 2: A schematic view of the $(\check{I}, \check{\phi})$ phase space, represented by the sphere. The circles $\check{\Theta} = \pi/2$, $0 \leq \check{\phi} < 2\pi$ (“equator”) and $\check{\phi} = 0, \pi$, $0 \leq \check{\Theta} \leq \pi$ (“Greenwich meridian”) are shown by dashed lines. The thick solid line represents the separatrix. The stationary points (one hyperbolic, at the separatrix self-crossing, and three elliptic) are shown by dark points.

To find the stationary points, we make a change of variables $\check{I} = (I/2) \cos \check{\Theta}$, $0 \leq \check{\Theta} \leq \pi$, thereby mapping the phase space onto a sphere (Fig. 2). From Eq. (5.3b) it is seen that the stationary points require $\check{\phi} = 0$ or π . It is convenient to fix $\check{\phi} = 0$, and extend $0 \leq \check{\Theta} < 2\pi$, parametrizing the circle by $\check{\Theta}$ only. Then we obtain an equation for stationary points:

$$\frac{\omega_1 - \omega_2}{2\Delta} \sin \check{\Theta} + \tau \cos \check{\Theta} + \frac{gI}{4\Delta} \sin 2\check{\Theta} = 0. \quad (5.4)$$

It has four solutions if and only if

$$|2\tau\Delta|^{2/3} + |\omega_1 - \omega_2|^{2/3} \leq (gI)^{2/3}. \quad (5.5)$$

Otherwise, it has two solutions. To see this, we introduce

$$r = 2 \sqrt{\frac{(\omega_1 - \omega_2)^2 + (2\tau\Delta)^2}{(gI)^2}}, \quad \Theta_0 = \arctan \frac{\omega_1 - \omega_2}{2\tau\Delta}, \quad (5.6)$$

so Eq. (5.4) becomes $\sin 2\check{\Theta} + r \cos(\check{\Theta} - \Theta_0) = 0$. At the borderline, it has three solutions, one of which is degenerate. Equating to zero $\sin 2\check{\Theta} + r \cos(\check{\Theta} - \Theta_0)$ together with its derivative, we obtain

$$r^2 = 1 + 3 \cos^2 2\check{\Theta} = 4 \frac{1 + \tan^6 \check{\Theta}}{(1 + \tan^2 \check{\Theta})^3}, \quad \tan(\check{\Theta} - \Theta_0) = -2 \cot 2\check{\Theta}.$$

From the second equation we obtain $\tan \check{\Theta} = (\cot \Theta_0)^{1/3}$. Substituting it into the first equation, we obtain Eq. (5.5).

Thus, for the separatrix to exist, it is absolutely necessary to have $2\tau\Delta < gI$. This is the reason for making the assumption $\tau \ll \rho$, as the typical value of $I \sim gT/|\mu|$. Given $\tau\Delta \ll gI$, the condition (5.5) can be taken in zero approximation, $|\omega_1 - \omega_2| < gI$. This is simply the condition for existence of $I_1, I_2 > 0$ satisfying $\omega_1 + gI_1 = \omega_2 + gI_2$, see Eq. (4.2). Also, at $\tau \ll gI$ the separatrix is concentrated in a narrow region of \check{I} around the resonant value $\check{I} = (\omega_2 - \omega_1)/(2g)$, so in the last term of Hamiltonian (5.2b) one can simply set $\check{I} = (\omega_2 - \omega_1)/(2g)$. Then the Hamiltonian becomes equivalent to that of a pendulum,

$$H = \frac{\omega_1 + \omega_2}{2} I + \frac{g}{4} I^2 - \frac{(\omega_1 - \omega_2)^2}{4g} + g \left(\check{I} - \frac{\omega_2 - \omega_1}{2g} \right)^2 - \frac{\Omega^2 \operatorname{sgn} \tau}{2g} \cos \check{\phi}, \quad (5.7)$$

and the pendulum frequency is given by

$$\Omega^2 = 2|\tau|\Delta \sqrt{(gI)^2 - (\omega_1 - \omega_2)^2}. \quad (5.8)$$

5.2. Two oscillators: stochastic layer

Suppose now that a time-dependent perturbation is added to the Hamiltonian (5.1):

$$H' = 2V(I_1, I_2) \cos(m_1\phi_1 + m_2\phi_2 - \omega t) \quad (5.9)$$

The frequency ω is a linear combination of frequencies of other oscillators. Their motion is taken in zero approximation, so effectively they exert an external time-dependent force on the resonant pair. This force produces a stochastic layer around the separatrix, as is discussed in detail in Refs. [54, 55, 59].

Perturbation (5.9) leads to a change in the old integrals of motion, I and H ,

$$\frac{dI}{dt} = -\frac{\partial H'}{\partial \phi}, \quad (5.10a)$$

$$\frac{dH}{dt} = -\frac{\partial H}{\partial I} \frac{\partial H'}{\partial \phi} - \frac{\partial H}{\partial \check{I}} \frac{\partial H'}{\partial \check{\phi}} + \frac{\partial H}{\partial \check{\phi}} \frac{\partial H'}{\partial \check{I}}. \quad (5.10b)$$

Out of the three terms on the right-hand side of Eq. (5.10b), the first one is essentially the repetition of Eq. (5.10a), while in the third term $\partial H/\partial \check{\phi} = O(\tau)$, so it can be neglected. Being interested in the perturbation of the pendulum motion in the vicinity of the separatrix, one can take the values of I_1, I_2 at the point of resonance, the unperturbed dependence of $\phi = (\partial H/\partial I)t$, and $\check{\phi}(t)$ right on the separatrix:

$$V(I_1, I_2) \rightarrow V\left(\frac{I}{2} + \frac{\omega_2 - \omega_1}{2g}, \frac{I}{2} - \frac{\omega_2 - \omega_1}{2g}\right), \quad (5.11a)$$

$$\phi(t) \rightarrow \frac{\omega_1 + \omega_2 + gI}{2} t, \quad (5.11b)$$

$$\check{\phi}(t) \rightarrow \pm \left[4 \arctan e^{\Omega(t-t_0)} - \pi \right]. \quad (5.11c)$$

The two signs of $\check{\phi}(t)$ correspond to the two branches of the separatrix (Fig. 2). The changes in I and H during one passage of the separatrix are given by

$$\begin{aligned}\delta I &= 2(m_1 + m_2)V \int_{-\infty}^{\infty} \sin \left[\frac{m_1 - m_2}{2} \check{\phi}(t) - \Lambda \Omega t \right] dt = \\ &= -\frac{2V}{\Omega} (m_1 + m_2) \mathcal{A}_{\pm(m_1 - m_2)}(\Lambda) \sin(\Lambda \Omega t_0),\end{aligned}\quad (5.12a)$$

$$\begin{aligned}\delta H &= \frac{\partial H}{\partial I} \delta I + (m_1 - m_2)V \int_{-\infty}^{\infty} \frac{d\check{\phi}(t)}{dt} \sin \left[\frac{m_1 - m_2}{2} \check{\phi}(t) - \Lambda \Omega t \right] dt = \\ &= -\frac{2V\omega}{\Omega} \mathcal{A}_{\pm(m_1 - m_2)}(\Lambda) \sin(\Lambda \Omega t_0),\end{aligned}\quad (5.12b)$$

where the Melnikov-Arnold integral $\mathcal{A}_m(\Lambda)$ is defined as

$$\begin{aligned}\mathcal{A}_m(\Lambda) &\equiv \int_{-\infty}^{\infty} \exp \left[\frac{im}{2} (4 \arctan e^s - \pi) \right] e^{-i\Lambda s} ds, \\ \Lambda &\equiv \frac{\omega - (m_1 + m_2)(\omega_1 + \omega_2 + gI)/2}{\Omega}.\end{aligned}\quad (5.13)$$

Since $\mathcal{A}_{-m}(\Lambda) = \mathcal{A}_m(-\Lambda)$, and $\mathcal{A}_{m>0}(\Lambda < 0) = (-1)^m \mathcal{A}_m(|\Lambda|) e^{-\pi|\Lambda|}$, for $|\Lambda| \gg 1$ and for a given perturbation (5.9), one of the branches of the separatrix is much more efficient than the other one. If we fix $\tau > 0$, $m_1 - m_2 > 0$, and $\Lambda > 0$ for definiteness, the main contribution comes from the upper branch of the separatrix, shown in Fig. 3. At $\Lambda \gg m$ the Melnikov-Arnold integral is exponentially suppressed,

$$\mathcal{A}_{m>0}(\Lambda \gg m) \approx 4\pi \frac{(2\Lambda)^{m-1}}{\Gamma(m)} e^{-\pi\Lambda/2},\quad (5.14)$$

where $\Gamma(m)$ is the Euler's gamma function.

Let us represent the pendulum Hamiltonian [the last two terms of Eq. (5.7)] as $(\Omega^2/2g)(h + 1)$, where h is the dimensionless energy of the pendulum, counted from the separatrix. Then h measures the distance of a trajectory from the separatrix. Denoting

$$h_s \equiv \frac{4gV}{\Omega^2} \Lambda^2 \mathcal{A}_{m_1 - m_2}(\Lambda), \quad \theta \equiv \Lambda \Omega t_0,\quad (5.15)$$

and using Eqs. (5.12a), (5.12b), we write the change in h upon passing the upper branch of the separatrix as

$$h \mapsto h + \frac{h_s}{\Lambda} \sin \theta,\quad (5.16a)$$

For trajectories close to separatrix, $|h| \ll 1$, the time spent in the vicinity of the hyperbolic point diverges as $(1/\Omega) \ln(32/|h|)$. This gives the value of the phase θ for the next

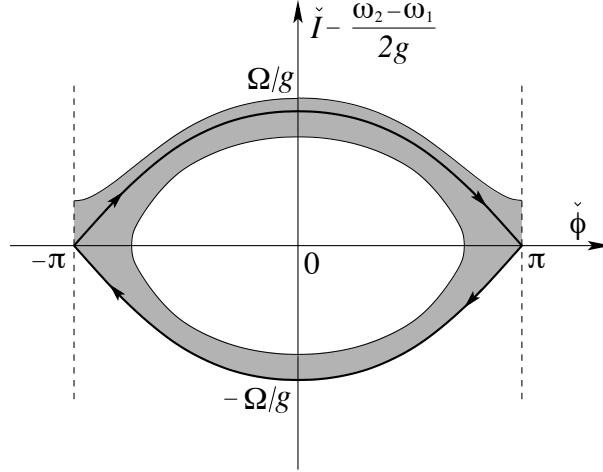


Figure 3: Stochastic layer around the separatrix in the $(\check{I}, \check{\phi})$ phase space, as shown by the shaded area ($\tau > 0$, $m_1 - m_2 > 0$, and $\Lambda > 0$ are assumed).

passage of the separatrix:

$$\theta \mapsto \theta + (2)\Lambda \ln \frac{32}{|h|}. \quad (5.16b)$$

The factor of 2 should be taken for trajectories inside the separatrix (pendulum oscillations), since the hyperbolic point is passed twice before the system returns to the upper branch. For trajectories just above the upper branch (pendulum rotations) there is no factor of 2. Trajectories below the lower branch are excluded from consideration since they never get to the upper branch. Eqs. (5.16a), (5.16b) define a mapping which is often called separatrix or whisker mapping. If the mapping is iterated starting with a sufficiently small value of h , the phase θ tends to randomize. For $|\Lambda \gg 1|$ the mapping can be linearized in h around one of the resonant values h_n by introducing a new variable z :

$$z = (2)\Lambda \frac{h - h_n}{h_n}, \quad h_n = 32 \exp \left[\frac{2\pi n}{(2)\Lambda} \right]. \quad (5.17)$$

The separatrix mapping then reduces to the so-called standard mapping, also called Chirikov-Taylor mapping:

$$z \mapsto z + K \sin \theta, \quad \theta \mapsto \theta - z, \quad (5.18)$$

where the stochasticity parameter is defined as $K(h_n) = (2)h_s/h_n$. As discussed in Refs. [54, 55, 59], the standard mapping becomes chaotic when $K > K_c$. Numerically, K_c is very close to 1, and we neglect $K_c - 1$ in what follows. This determines the stochastic region for the separatrix mapping (5.16a)–(5.16b) as $|h| < (2)h_s$. Using this

result, one can calculate the total phase volume of the stochastic layer (the shaded area in Fig. 3):

$$W_s \equiv \int_{\text{layer}} \frac{d\check{I} d\check{\phi}}{2\pi} = \frac{\Omega}{2\pi g} \left(2h_s \ln \frac{32e}{2h_s} + \frac{h_s}{2} \ln \frac{32e}{h_s} \right). \quad (5.19)$$

For $|\Lambda| \gg 1$ the change in h upon one iteration is much smaller than the layer width, so the dynamics of h is diffusive. If the phases at successive iterations are assumed uncorrelated, the average square of displacement in h after N iterations is $(N/2)(h_s/\Lambda)^2$. It takes the time $N\delta t$, where $\delta t = (2)\Omega^{-1} \ln(32/(2)h)$ is the time step, which gives the following estimate for the diffusion coefficient in h :

$$D_h(h) = \frac{\Omega}{2} \frac{h_s^2}{\Lambda^2} \left[(2) \ln \frac{32}{(2)h} \right]^{-1}. \quad (5.20)$$

In fact, the assumption of completely random phases is never fully correct. For the standard mapping, Eq. (5.18), even at relatively large $K \sim 10-20$ small residual correlations of the phase (at the level of $10^{-3} - 10^{-4}$) have been found [67]. These residual correlations are usually explained by the system sticking to various structures inside the chaotic region, such as stability islands where the diffusion is anomalously slow, or accelerator modes, where the diffusion is anomalously fast. Still, in spite of the residual correlations, the diffusion coefficient in z for the standard mapping for $K > 2$ was found in Ref. [67] to agree quite well with its random-phase value $K^2/2$ together with the leading in $1/\sqrt{K}$ correction [81]; the largest relative deviations from $K^2/2$ were less than 100% and occurred for special values of K corresponding to accelerator modes. The accelerator modes should be much less important for the separatrix mapping than for the standard mapping; indeed, since $K = K(h)$, the fast diffusion in h will quickly move the system away from the special values of K .

The random phase assumption is completely wrong close to the stochastic layer boundary. Indeed, the system cannot leave the stochastic layer and end up on a stable periodic orbit, so the diffusion coefficient must vanish at the boundary. According to numerics, it vanishes as a power law, $D_h(h) \propto ((2)h_s - |h|)^{2.55\dots}$ [54]. As will be seen later (see Eq. (8.28a) and Appendix F), what will matter for the present problem is a certain average of the diffusion coefficient over the stochastic layer, so we estimate the relative error of Eq. (5.20) to be ~ 1 , which is beyond the accuracy of our final result, Eq. (3.6a).

As the perturbation causes changes in I , the latter also undergoes diffusion. However, Eqs. (5.12a), (5.12b), rigidly relate the change in I to the change in h on each step:

$$\delta I = \frac{(m_1 + m_2)\Omega}{2g\Lambda} \delta h, \quad (5.21)$$

so, as h is limited to a thin stochastic layer, a single perturbation term (5.9) cannot produce a large excursion in I .

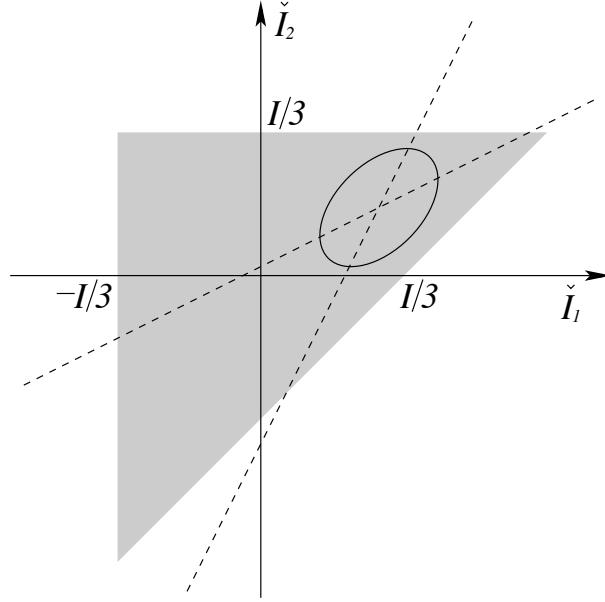


Figure 4: The allowed region of \check{I}_1, \check{I}_2 , shown by the shaded area. The resonance manifolds defined by Eqs. (5.24a), (5.24b) are shown by dashed lines. The ellipse represents a constant-energy surface.

5.3. Three oscillators: resonances

The Hamiltonian of the triple is given by

$$H = \sum_{n=1}^3 \left[\omega_n I_n + \frac{g}{2} I_n^2 \right] - 2\tau\Delta \sum_{n=1}^2 \sqrt{I_n I_{n+1}} \cos(\phi_n - \phi_{n+1}). \quad (5.22)$$

We perform the following canonical change of variables:

$$\phi = \frac{\phi_1 + \phi_2 + \phi_3}{3}, \quad \check{\phi}_1 = \phi_1 - \phi_2, \quad \check{\phi}_2 = \phi_2 - \phi_3, \quad (5.23a)$$

$$I = I_1 + I_2 + I_3, \quad \check{I}_1 = \frac{2I_1 - I_2 - I_3}{3}, \quad \check{I}_2 = \frac{I_1 + I_2 - 2I_3}{3}, \quad (5.23b)$$

$$\begin{aligned} H = & \frac{\omega_1 + \omega_2 + \omega_3}{3} I + \frac{gI^2}{6} + \\ & + (\omega_1 - \omega_2)\check{I}_1 + g\check{I}_1^2 + (\omega_2 - \omega_3)\check{I}_2 + g\check{I}_2^2 - g\check{I}_1\check{I}_2 - \\ & - 2\tau\Delta \sqrt{I_1 I_2} \cos \check{\phi}_1 - 2\tau\Delta \sqrt{I_2 I_3} \cos \check{\phi}_2. \end{aligned} \quad (5.23c)$$

The allowed region of \check{I}_1, \check{I}_2 , determined by the conditions $I_1, I_2, I_3 > 0$, is a triangle $-1/3 < \check{I}_1 < 2I/3, \check{I}_1 - I/3 < \check{I}_2 < I/3$, shown in Fig. 4.

We consider two possibilities for the guiding resonance: either $\omega_1 + gI_1 = \omega_2 + gI_2$ or $\omega_2 + gI_2 = \omega_3 + gI_3$. The resonance between the oscillators 1 and 3 has the effective coupling $\sim \tau^2$, so its stochastic layer is negligibly thin. The resonance conditions are

$$\frac{d\check{\phi}_1}{dt} = 0 \Rightarrow \check{I}_2 - 2\check{I}_1 = \frac{\omega_1 - \omega_2}{g}, \quad (5.24a)$$

$$\frac{d\check{\phi}_2}{dt} = 0 \Rightarrow \check{I}_1 - 2\check{I}_2 = \frac{\omega_2 - \omega_3}{g}. \quad (5.24b)$$

They intersect at the point

$$\check{I}_{1r} = \frac{-2\omega_1 + \omega_2 + \omega_3}{3g}, \quad \check{I}_{2r} = \frac{-\omega_1 - \omega_2 + 2\omega_3}{3g}. \quad (5.25)$$

This point lies inside the allowed triangle if $gI > 2\omega_i - \omega_j - \omega_k$ for any $\{i, j, k\}$ being a permutation of $\{1, 2, 3\}$, or, equivalently,

$$gI > 3 \max_{1 \leq n \leq 3} \{\omega_n\} - \sum_{n=1}^3 \omega_n \equiv gI_{min}. \quad (5.26)$$

The importance of the intersection point can be seen by considering the result of the previous subsection for the 1-2 resonance, where the separatrix-destroying perturbation comes from the coupling to the third oscillator. Let us set $m_1 = 0, m_2 = 1, \omega = \omega_3 + gI_3, V = -\tau\Delta\sqrt{I_2I_3}$ in Eq. (5.9), and take the large- Λ asymptotics (5.14) of the Melnikov-Arnold integral appearing in Eq. (5.15) for h_s , which, in turn, enters Eq. (5.19). This gives the following estimate for the I_3 -dependent volume of the stochastic layer around the 1-2 separatrix (numerical and logarithmic factors are omitted):

$$W_s^{(12)} \sim \frac{\Delta}{\Omega} \sqrt{I_2I_3} \tau \Lambda^2 e^{-\pi\Lambda/2}, \quad \Lambda = \frac{|\omega_2 - \omega_3 + g(I_2 - I_3)|}{\Omega}. \quad (5.27)$$

If we now integrate $W_s^{(12)}$ over I_3 to find the total volume of the stochastic region in the space (I_1, I_2, I_3) , the exponential factor will ensure that the integral is dominated by values of I_3 close to the resonance intersection point.

5.4. Three oscillators: chaotic phase space

Let us expand the Hamiltonian, Eq. (5.23c), around the resonance intersection point, Eq. (5.25), writing $\check{I}_{1,2} = \check{I}_{1,2}^r + p_{1,2}$:

$$\begin{aligned} H &= H_r(I) + \check{H}(p_1, p_2; \check{\phi}_1, \check{\phi}_2) = \\ &= -\frac{(\omega_1 - \omega_2)^2 + (\omega_2 - \omega_3)^2 + (\omega_1 - \omega_3)^2}{6g} + \frac{\omega_1 + \omega_2 + \omega_3}{3} I + \frac{gI^2}{6} + \\ &\quad + gp_1^2 - gp_1p_2 + gp_2^2 - 2V_1 \cos \check{\phi}_1 - 2V_2 \cos \check{\phi}_2. \end{aligned} \quad (5.28)$$

Taking $V_{1,2}$ at the intersection point is allowed when the resonance intersection point $(\check{I}_1^r, \check{I}_2^r)$ is not too close to the sides of the allowed triangle in the $(\check{I}_1, \check{I}_2)$ plane. This is possible when $gI \gg \tau\Delta$.

The main task of the present section is to estimate the fraction of the total (thermally weighted) phase volume, occupied by the chaotic part:

$$w = \frac{\int_{\text{chaotic}} e^{-(H-\mu I)/T} \prod_{n=1}^3 dI_n d\phi_n / (2\pi)}{\int e^{-(H-\mu I)/T} \prod_{n=1}^3 dI_n d\phi_n / (2\pi)}. \quad (5.29)$$

At $gT/|\mu| \ll \Delta \ll |\mu|$, the denominator can be simply taken to be $(T/|\mu|)^3$. Inside the allowed triangle the typical value of $\check{H} \sim gI^2 \ll T$, so its contribution to the thermal weight can be neglected. Then the calculation of w can be done in two steps:

$$W_{ss}(I) = \int_{\text{chaotic}} \frac{d\check{I}_1 d\check{\phi}_1}{2\pi} \frac{d\check{I}_2 d\check{\phi}_2}{2\pi}, \quad (5.30a)$$

$$w = \left(\frac{|\mu|}{T}\right)^3 \int_0^\infty e^{-[H_r(I)-\mu I]/T} W_{ss}(I) dI. \quad (5.30b)$$

Not being able to calculate $W_{ss}(I)$ at arbitrary V_1, V_2 , we first consider the case when one of the couplings is much stronger than the other (e. g., $V_1 \gg V_2$), and then extrapolate to $V_1 \sim V_2$. At $V_2 = 0$ we write \check{H} as

$$\check{H}|_{V_2=0} = g \left(p_1 - \frac{p_2}{2} \right)^2 - 2V_1 \cos \check{\phi}_1 + \frac{3}{4} g p_2^2 \equiv \check{H}_1 + \frac{3}{4} g p_2^2, \quad (5.31)$$

and find the separatrix solution for $\check{\phi}_1$, as in Sec. 5.2:

$$\check{\phi}_1(t) = \pm \left[4 \arctan e^{\Omega_1(t-t_0)} - \pi \right], \quad \check{\phi}_2(t) = -\frac{\check{\phi}_1(t)}{2} + \frac{3}{2} g p_2 t, \quad \Omega_1 = \sqrt{4gV_1}. \quad (5.32)$$

Again, we calculate the changes in the action p_2 and the pendulum energy \check{H}_1 :

$$\delta p_2 = - \int 2V_2 \sin \check{\phi}_2(t) dt = -\frac{V_2}{\sqrt{gV_1}} \mathcal{A}_{\pm 1} \left(\frac{3gp_2}{4\sqrt{gV_1}} \right) \sin \frac{3gp_2 t_0}{4\sqrt{gV_1}}, \quad (5.33a)$$

$$\delta \check{H}_1 = - \int \frac{\partial \check{H}_1}{\partial p_2} 2V_2 \sin \check{\phi}_2(t) dt = \frac{3gp_2 V_2}{2\sqrt{gV_1}} \mathcal{A}_{\pm 1} \left(\frac{3gp_2}{4\sqrt{gV_1}} \right) \sin \frac{3gp_2 t_0}{4\sqrt{gV_1}}, \quad (5.33b)$$

where $\mathcal{A}_{\pm 1}(\Lambda) = \pm 2\pi e^{\pm \pi \Lambda / 2} / \sinh(\pi \Lambda)$.

Again, one arrives at the separatrix mapping, analogous to Eqs. (5.16a)–(5.16b). The main contribution to the stochastic phase volume comes from $g|p_2| \sim \sqrt{gV_1}$, i. e. $|\Lambda| \sim 1$. This is still much larger than the inverse time of the passage of the separatrix due to the

logarithmic factor, so the phase is randomized after a few iterations. However, at $|\Lambda| \sim 1$ the change in the Hamiltonian per iteration is not small compared to the stochastic layer width, so the standard approach for determining the layer width (linearization of Eq. (5.16a) around some value of h and reduction to the standard mapping) does not apply in this case. The diffusive picture for the motion across the stochastic layer is not valid either. Also, for the pendulum rotation, $\check{H}_1 > 2V_1$, the contribution $\propto e^{-3\pi|\Lambda|/2}$ from the “inefficient” rotation direction should also be kept. Thus, the stochastic layer is determined by the inequalities

$$-4V_2\Lambda^2\tilde{\mathcal{A}}_o(\Lambda) < \check{H}_1 - 2V_1 < 2V_2\Lambda^2\tilde{\mathcal{A}}_{\pm}(\Lambda), \quad (5.34)$$

where $\tilde{\mathcal{A}}_{o,\pm}(\Lambda)$ are some functions, analogous to Melnikov-Arnold integral (5.13), about which we only know that

$$\tilde{\mathcal{A}}_o(-\Lambda) = \tilde{\mathcal{A}}_o(\Lambda), \quad \tilde{\mathcal{A}}_{\pm}(-\Lambda) = \tilde{\mathcal{A}}_{\mp}(\Lambda), \quad (5.35a)$$

$$|\Lambda| \sim 1 : \quad \tilde{\mathcal{A}}_{o,\pm}(\Lambda) \sim 1, \quad (5.35b)$$

$$|\Lambda| \gg 1 : \quad \tilde{\mathcal{A}}_o(\Lambda) \approx 2\pi e^{-\pi|\Lambda|/2}, \quad \tilde{\mathcal{A}}_{\pm}(\Lambda) \approx 2\pi e^{-\pi|\Lambda| \pm \pi\Lambda/2}. \quad (5.35c)$$

Now we can calculate the volume of the stochastic layer in the pendulum phase space analogously to Eq. (5.19) for each p_2 , and then integrate over p_2 [equivalently, over $\Lambda = 3gp_2/(4\sqrt{gV_1})$]:

$$W_{ss} = \frac{2}{3\pi} \frac{V_2}{g} \int_{-\infty}^{\infty} d\Lambda \left[4\Lambda^2 \tilde{\mathcal{A}}_o(\Lambda) \ln \frac{16eV_1/V_2}{\Lambda^2 \tilde{\mathcal{A}}_o(\Lambda)} + \sum_{\pm} \Lambda^2 \tilde{\mathcal{A}}_{\pm}(\Lambda) \ln \frac{32eV_1/V_2}{\Lambda^2 \tilde{\mathcal{A}}_{\pm}(\Lambda)} \right]. \quad (5.36)$$

The integral is dominated by $|\Lambda| \sim 1$ where the functions $\tilde{\mathcal{A}}_{o,\pm}(\Lambda)$ are not known. Thus, one can only conclude that

$$W_{ss} = C_{ss} \frac{V_2}{g} \ln \frac{V_1}{V_2}, \quad (5.37)$$

with some unknown constant $C_{ss} \sim 1$.

At $V_2 \ll V_1$, the main region of integration over p_2 , $|p_2| \sim \sqrt{V_1/g}$, is far away from the separatrix of the $(p_2, \check{\phi}_2)$ motion, which occurs at $|p_2| \sim \sqrt{V_2/g}$. When $V_2 \sim V_1$, the two separatrices should be treated on equal footing, and the author is not aware of any accurate method for description of the stochastic layer. A reasonable extrapolation of Eq. (5.37) is

$$W_{ss} = C_{ss} \frac{V_{min}}{g} \ln \frac{C'_{ss} V_{max}}{V_{min}}, \quad (5.38)$$

where $V_{max} = \max\{V_1, V_2\}$, $V_{min} = \min\{V_1, V_2\}$, and $C_{ss}, C'_{ss} \sim 1$ are some bounded functions of V_{max}/V_{min} . It is worth reminding that this expression is valid when the resonance intersection point is inside the allowed triangle and not too close to its boundaries, i. e., I satisfies inequality (5.26) with a positive correction $\sim \tau\Delta$ to its right-hand side.

Now let us turn to the integral in Eq. (5.30b). The whole I integration range consists of three parts: (i) the smallest I , $0 < I < I_{min}^{(line)}$, when the allowed triangle is so small that none of the dashed lines in Fig. 4 enters it, (ii) intermediate I , $I_{min}^{(line)} < I < I_{min}$ when one or both dashed lines enter the triangle, but not their intersection point, and (iii) sufficiently large $I > I_{min}$, when the triangle contains the resonance intersection point [Eq. (5.26)]. For a typical configuration of the random oscillator frequencies, $I_{min}^{(line)}, I_{min}, I_{min} - I_{min}^{(line)} \sim \Delta/g$. Hence, even though W_{ss} in the intermediate region has an additional smallness $\sim e^{-1/\sqrt{\tau}}$ from the Melnikov-Arnold integral, a thermal factor $\sim e^{1/\rho}$ is gained with respect to $I > I_{min}^{(point)}$ due to the higher activation barrier of the latter. However, as will be seen below, the main contribution to the disorder average of w comes not from the typical configurations, but from those where $I_{min} \sim T/|\mu|$. In this case the contribution from the region $I_{min}^{(line)} < I < I_{min}$ can be neglected, and one can focus on I satisfying inequality (5.26) and use Eq. (5.38) for W_{ss} .

As \check{I} increases, the intersection point enters the triangle through one of its sides, depending on which of $\omega_1, \omega_2, \omega_3$ is the largest. It is convenient to rewrite $H_r(I)$ as

$$H_r(I) = E_a + \max_{1 \leq n \leq 3} \{\omega_n - \mu\} (I - I_{min}) + \frac{g}{6} (I - I_{min})^2, \quad (5.39a)$$

$$E_a = 3 \max_{1 \leq n \leq 3} \frac{(\omega_n - \mu)^2}{2g} - \sum_{n=1}^3 \frac{(\omega_n - \mu)^2}{2g}. \quad (5.39b)$$

The contribution of the last term in Eq. (5.39a) to the thermal weight can be neglected. E_a can be viewed as the activation barrier for the triple. Its probability distribution is calculated as (using $\Delta \ll |\mu|$)

$$\begin{aligned} p_\omega(E_a) &= \int_{-\Delta/2}^{\Delta/2} \frac{d\omega_1}{\Delta} \frac{d\omega_2}{\Delta} \frac{d\omega_3}{\Delta} \delta \left(3 \max_{1 \leq n \leq 3} \frac{(\omega_n - \mu)^2}{2g} - \sum_{n=1}^3 \frac{(\omega_n - \mu)^2}{2g} - E_a \right) = \\ &= \frac{3g}{|\mu|\Delta} \begin{cases} \frac{gE_a}{|\mu|\Delta} \left(1 - \frac{3}{4} \frac{gE_a}{|\mu|\Delta} \right), & 0 < \frac{gE_a}{|\mu|\Delta} < 1, \\ \left(1 - \frac{1}{2} \frac{gE_a}{|\mu|\Delta} \right)^2, & 1 < \frac{gE_a}{|\mu|\Delta} < 2, \\ 0, & \text{otherwise.} \end{cases} \end{aligned} \quad (5.40)$$

Let us assume that $\omega_1 > \omega_2, \omega_3$, which occurs with probability 1/3. Denoting $g(I - I_{min}) = \omega'$, $\omega_1 - \omega_2 = \omega_{12}$, $\omega_1 - \omega_3 = \omega_{13}$, we obtain

$$w = \frac{2C_{ss}T\Delta}{3(gT/|\mu|)^3} e^{-E_a/T} \int_0^\infty \sqrt{\omega'(\omega' + 3\omega_{12})} e^{-\omega_1\omega'/(gT)} \ln \frac{C'_{ss} \sqrt{\omega' + 3\omega_{13}}}{\sqrt{\omega'}} d\omega'. \quad (5.41)$$

The integral can be calculated analytically in two limiting cases:

$$w = \frac{2C_{ss}\tau}{3} \frac{|\mu|\Delta}{gT} e^{-E_a/T} \begin{cases} \ln C'_{ss}, & \omega_{12}, \omega_{13} \ll gT/|\mu|, \\ \sqrt{\frac{3\pi}{16} \frac{\omega_1\omega_{12}}{gT}} \ln \frac{C''_{ss}\omega_{13}\omega_1}{gT}, & \omega_{12}, \omega_{13} \gg gT/|\mu|, \end{cases} \quad (5.42a)$$

$$C''_{ss} = 3(C'_{ss})^2 e^{\ln 2 - 1 + \gamma/2},$$

where $\gamma = 0.577\dots$ is the Euler-Mascheroni constant. For $\omega_3 > \omega_1, \omega_2$ one obtains the same result with ω_1 and ω_3 interchanged. For $\omega_2 > \omega_1 > \omega_3$ the calculation is fully analogous, and one obtains

$$w = \frac{2C_{ss}\tau}{3} \frac{|\mu|\Delta}{gT} e^{-E_a/T} \begin{cases} \ln C'_{ss}, & \omega_{21}, \omega_{23} \ll gT/|\mu|, \\ \sqrt{\frac{3\pi}{16} \frac{\omega_2\omega_{21}}{gT}} \ln \frac{(C'_{ss})^2\omega_{23}}{\omega_{21}}, & \omega_{21}, \omega_{23} \gg gT/|\mu|. \end{cases} \quad (5.42b)$$

Again, for $\omega_2 > \omega_3 > \omega_1$ it is sufficient to interchange ω_1 and ω_3 .

Now one can average w over the disorder, which gives the average spatial density of the chaotic spots:

$$\bar{w} \equiv \int_{-\Delta/2}^{\Delta/2} \frac{d\omega_1}{\Delta} \frac{d\omega_2}{\Delta} \frac{d\omega_3}{\Delta} w = C_w \tau \frac{gT}{|\mu|\Delta} \equiv C_w \tau \rho, \quad (5.43)$$

where C_w is a constant. The average is dominated by rare triples which have $E_a \sim T$, that is $|\omega_{12}| \sim |\omega_{23}| \sim gT/|\mu|$. Since expressions (5.42a)–(5.42b) cover only limiting cases, no analytical expression for the constant C_w is available.

The estimate (5.43) is not very much sensitive to the fact that in Eq. (5.29) the chaotic fraction is defined using the thermal weight. The latter only fixes the typical value of the action $I_n \sim gT/|\mu|$. Let us repeat the estimate simply fixing $I_1 = I_2 = I_3 = I/3$, so instead of the thermal exponential in Eq. (5.29) we put $\delta(I_1 - I/3) \delta(I_2 - I/3) \delta(I_3 - I/3)$. Then $V_1 = V_2 = (2/3)\tau\Delta I$, and \bar{w} is simply given by the probability that the point $\check{I}_1 = \check{I}_2 = 0$ lies inside the area $W_{ss}(I) = C'''_{ss}\tau\Delta I/g$ (we denote $C'''_{ss} = (2/3)C_{ss} \ln C'_{ss}$) around the resonance point (5.25), which gives $\bar{w} = 3C'''_{ss}\tau gI/\Delta$. Defining $\rho = gI/(3\Delta)$, we obtain an estimate fully analogous to Eq. (5.43).

6. Perturbation theory

6.1. General remarks

One could formulate the perturbation theory for Eq. (2.1) by taking independent oscillations, $\psi_n^{(0)}(t) = \sqrt{I_n} e^{-i(\omega_n + gI_n)t + i\phi_n^0}$, as the zero approximation and solving Eq. (2.1) for $\psi_n(t)$ by iterations. Clearly, such perturbation theory is divergent. Indeed, if it were

convergent, there would be no chaos. Formally, its divergent character can be seen already from the exact solution for two oscillators, given in Sec. 5.1. The pendulum frequency depends on τ as $\Omega \propto \sqrt{|\tau|}$ [Eq. (5.8)], while the dependence on g has a threshold [Eq. (5.5)]. As the dependence on τ and g is non-analytic at $\tau, g \rightarrow 0$, the perturbation series has zero radius of convergence.

The crucial point of the present work is that instead of studying the whole perturbation series, the most dangerous terms of this series should be identified (more, precisely, the probability for them to occur), and the subsequent analysis of their effect should be performed non-perturbatively, using an effective model, such as driven pendulum. In other words, once a small frequency difference in the denominator has occurred in the perturbation series, one step back should be taken, the combination of the oscillator phases corresponding to this frequency combination should be called the phase $\check{\phi}$ of the effective pendulum, while the prefactor multiplying the inverse of this frequency difference should be called the effective coupling, which multiplies $\cos \check{\phi}$ in the effective pendulum Hamiltonian.

Divergence of the perturbation theory due to resonances corresponds to an instability at long times. Indeed, perturbation theory in the time domain in the nonlinearity has been shown to converge only for not too long times [17, 22]. Its divergence at long times signals the chaotic instability. In fact, the perturbation theory developed here is closely related to that of Refs. [17, 22], as will be discussed in more detail the end of Sec. 6.3.

The perturbation theory developed here is designed to generate the effective many-oscillator coupling in high orders in τ and g . We define the effective coupling between $2N$ oscillators $n_1, \dots, n_N, \bar{n}_1, \dots, \bar{n}_N$ (these are, generally speaking, $2N$ arbitrary integers) as the coupling term in the Hamiltonian which involves no other oscillators and leads to the same equations of motion for these $2N$ oscillators, as the equations obtained by eliminating all other oscillators from the full equations of motion, Eq. (2.1). Thus, the effective coupling is the sum of terms of the kind

$$V^{(N)} = \frac{1}{N} \mathcal{K}_{n_1 \dots n_N \bar{n}_1 \dots \bar{n}_N} \psi_{n_1}^* \dots \psi_{n_N}^* \psi_{\bar{n}_1} \dots \psi_{\bar{n}_N}, \quad (6.1)$$

Strictly speaking, the above definition of the effective coupling is meaningful only exactly at resonance, $\omega_{n_1} + \dots + \omega_{n_N} = \omega_{\bar{n}_1} + \dots + \omega_{\bar{n}_N}$, as will be seen in Sec. 6.3. This does not pose a problem, since it is just in the vicinity of the resonance that this coupling is needed, where it determines the parameters of the effective pendulum. Thus, the frequency difference $|\omega_{n_1} + \dots + \omega_{n_N} - \omega_{\bar{n}_1} - \dots - \omega_{\bar{n}_N}|$ is assumed to be smaller than any of the intermediate frequency denominators involved in the coefficient \mathcal{K} . In other words, the $2N$ -oscillator perturbation term is generated under the assumption of no resonances for $2N' < 2N$ oscillators, involved in the construction of this $2N$ -oscillator term. Indeed, if a $2N'$ -oscillator resonance occurs, it would be more efficient in producing chaos due to larger effective coupling obtained in a lower order of the perturbation theory, and then $V^{(N)}$ is not needed at all.

To illustrate the diagram generation, all distinct diagrams for $N = 2, 3, 4$ are shown explicitly in Fig. 5.

2. Each of the free ends of solid lines corresponds to some of the sites $n_1, \dots, n_N, \bar{n}_1, \dots, \bar{n}_N$. Each dotted-solid-solid vertex also has a site index, the two ends of the same dotted line corresponding to the same site.
3. Each solid line has a frequency argument. For external lines it is the frequency of the site at its free end. For internal lines it is determined from the conservation law holding for each dotted line: the sum of the two frequencies of the entering solid lines is equal to the sum of the two outgoing frequencies. An example of labeling a diagram is shown in Fig. 6. Note that this procedure is consistent only when $\omega_{n_1} + \dots + \omega_{n_N} = \omega_{\bar{n}_1} + \dots + \omega_{\bar{n}_N}$.
4. One obtains an analytical expression corresponding to each diagram by (i) associating a factor g to each dotted line; (ii) associating a factor $G_{nm'}(\omega)$ to each internal solid line which starts on site n , ends on site n' , and carries frequency ω ; (iii) associating a factor $G'_{n_k n}(\omega_{n_k})$ or $G''_{n \bar{n}_k}(\omega_{\bar{n}_k})$ to each external outgoing or incoming line, respectively, with free end on site n_k or \bar{n}_k ; (iv) summing over internal site indices. For example, the diagram in Fig. 6 produces an expression

$$g^2 \sum_{n'_1, n'_2} G'_{n_1 n'_1}(\omega_{\bar{n}_1} + \omega_{\bar{n}_2} + \omega_{\bar{n}_3} - \omega_{n_2} - \omega_{n_3}) G''_{n'_1 \bar{n}_1}(\omega_{\bar{n}_1}) G'_{n_2 n'_2}(\omega_{n_2}) G''_{n'_2 \bar{n}_2}(\omega_{\bar{n}_2}) \\ \times G'_{n_3 n'_2}(\omega_{n_3}) G_{n'_2 n'_1}(\omega_{n_3} + \omega_{n_2} - \omega_{\bar{n}_2}) G''_{n'_1 \bar{n}_3}(\omega_{\bar{n}_3}).$$

5. Summation over all diagrams gives the coefficient $\mathcal{K}_{n_1 \dots n_N \bar{n}_1 \dots \bar{n}_N}^{(N)}$ in Eq. (6.1).

6.3. Derivation of the diagrammatic rules

Let us write the equations of motion, Eq. (2.1) in the form

$$(i\partial_t - \omega_n)\psi_n = -\tau\Delta(\psi_{n+1} + \psi_{n-1}) + \psi_n \sum_{n'} g_{nn'} \psi_{n'}^* \psi_{n'}, \quad (6.4)$$

where $g_{nn'} = g\delta_{nn'}$ is introduced to simplify the diagrammatic rules (otherwise, additional combinatorial coefficients would have to be assigned to each diagram). The right-hand side of Eq. (6.4) can be viewed as an external force acting on the oscillator n . Then, the response of the oscillator to an external periodic force is determined as

$$(i\partial_t - \omega_n)\psi_n = \sum_{\alpha} f_{\alpha} e^{-i\omega_{\alpha} t} \Rightarrow \psi_n = \psi_n^{(0)} e^{-i\omega_n t} + \sum_{\alpha} \frac{f_{\alpha} e^{-i\omega_{\alpha} t}}{\omega_{\alpha} - \omega_n}. \quad (6.5)$$

Let us start with two oscillators, n and \bar{n} (assume $n < \bar{n}$ for concreteness). Suppose the \bar{n} th oscillator performs some given motion

$$\psi_{\bar{n}}(t) = \int \frac{d\omega}{2\pi} \tilde{\psi}_{\bar{n}}(\omega) e^{-i\omega t}, \quad (6.6)$$

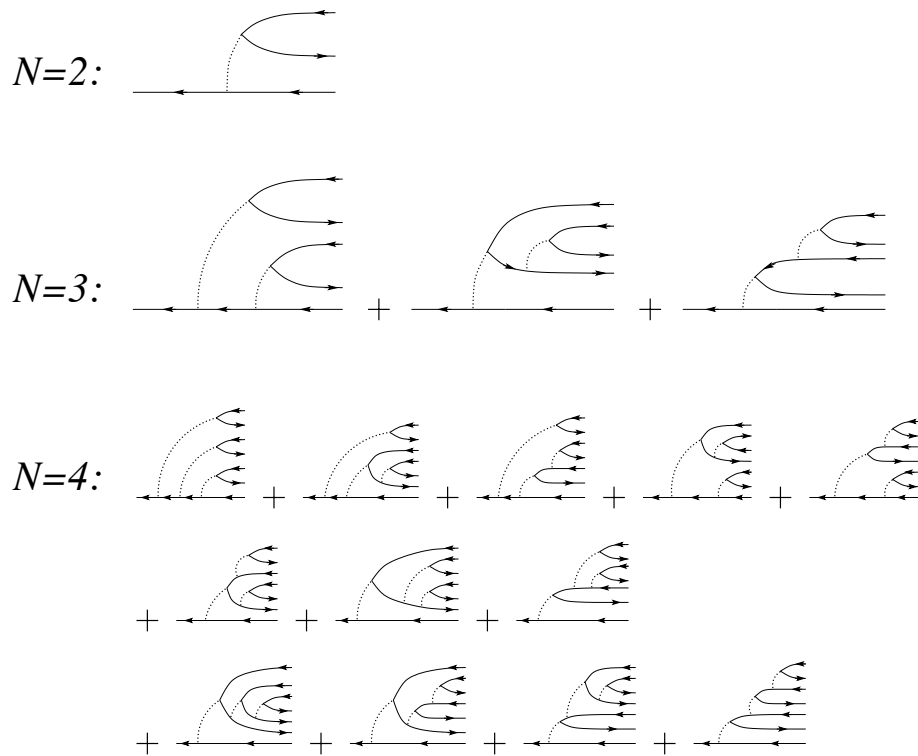


Figure 5: All distinct diagrams generating effective couplings for $N = 2, 3, 4$ oscillators.

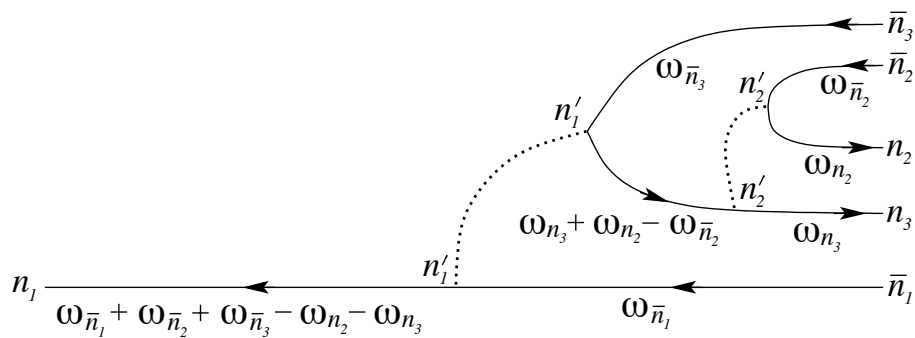


Figure 6: Labeling the lines and vertices of a diagram.

and let us find the corresponding force acting on oscillator n . To the leading order in τ (which is $\bar{n} - n$) and g (which is zero), this force is found by writing Eq. (6.4) in the Fourier space, and eliminating oscillators $n + 1, \dots, \bar{n} - 1$ perturbatively:

$$\begin{aligned} f_{n \leftarrow \bar{n}}(t) &= \int \frac{d\omega}{2\pi} (-\tau\Delta) \frac{1}{\omega - \omega_{n+1}} (-\tau\Delta) \dots (-\tau\Delta) \frac{1}{\omega - \omega_{\bar{n}-1}} (-\tau\Delta) \tilde{\psi}_{\bar{n}}(\omega) e^{-i\omega t} \equiv \\ &\equiv \int \frac{d\omega}{2\pi} G''''_{n\bar{n}}(\omega) \tilde{\psi}_{\bar{n}}(\omega) e^{-i\omega t}. \end{aligned} \quad (6.7)$$

We are interested in the case when the spectrum of $\tilde{\psi}_{\bar{n}}$ is concentrated around $\omega \approx \omega_{\bar{n}} \approx \omega_n$, i. e. slow modulations of the periodic oscillator motion. Then one can replace $G''''_{n\bar{n}}(\omega) \rightarrow G''''_{n\bar{n}}(\omega_{\bar{n}})$ and take it out of the integral. Then the effective equation of motion for the n th oscillator is

$$(i\partial_t - \omega_n) \psi_n(t) = G''''_{n\bar{n}}(\omega_{\bar{n}}) \psi_{\bar{n}}(t), \quad (6.8)$$

which can be obtained from the effective coupling Hamiltonian

$$V = G''''_{n\bar{n}}(\omega_{\bar{n}}) \psi_n^* \psi_{\bar{n}}. \quad (6.9)$$

This corresponds to the diagram consisting of a single solid line with two free ends, so we have introduced the Green's function G'''' , shortened on both ends. To the coupling Hamiltonian in Eq. (6.9) another term should be added, which has the same form, but with n and \bar{n} interchanged. The resulting Hamiltonian is real only when the expression $G''''_{n\bar{n}}(\omega_{\bar{n}})$ is symmetric with respect to interchange $n \leftrightarrow \bar{n}$, that is only when $\omega_{\bar{n}} = \omega_n$.

To see how the procedure works for a larger number of oscillators, let us calculate the force acting on oscillator n_1 . First, we write

$$f_{n_1}(t) = \sum_n \int \frac{d\omega}{2\pi} G''''_{n_1 n}(\omega) \tilde{\psi}_n(\omega) e^{-i\omega t}, \quad (6.10)$$

as before. Now, we find $\tilde{\psi}_n(\omega)$ from Eq. (6.5) where the force comes from the nonlinear term:

$$\begin{aligned} \tilde{\psi}_n(\omega) &= \frac{1}{\omega - \omega_n} \sum_{n'} \int dt e^{i\omega t} [\psi_n(t) g_{nn'} \psi_{n'}(t) \psi_{n'}^*(t)] = \\ &= \sum_{n'} \frac{g_{nn'}}{\omega - \omega_n} \int \frac{d\omega'}{2\pi} \frac{d\omega''}{2\pi} \tilde{\psi}_n(\omega') \tilde{\psi}_{n'}(\omega'') \tilde{\psi}_{n'}^*(\omega' + \omega'' - \omega) \end{aligned} \quad (6.11)$$

Expressing $\tilde{\psi}_n, \tilde{\psi}_{n'}, \tilde{\psi}_{n'}^*$ in terms of some other oscillators $n_2, \bar{n}_1, \bar{n}_2$, we obtain

$$\begin{aligned} f_{n_1}(t) &= \int \frac{d\omega}{2\pi} e^{-i\omega t} \int \frac{d\omega'}{2\pi} \frac{d\omega''}{2\pi} \sum_{n, \bar{n}_1} G'_{n_1 n}(\omega) G''_{\bar{n}_1}(\omega') \tilde{\psi}_{\bar{n}_1}(\omega') \sum_{n'} g_{nn'} \times \\ &\times \sum_{n_2, \bar{n}_2} \tilde{\psi}_{n_2}^*(\omega' + \omega'' - \omega) G'_{n_2 n'}(\omega' + \omega'' - \omega) G''_{n' \bar{n}_2}(\omega'') \tilde{\psi}_{\bar{n}_2}(\omega''). \end{aligned} \quad (6.12)$$

Again, inside the Green's functions one can replace $\omega' \rightarrow \omega_{\bar{n}_1}$, $\omega'' \rightarrow \omega_{\bar{n}_2}$, $\omega' + \omega'' - \omega \rightarrow \omega_{n_2}$. When they are taken out of the triple frequency integral, the latter evaluates to $\psi_{\bar{n}_1}(t) \psi_{\bar{n}_2}(t) \psi_{n_2}^*(t)$. As a result,

$$(\partial_t - \omega_{n_1})\psi_{n_1} = \sum_{n_2, \bar{n}_1, \bar{n}_2} \mathcal{K}_{n_1 n_2 \bar{n}_1 \bar{n}_2}^{(2)} \psi_{n_2}^* \psi_{\bar{n}_1} \psi_{\bar{n}_2}, \quad (6.13)$$

where $\mathcal{K}_{n_1 n_2 \bar{n}_1 \bar{n}_2}^{(2)}$ is the expression corresponding to the diagram for $N = 2$ in Fig. 5, according to the rules of the previous subsection. Finally, the factor 1/2 has to be added when deducing $V^{(2)}$ from \mathcal{K}_2 , in order to avoid double counting upon differentiation $\partial V^{(2)}/\partial \psi_{n_1}^*$.

Generalization to the N -oscillator case is straightforward: calculation of the force by iterative solution of Eq. (6.4) corresponds to iterations of diagrammatic equations (6.3a), (6.3b). The factor $1/N$ in $V^{(N)}$ takes care of double counting upon differentiation.

To conclude this subsection, we note that the perturbation theory, developed here, is closely related to that of Refs. [17, 22]. One obvious difference is that the linear part of the problem was assumed to be diagonalized in Refs. [17, 22], while here the linear coupling is treated perturbatively. This difference is purely technical; the present calculation corresponds just to the perturbative evaluation of the overlap sums which dress the nonlinear coupling in the approach of Refs. [17, 22]. Second, in Refs. [17, 22] one starts from a single excited normal mode as zero approximation and then calculates the force acting on other oscillators. Here, the independently excited oscillators are taken as the zero approximation, and the force acting on some given oscillator n is calculated. Clearly, the two approaches are closely related, so the structure of the perturbation theory is very similar in the two cases. It is the subsequent use of the information obtained from the perturbation theory which is quite different.

6.4. On the number of diagrams

It turns out that the total number of diagrams of the order g^{N-1} , generated according to the rules given in Sec. 6.2, is given by the following exact expression:

$$\mathcal{D}_N = \sum_{k=1}^{N-1} \frac{2^{N-1}}{2^k k!} \sum_{0 \leq m_1 \leq \dots \leq m_{k-1} \leq N-1-k} (3m_1 + 2)(3m_2 + 3) \dots (3m_{k-1} + k), \quad (6.14)$$

to be derived below. Even though explicit, this expression is not straightforward to evaluate. Still, it can be shown that \mathcal{D}_N grows exponentially with N . Let us estimate it from below and from above:

$$\sum_{k=1}^{N-1} \frac{2^{N-1}}{2^k k!} \frac{(3N-3-2k)!}{(3N-2-3k)!} < \mathcal{D}_N < \sum_{k=1}^{N-1} \frac{2^{N-1}}{2^k k!} \frac{(3N-3-2k)!}{(3N-2-3k)!} \frac{(N-2)!}{(k-1)!(N-1-k)!}. \quad (6.15)$$

The lower bound is obtained by simply taking one term of the m -sum with all $m_i = N - 1 - k$; this is the largest term, so the upper bound is obtained by multiplying it by the total number of terms in the sum, where we use the formula⁹

$$\sum_{1 \leq m_1 \leq \dots \leq m_k \leq n} 1 = \frac{(n-1+k)!}{k!(n-1)!}. \quad (6.16)$$

At $N \gg 1$ we approximate the factorials by Stirling's formula, denote $k/N = x$, and pass to the integral:

$$\begin{aligned} & \int_0^1 \frac{dx}{\sqrt{8\pi N^3}} \sqrt{\frac{(3-3x)^3}{(3-2x)^5} \left[\frac{2^{1-x}(3-2x)^{3-2x}}{x^x(3-3x)^{3-3x}} \right]^N} < \\ & < \mathcal{D}_N < \int_0^1 \frac{dx}{4\pi N^2} \sqrt{\frac{(3-3x)^3}{x(1-x)(3-2x)^5} \left[\frac{2^{1-x}(3-2x)^{3-2x}}{(1-x)^{(1-x)}x^{2x}(3-3x)^{3-3x}} \right]^N}, \end{aligned} \quad (6.17)$$

The maxima of the expressions in the square brackets on the left and on the right are 4.365... and 8.722..., respectively. For the numerical evaluation of \mathcal{D}_N it is convenient to cast Eq. (6.14) into a recursive form:

$$\mathcal{D}_N = \sum_{k=1}^{N-1} \frac{2^{N-1}}{2^k} S_{k,N-1-k}, \quad (6.18a)$$

$$S_{k+1,n} = \sum_{m=0}^n \left(1 + \frac{3m}{k+1} \right) S_{k,m}, \quad S_{1,n} = 1. \quad (6.18b)$$

Numerical evaluation of the leading exponential gives

$$\frac{\mathcal{D}_{N+1}}{\mathcal{D}_N} \underset{N \rightarrow \infty}{\sim} (6.75\dots) \times \left(1 + \frac{1}{N} \right)^{-1.5\dots}. \quad (6.19)$$

To derive Eq. (6.14) let us view the diagrams as trees formed by the dotted lines (Fig. 7). The simplest one is a single-branch tree: in the order g^{N-1} there are 2^{N-2} such diagrams. If there is one lateral branch, the number of such diagrams is

$$\mathcal{D}_N^{(2)} = \frac{1}{2} \sum_{l_1, l_2=1}^{N-1} [3(l_1-1) + 2] 2^{l_1-1} 2^{l_2-1} \delta_{l_1+l_2, N-1}, \quad (6.20)$$

⁹This formula can be obtained by noting that the sum, denoted by $s_{k,n}$, satisfies the recurrence relation $s_{k,n} = s_{k-1,n} + s_{k,n-1}$. Then one can (i) check directly that it is satisfied by $(n+k-1)!/[k!(n-1)!]$, or (ii) introduce the characteristic function, $\chi(\phi, \theta) = \sum_{k,n} e^{ik\phi+i(n-1)\theta} s_{k,n}$, for which the recurrence relation reduces to a simple algebraic equation, so that $\chi(\phi, \theta) = (1 - e^{i\phi} - e^{i\theta})^{-1}$, from which $s_{k,n}$ is easily reconstructed.

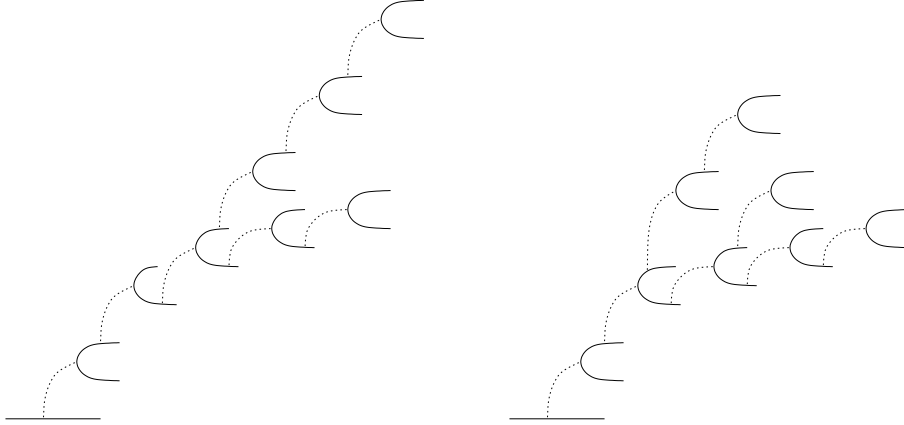


Figure 7: Examples of two- and three-branch diagrams for effective 18-oscillator coupling.

because 2^{l_1-1} is the number of ways to build the main branch, 2^{l_2-1} is the number of ways to build the lateral branch, $3(l_1 - 1) + 2$ is the number of electron lines where the lateral branch can be attached to the main one, and $1/2$ stands because of the arbitrary choice of which branch is main and which one is lateral. Summing over the number of branches, we obtain

$$\mathcal{D}_N = \sum_{k=1}^{N-1} \sum_{l_1, \dots, l_k \geq 0} \frac{1}{k!} (3l_1 + 2)(3l_1 + 3l_2 + 3) \dots (3l_1 + \dots + 3l_{k-1} + k) \times \\ \times 2^{l_1 + \dots + l_k} \delta_{l_1 + \dots + l_k, N-1-k}, \quad (6.21)$$

which is equivalent to Eq. (6.14).

It turns out that Eq. (6.22) is equivalent to the following recursive relation, derived in Ref. [22]:¹⁰

$$\mathcal{D}_N = \sum_{N_1, N_2, N_3 \geq 1} \mathcal{D}_{N_1} \mathcal{D}_{N_2} \mathcal{D}_{N_3} \delta_{N_1 + N_2 + N_3, N+1}, \quad \mathcal{D}_1 = \mathcal{D}_2 = 1. \quad (6.22)$$

The author was not able to prove the equivalence between Eq. (6.22) and Eq. (6.14) algebraically, however, it can be checked numerically for quite large N . For example, both equations give $\mathcal{D}_{50} = 30426054945480277365983787382745806500$.

¹⁰Strictly speaking, the quantity, for which Eq. (6.22) was derived in Ref. [22], is not defined in exactly the same way as \mathcal{D}_N , since the perturbation theory developed in Ref. [22] is not strictly identical to the present one. Still, the two perturbation theories are closely related, as discussed in the end of Sec. 6.3, and the equivalence between Eq. (6.22) and Eq. (6.14) is a manifestation of this relation.

6.5. On the statistics of diagrams

Let us define a resonance r as a sequence $n_1^r \leq n_2^r \leq \dots \leq n_{N_r}^r$, $\bar{n}_1^r \leq \bar{n}_2^r \leq \dots \leq \bar{n}_{N_r}^r$, where none of the n 's coincides with any of the \bar{n} 's. The freedom of interchanging $n \leftrightarrow \bar{n}$ can be fixed by requiring

$$\omega_{n_1^r} + \dots + \omega_{n_{N_r}^r} < \omega_{\bar{n}_1^r} + \dots + \omega_{\bar{n}_{N_r}^r}. \quad (6.23)$$

The frequency mismatch of the resonance is thus defined to be positive:

$$\varpi_r = \omega_{\bar{n}_1^r} + \dots + \omega_{\bar{n}_{N_r}^r} - (\omega_{n_1^r} + \dots + \omega_{n_{N_r}^r}). \quad (6.24)$$

To associate the resonance with a single site n , one can fix $n_1^r = n$. In the case when some of the n 's or some of the \bar{n} 's coincide, one can introduce the multiplicity of each site n , m_n^r , defined as the number of times it occurs in the sequence of n^r 's or minus the number of times it occurs in the sequence of \bar{n}^r 's. For sites n that do not participate in the resonance, $m_n^r = 0$. Due to action conservation,

$$\sum_n m_n^r = 0, \quad \sum_n |m_n^r| = 2N_r. \quad (6.25)$$

Viewing the sequence $\{m_n^r\}$ as a vector, we define the scalar product and the norm in the usual way:

$$(\underline{m}^r, \underline{m}^{r'}) = \sum_{n=-\infty}^{\infty} m_n^r m_n^{r'}, \quad |\underline{m}^r|^2 = (\underline{m}^r, \underline{m}^r). \quad (6.26)$$

The oscillators are coupled by an effective Hamiltonian

$$\begin{aligned} V &= 2V_r \cos(\phi_{n_1^r} + \dots + \phi_{n_{N_r}^r} - \phi_{\bar{n}_1^r} - \dots - \phi_{\bar{n}_{N_r}^r}), \\ V_r &= \mathcal{K}_r \sqrt{I_{n_1^r} \dots I_{n_{N_r}^r} I_{\bar{n}_1^r} \dots I_{\bar{n}_{N_r}^r}}, \\ \mathcal{K}_r &= \frac{1}{N} \sum \mathcal{K}_{n_1 \dots n_{N_r} \bar{n}_1 \dots \bar{n}_{N_r}}^{(N)}. \end{aligned} \quad (6.27)$$

The summation is performed over $(N_r!)^2 / \prod_n |m_n^r|!$ distinct permutations of $n_1^r, \dots, n_{N_r}^r$ and of $\bar{n}_1^r, \dots, \bar{n}_{N_r}^r$. Besides the summation over permutations, \mathcal{K}_r represents a sum over different diagrams whose number was estimated in Sec. 6.4, and for each diagram the summation over the positions of $N_r - 1$ nonlinear vertices should be performed. Thus, \mathcal{K}_r is a sum of many terms, whose number will be denoted by \mathcal{N} . Each term contains a product of $L_r + N_r - 2$ frequency denominators, where $L_r \geq N_r$ is the minimal order in τ which couples all oscillators together.

It is convenient to explicitly separate all trivial deterministic factors and introduce the dimensionless random quantity

$$\tilde{\mathcal{K}}_r = \frac{2^{L_r + N_r - 2} \Delta^{N_r - 2}}{\tau^{L_r} g^{N_r - 1}} \mathcal{K}_r. \quad (6.28)$$

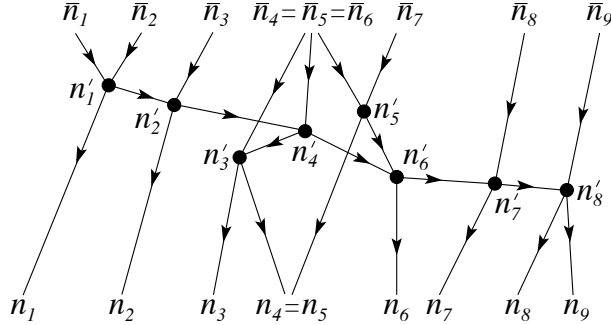


Figure 8: An example of the spatial structure for an $N = 9$ diagram.

Our primary interest will be the probability that $\tilde{\mathcal{K}}_r$ exceeds a certain value $e^{-\lambda}$:

$$\mathcal{P}\{\tilde{\mathcal{K}}_r < e^{-\lambda}\} = \overline{\theta\left(\ln \frac{1}{\tilde{\mathcal{K}}_r} - \lambda\right)}, \quad (6.29)$$

where $\theta(x)$ is the Heaviside step function, and the overline denotes the statistical averaging over the static frequency disorder.

First, let us argue that the number of terms \mathcal{N} is at most exponential in N_r, L_r . It is convenient to introduce a pictorial representation of each term, which illustrates its spatial structure. Namely, let the direction from left to right represent the position on the chain. Then, each term of the perturbation theory, contributing to \mathcal{K} , corresponds to definite locations of the free ends of the solid lines and definite locations of the dotted lines of the corresponding diagram. For the latter reason it is more convenient to represent the nonlinear vertex by a small circle:

$$\text{Diagram} = \text{Diagram} + \text{Diagram} \quad (6.30)$$

An example of a diagram with a spatial structure is shown in Fig. 8. The vertical direction on the picture has no particular meaning and is used just for the convenience of presentation. What really counts is the length of the projection of each solid line on the horizontal axis, as the sum of these projections for all lines determines the order in τ .

Now it is quite easy to see that out of a factorially large number of permutations of n' 's and \bar{n} 's, very few actually contribute. Indeed, while permutation $\bar{n}_1 \leftrightarrow \bar{n}_2$ in Fig. 8 does not change the order in τ , the permutation $\bar{n}_2 \leftrightarrow \bar{n}_3$ already increases the order in τ , and $\bar{n}_1 \leftrightarrow \bar{n}_9$ almost doubles the order. In fact, a typical permutation contributing to the factorial number, has a smallness $\tau \sim L_r^2$, which suppresses even the large factorial factor. In fact, the number of permutations which preserve the order in τ cannot exceed the number of vertices, i. e., $N_r - 1$.

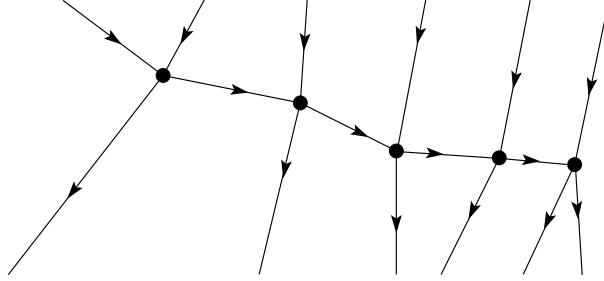


Figure 9: The structure of the diagram for a sparse resonance.

Another source of different terms is the summation over the positions of the nonlinear vertices. In Fig. 8, for example, n'_1 can be varied between \bar{n}_1 and \bar{n}_2 without changing the order in τ . Clearly, this freedom is most important when the sites n'_1, \dots, n'_{N_r} and $\bar{n}'_1, \dots, \bar{n}'_{N_r}$ are sparse, i. e., $L_r \gg N_r$ (which will be called a sparse resonance). In this case the most important diagrams have the structure shown in Fig. 9: the solid lines should be drawn as vertically as possible, but at least one should go across the whole spatial region in order to connect all the oscillators. Moreover, for sparse resonances having $|m_n| > 1$ clearly represents a disadvantage since imposing constraints on the oscillator positions decreases the freedom in making ϖ_r small, without any gain in τ . Then, each nonlinear vertex can be moved within a segment $\sim L_r/N_r$, so all vertices together give a factor $\sim (L_r/N_r)^{N_r}$. Using the fact that $\lim(\mathcal{D}_{N+1}/\mathcal{D}_N) = 6.75\dots < e^2$, we arrive at the following bounds:

$$1 \leq \mathcal{N} < \left(\frac{L_r}{N_r}\right)^{N_r} e^{2N_r}. \quad (6.31)$$

Let us now turn to the statistics of each individual term contributing to $\tilde{\mathcal{K}}_r$. The denominators of the $2N_r$ external Green's functions contain differences of two frequencies only, whose probability distribution is

$$\varpi = |\omega_n - \omega_{n'}| \Rightarrow p_{1,-1}(\varpi) = \frac{2}{\Delta} \left[1 - \frac{\varpi}{\Delta}\right], \quad (6.32)$$

where we denoted $[x] \equiv x\theta(x)$, i. e., $[x] = x$ for $x > 0$ and $[x] = 0$ otherwise. The $N_r - 2$ internal Green's functions contain linear combinations of many frequencies, so their probability distribution can be estimated from the central limit theorem:

$$\varpi = \left| \sum_{n=-\infty}^{\infty} m_n \omega_n \right| \Rightarrow p_{\underline{m}}(\varpi) = \frac{2}{\Delta} \sqrt{\frac{6}{\pi|\underline{m}|^2}} \exp\left(-\frac{6\varpi^2}{|\underline{m}|^2\Delta^2}\right), \quad (6.33)$$

since the dispersion of a single frequency is

$$\int_{-\Delta/2}^{\Delta/2} \frac{d\omega}{\Delta} \omega^2 = \frac{\Delta^2}{12}. \quad (6.34)$$

When the number of terms \mathcal{N} is very large, the distribution at $\varpi \rightarrow 0$ is the most important (the main contribution to $\tilde{\mathcal{K}}_r$ coming from largest terms, thus small denominators), so we replace $p(\varpi)$ by a box distribution of the height $p(\varpi \rightarrow 0)$. The factor $(2/\Delta)$ has been included explicitly in Eq. (6.28), and for external Green's functions nothing else is needed. For internal ones, however, $\sqrt{6/(\pi|m|^2)}$ should be included. Since the contribution of the internal Green's functions to L_r can vary from 0 to 100%, and internal Green's functions can involve up to $2N_r$ frequencies, so that $|m|^2$ can approach $2N_r^2$, we can represent each term contributing to $\tilde{\mathcal{K}}_r$ as

$$\tilde{\mathcal{K}}_r^{(1 \text{ term})} = a\zeta, \quad (6.35)$$

where the non-random coefficient a is bounded by

$$\frac{1}{(\sqrt{3}/\pi N_r)^{L_r}} < a < 1, \quad (6.36)$$

and ζ is a random variable constructed as

$$\zeta = \frac{1}{x_1 \dots x_{L_r+N_r-2}}, \quad (6.37)$$

$x_1, \dots, x_{L_r+N_r-2}$ being random variables uniformly distributed between 0 and 1.

Strictly speaking, x_i 's are not statistically independent, since the same oscillator frequency can enter several factors in the denominator. The resulting correlations can lead to both bunching (meaning that if one of x_i 's is small, than some others are also likely to be small) and antibunching (if one of x_i 's is small, than some others are less likely to be small) of x_i 's. First, we will estimate $\tilde{\mathcal{K}}_r$ assuming all x_i 's to be statistically independent. After that, we will study the effect of both type of correlations on the obtained estimate.

The probability distribution for ζ , defined by Eq (6.37) with independent x_i 's,

$$p_{N_r+L_r-2}(\zeta) = \frac{\theta(\zeta - 1)}{\zeta^2} \frac{\ln^{N_r+L_r-3} \zeta}{(N_r + L_r - 3)!}, \quad (6.38)$$

is discussed in detail in Appendix C. It is crucial that all moments of this distribution diverge, so for the sum of \mathcal{N} such random variables with random signs, $\pm\zeta_1 \pm \dots \pm \zeta_{\mathcal{N}}$, the central limit theorem does not hold. Unable to calculate explicitly the probability distribution of this sum, we estimate the sum from above and from below. This corresponds to estimating the probability for the absolute value of the sum to be smaller than some value z , $\mathcal{P}\{|\pm\zeta_1 \pm \dots \pm \zeta_{\mathcal{N}}| < z\}$, from below and from above, respectively.

As discussed in Appendix C, the lower bound for the probability is obtained if one replaces the sum by its largest term:

$$\mathcal{P}\{|\pm \zeta_1 \pm \dots \pm \zeta_N| < z\} \geq \mathcal{P}\{\zeta_1, \dots, \zeta_N < z\} \approx \exp\left[-\mathcal{N} \int_z^\infty p_{N_r+L_r-2}(\zeta) d\zeta\right]. \quad (6.39)$$

When \mathcal{N} is sufficiently large (exponential in N_r, L_r), it can be approximated as

$$\mathcal{P}\{\zeta_1, \dots, \zeta_N < z\} \approx \exp\left[-\frac{1}{z} \frac{\mathcal{N}}{(N_r + L_r - 3)!} \frac{\ln^{N_r+L_r-2} z}{\ln(z/e^{N_r+L_r-3})}\right]. \quad (6.40)$$

This probability is (i) very strongly suppressed for z smaller than a typical value at which the argument of the exponential is of the order of unity, and (ii) slowly approaches unity for larger z , so that all moments of z diverge. This typical value of z is found from

$$\frac{1}{z(N_r + L_r - 3)!} \frac{\ln^{N_r+L_r-2} z}{\ln(z/e^{N_r+L_r-3})} = \frac{1}{\mathcal{N}}. \quad (6.41)$$

At large N_r, L_r the solution of this equation is given by

$$z \sim \left[e f(\mathcal{N}^{1/(N_r+L_r)})\right]^{N_r+L_r}, \quad (6.42)$$

where we omitted the prefactor, a power of $N_r + L_r$, and the function $f(x)$ is defined as the solution of the equation

$$\frac{f}{1 + \ln f} = x. \quad (6.43)$$

In particular, if $\mathcal{N} \sim c^{N_r+L_r}$, then the typical $z \sim (ef(c))^{N_r+L_r}$. To give an idea of the behavior of $f(x)$, we note that $f(1) = 1$, and $x \ln(ex) \leq f(x) < 2x \ln(ex)$ for $x > 1$. To obtain the approximate expression in the region around the typical value of z , we linearize the logarithm of the argument of the exponential in Eq. (6.40) with respect to $\ln z$. Using the right inequality (6.31) the inequality

$$f\left(\left(\frac{L}{N}\right)^{N/(L+N)} e^{2N/(L+N)}\right) < e^2, \quad L \geq N, \quad (6.44)$$

and the right inequality (6.36) we arrive at the following bound:

$$\mathcal{P}\{\tilde{\mathcal{K}}_r < e^{-\lambda}\} > \exp\left[-e^{\lambda+3(L_r+N_r)}\right]. \quad (6.45)$$

A lower bound for $|\pm \zeta_1 \pm \dots \pm \zeta_N|$ is obtained by ‘‘squeezing’’ its probability distribution towards smaller values. As discussed in Appendix C, this is done by first replacing distribution (6.38) for each term ζ by the log-normal distribution, applying the central limit theorem to the latter, and squeezing the resulting Gaussian into a box of the same height. This corresponds to assuming the sum to be uniformly distributed in the range

$$0 < |\pm \zeta_1 \pm \dots \pm \zeta_N| < \sqrt{\frac{\pi}{2}} e^{2(L_r+N_r-3)}, \quad (6.46)$$

where the left inequality (6.31) was used. Using the left inequality (6.36), we translate it into the uniform distribution of $\tilde{\mathcal{K}}_r$ in the range

$$0 < \tilde{\mathcal{K}}_r < \sqrt{\frac{\pi}{2}} \frac{e^{2(L_r+N_r-3)}}{(\sqrt{3/\pi} N_r)^{L_r}}. \quad (6.47)$$

Squeezing this range further, down to $1/N_r^{L_r}$, for pure analytical convenience, we obtain

$$\mathcal{P}\{\tilde{\mathcal{K}}_r < e^{-\lambda}\} < e^{L_r \ln N_r - \lambda} \theta(\lambda - L_r \ln N_r) + \theta(L_r \ln N_r - \lambda). \quad (6.48)$$

Having found the bounds for the statistics of $\tilde{\mathcal{K}}_r$, let us obtain bounds for the following average:

$$\overline{[\tilde{\lambda} + \ln \tilde{\mathcal{K}}_r]^N} = - \int_{-\infty}^{\tilde{\lambda}} (\tilde{\lambda} - \lambda)^N \frac{d}{d\lambda} \mathcal{P}\{\tilde{\mathcal{K}}_r < e^{-\lambda}\} d\lambda, \quad [x] \equiv x \theta(x). \quad (6.49)$$

For the bound (6.45) the integral can be calculated as

$$\begin{aligned} & - \int_{-\infty}^{\tilde{\lambda}} (\tilde{\lambda} - \lambda)^N \frac{d}{d\lambda} \exp(-e^{\lambda-\lambda_r}) d\lambda \approx \int_{\max\{0, \tilde{\lambda}-\lambda_r\}}^{\infty} \lambda^N e^{\tilde{\lambda}-\lambda_r-\lambda} d\lambda = \\ & = \begin{cases} (\tilde{\lambda} - \lambda_r)^{N+1} / (\tilde{\lambda} - \lambda_r - N), & \tilde{\lambda} - \lambda_r - N \gg \sqrt{N}, \\ N! e^{\tilde{\lambda}-\lambda_r}, & N - (\tilde{\lambda} - \lambda_r) \gg \sqrt{N}, \end{cases} \end{aligned} \quad (6.50)$$

where the abrupt cutoff of $\exp(-e^{\lambda-\lambda_r})$ at $\lambda > \lambda_r$ was simply replaced by a step function. For the bound (6.48) we obtain the integral

$$\theta(\tilde{\lambda} - \lambda_r) \int_{\lambda_r}^{\tilde{\lambda}} (\tilde{\lambda} - \lambda)^N e^{\lambda_r-\lambda} d\lambda = \begin{cases} (\tilde{\lambda} - \lambda_r)^{N+1} / (\tilde{\lambda} - \lambda_r - N), & N \gg 1, \\ (\tilde{\lambda} - \lambda_r)^N, & N \ll \tilde{\lambda} - \lambda_r. \end{cases} \quad (6.51)$$

In the following, we will be interested in the situation $\tilde{\lambda} - \lambda_r \gg N$, so our working estimate will be

$$[\tilde{\lambda} - L_r \ln N_r]^N < \overline{[\tilde{\lambda} + \ln \tilde{\mathcal{K}}_r]^N} < [\tilde{\lambda} + 3(L_r + N_r)]^N. \quad (6.52)$$

Let us now see how the above estimates are modified by correlations between different x_i 's in Eq. (6.37). To estimate the effect of bunching, we consider its extreme case by requiring that variables in groups of m are identical: $x_1 = x_2 = \dots = x_m$, $x_{m+1} = \dots = x_{2m}$, etc., This corresponds to replacement $\zeta \rightarrow \zeta^{1/m}$, $L_r + N_r - 2 \rightarrow (L_r + N_r - 2)/m$ is Eq. (6.37). Repeating the same steps, we obtain Eq. (6.45) with $e^{\lambda+3(L_r+N_r)} \rightarrow e^{\lambda/m+3(L_r+N_r)/m}$, and Eq. (6.47) with $e^{2(L_r+N_r-3)} \rightarrow e^{2m(L_r+N_r-3)}$. Note that

m cannot be too large, as this imposes strong restrictions on the structure of the resonance, so we assume $m \ll L_r, N_r$. Thus, the modification of Eq. (6.45) has no effect on the estimate (6.52) since one still can replace $\exp(-e^{(\lambda-\lambda_r)/m})$ by a step function in Eq. (6.50). As for modification of Eq. (6.47), it is completely absorbed in the passage from Eq. (6.47) to Eq. (6.48). To estimate the effect of antibunching, we set some of the variables in Eq. (6.37) to $x_i = 1$, thereby replacing $L_r + N_r - 2$ by a smaller number N' . This replacement can only decrease the value of ζ , so the probabilistic upper bound on ζ , expressed by Eq. (6.45), remains valid. In Eq. (6.47) we have to replace $e^{2(L_r+N_r-3)} \rightarrow e^{2(N'-1)}$, so this modification is also absorbed in the passage to Eq. (6.48). To summarize, the bounds established previously for uncorrelated x_i 's, are loose enough, so that the effects of correlations fit in these bounds as well.

6.6. On the number of resonances

Here we estimate the number of different coupling terms of the form (6.1), $\mathcal{R}(N_r, L_r)$, corresponding to given values of N_r and L_r . One of the oscillators is assumed to be fixed; otherwise, $\mathcal{R}(N_r, L_r)$ would be infinite due to the translational degree of freedom. As will be seen shortly, $\mathcal{R}(N_r, L_r)$ at large N_r, L_r can be represented as

$$\mathcal{R}(N_r, L_r) = \mathcal{R}_0(N_r, L_r) [R(L_r/N_r)]^{N_r}, \quad (6.53)$$

where $\mathcal{R}_0(N_r, L_r)$ is a power-law prefactor. Thus, most interesting for us is the quantity

$$R(p) = \lim_{N_r \rightarrow \infty} [\mathcal{R}(N_r, pN_r)]^{1/N_r}. \quad (6.54)$$

Finiteness of this quantity (i. e., the fact that it is neither zero, nor infinity) is equivalent to the validity of representation (6.53). The quantity $p = L_r/N_r$ is nothing but the ratio between the order of the perturbation theory in τ and the order in g . Note that $L_r \geq N_r$, since $n'_k \neq \bar{n}'_{k'}$ for any k, k' , and the oscillators must be coupled. Thus,

$$R(p < 1) = 0. \quad (6.55)$$

To obtain an upper bound on $R(p)$, let us choose some $2N_r$ -oscillator diagram and fix one of its free ends to a given site. Let us now count all possible positions of all other free ends and nonlinear vertices which produce the required L_r . In total, the diagram has $2N_r - 2$ Green's functions, each corresponding to a certain displacement along the chain. Thus, we simply have to sum over all possible displacements, keeping their sum equal to L_r . As mentioned above, N_r displacements cannot be smaller than unity, others can be zero:

$$\begin{aligned} & \sum_{k_1, \dots, k_{N_r} \geq 1} \sum_{k_{N_r+1}, \dots, k_{3N_r-2} \geq 0} \delta_{k_1 + \dots + k_{3N_r-2}, L_r} = \sum_{k_1, \dots, k_{3N_r-2} \geq 0} \delta_{k_1 + \dots + k_{3N_r-2}, L_r - N_r} = \\ & = \int_0^{2\pi} \frac{d\phi}{2\pi} \frac{e^{-i(L_r - N_r)\phi}}{(1 - e^{i\phi})^{3N_r-2}} = \frac{(L_r + 2N_r - 3)!}{(L_r - N_r)! (3N_r - 3)!}. \end{aligned} \quad (6.56)$$

This expression should be multiplied by 2^{3N_r-2} , since each k_j can correspond to a step to the left or to the right. This procedure produces all resonances with the given L_r which involve the starting site. Moreover, each resonance is counted several times, because the spatial arrangements of the diagram, differing by the positions of the nonlinear vertices, but with the same positions of the ends, are counted as different configurations. Thus, it indeed produces an upper bound, and we have

$$R(p) \leq \frac{8(p+2)^{p+2}}{27(p-1)^{p-1}} \leq 8(2p-1)^3. \quad (6.57)$$

To obtain a lower bound, consider a resonance with $n_k = 2k - 1$, $\bar{n}_k = 2k$, $k = 1, \dots, N_r$. Coupling the oscillators by a diagram similar to the one shown in Fig. 9 gives $L_r = 3N_r - 2$. If one exchanges $\bar{n}_k \leftrightarrow n_{k+1}$ for some k , L_r is not changed, but a different resonance is obtained. Thus, we can construct explicitly 2^{N_r-1} resonances with $L_r = 3N_r - 2$, which means that $R(p=3) \geq 2$. One can generalize this estimate by considering resonances with $\bar{n}_{N_r} - n_1 = L - 1$, and fixed $|\bar{n}_k - n_{k+1}| = 1$. Then $L_r = L + N_r - 2$, while the number of such resonances is at least $2^{N_r-1} (L/2 - 1)! / [(N_r - 1)! (L/2 - N_r)!]$ (L is divided by two, since we are counting the ways to distribute nearest-neighbor pairs). This gives

$$R(p \geq 3) \geq \sqrt{\frac{(p-1)^{p-1}}{(p-3)^{p-3}}} \geq e(p-3). \quad (6.58)$$

Taking into account the power-law prefactors, we obtain the upper and lower bounds as

$$\frac{e^{N_r}}{\sqrt{2\pi N_r}} \left[\frac{L_r}{N_r} - 3 \right]^{N_r-1} \leq \mathcal{R}(N_r, L_r) \leq 64^{N_r} \left[\frac{L_r}{N_r} - \frac{1}{2} \right]^{3N_r}, \quad (6.59)$$

where $\lfloor x \rfloor \equiv x \theta(x)$, i. e., $\lfloor x \rfloor = x$ for $x > 0$ and $\lfloor x \rfloor = 0$ otherwise. We will also need an upper bound for the contribution to $\mathcal{R}(N_r, L_r)$ from resonances with typical values of multiplicities $|m'_n| \sim m_r$. If we constrain $|m'_n| \geq m_r$, the number of oscillators is m^r times smaller. Thus, in the number of combinations we replace $N_r \rightarrow N_r/m_r$ (but not in the ratio L_r/N_r , since it cannot be too small even for high multiplicities):

$$\mathcal{R}(N_r, L_r) \leq \sum_{m_r=1}^{N_r} 64^{N_r/m_r} \left[\frac{L_r}{N_r} - \frac{1}{2} \right]^{3N_r/m_r}. \quad (6.60)$$

6.7. On resonant triples for not too weak disorder

The analysis of the stochastic phase volume of nearest-neighbor triples was performed in Sec. 5 under the condition $\tau \ll \rho$. This condition guaranteed that for two neighboring oscillators the phase space had a separatrix when the difference between their bare frequencies $|\omega_n - \omega_{n+1}|$ was sufficiently small. In the opposite case, $\tau \gg \rho$,

the minimal splitting of frequencies of the neighboring oscillators is $2\tau\Delta$ because of the coupling (also known as level repulsion, in the quantum-mechanical language), so the nonlinearity is too weak to produce the separatrix, as seen from Eq. (twoosboundary=).

Two normal modes of the disordered linear chain can have eigenfrequencies much closer than $\tau\Delta$ only if they are well separated in space. Indeed, the effective coupling between two oscillators separated by a distance l can be obtained in the $(l - 1)$ st order of the perturbation theory, and is given by Eq. (6.9). Strictly speaking, it is a random quantity, so its statistics should be analyzed. However, we note that the typical value of the splitting scales as $\tau^l\Delta$, rapidly falling off with the distance. As soon as this splitting becomes $\sim \rho\Delta$ or smaller, the separatrix can appear. On the one hand, this can always be satisfied when l is large. On the other, if l is too large, the coupling will be very weak, so the effective pendulum frequency will be very small, and the stochastic layer will be very thin due to Melnikov-Arnold exponential. Thus, the optimal value of l is such that $\tau^l \sim \rho$. The same arguments can be used for the choice the third oscillator, needed to destroy the separatrix and to produce the stochastic layer. Thus, we face the situation similar to that of Sec. 5, but the coupling constant τ should be replaced by $\tau \rightarrow \tau^l \sim \rho$. Hence, the average density of the chaotic spots for $\tau \gg \rho$ is $\bar{w} \sim \rho^2$.

Finally, we note that the situation described above (effective tunnelling coupling between two oscillators being of the same order as the nonlinearity and their frequency mismatch) corresponds to nonlinear coupling between two double-humped eigenstates of the linear problem. The distance between the two humps is given by l , and the two eigenstates correspond to different mutual signs of the humps of the wavefunction. The importance of double-humped states for the wave-packet spreading was discussed in Ref. [29].

7. Probability distribution of the chaotic fraction

7.1. General remarks on the procedure

Each site n of the chain can be characterized by a variable w_n , the chaotic fraction of the thermally-weighted phase volume, summed over all possible guiding resonances involving the site n and sites to the right of it [to be formally defined below, Eq. (7.8)]. For a resonant nearest-neighbor triple at $\tau \ll \rho$ this quantity was defined in Eq. (5.29) and estimated in Sec. 5.4, the result being [see Eqs. (5.42a), (5.42b)]

$$w_n \sim \frac{\tau}{\rho} e^{-E_n/T}, \quad 2gE_n = 3 \max_{k=n,n+1,n+2} (\omega_k - \mu)^2 - \sum_{k=n}^{n+2} (\omega_k - \mu)^2. \quad (7.1)$$

Note that the definition of w_n involves the thermal averaging but not the disorder averaging. Thus, w_n is still a random quantity, determined by random frequencies of the oscillators in the vicinity of the site n . Our goal in this section is to find its probability distribution function for values w much smaller than its disorder-averaged value, $w \ll$

$\min\{\tau\rho, \rho^2\}$. For this purpose Eq. (7.1) is of no use, as it greatly underestimates the typical value of w (the value where the probability distribution has a maximum), giving $w \sim (\tau/\rho)e^{-1/\rho}$. In fact, one can typically find chaotic phase volume at lower energies by taking into consideration guiding and layer resonances which involve many oscillators.

Typically, for a given guiding resonance g and a given layer resonance ℓ , the corresponding contribution to the chaotic fraction, $w^{(g,\ell)}$, is very small (much smaller than for a nearest-neighbor triple, as high orders of perturbation theory have to be involved). That is, the probability that it exceeds some value $w_0 = e^{-\lambda}$, $\mathcal{P}\{w^{(g,\ell)} > w_0\}$, is small unless w_0 itself is very small. However, $w < w_0$ means that $w^{(g,\ell)} < w_0$ for all of the numerous candidates for guiding and layer resonances. The probability of this event can be written as (assuming statistical independence of the contributions from different resonances)

$$\mathcal{P}\{w < w_0\} = \prod_{g,\ell} \left(1 - \mathcal{P}\{w^{(g,\ell)} > w_0\}\right) \approx \exp\left[-\sum_{g,\ell} \mathcal{P}\{w^{(g,\ell)} > w_0\}\right] \equiv e^{-S}. \quad (7.2)$$

Thus, S is determined by the competition of the smallness of each individual probability $\mathcal{P}\{w^{(g,\ell)} > w_0\}$ and the large number of terms in the sum.

It is more convenient technically to perform the summation in Eq. (7.2) in two steps. First, we calculate

$$S_g(\lambda) = \sum_{\ell} \overline{\theta(w^{(g,\ell)} - e^{-\lambda})}, \quad (7.3a)$$

where $\theta(x)$ is the Heaviside step function, and the overline denotes the statistical averaging over the frequencies involved in the layer resonance, while the guiding resonance is kept fixed. Thus, e^{-S_g} is the probability of $w^{(g)} < e^{-\lambda}$ for a given guiding resonance, but after the optimization over the layer resonances. On the second step, we calculate

$$S(\lambda) = \sum_g \mathcal{P}\{w^{(g)} > e^{-\lambda}\} = \sum_g \left(1 - \overline{e^{-S_g(\lambda)}}\right), \quad (7.3b)$$

where the averaging is performed over the frequencies of the guiding resonance. This latter averaging is assumed to be independent from the former one. Note that expanding the exponential and simply averaging $\overline{S_g}$ would produce a wrong result, since at large λ (the ones we are interested in) the main contribution to the average would come from configurations for which the expansion $1 - e^{-S_g} \approx S_g$ is not valid. This point will be discussed in more detail in Sec. 7.5.1.

The main body of the bulky calculations is presented in Secs. 7.3–7.5, and the result is summarized in Sec. 7.6.

7.2. Definitions

Consider a guiding resonance g (defined as in Sec. 6.5, $r = g$) with the effective coupling as in Eq. (6.27):

$$V = -2V_g \cos\left(\phi_{n_1^g} + \dots + \phi_{n_{N_g}^g} - \phi_{\bar{n}_1^g} - \dots - \phi_{\bar{n}_{N_g}^g}\right). \quad (7.4)$$

This coupling determines the effective pendulum Hamiltonian \check{H}_g and the frequency Ω_g ,

$$\check{H}_g = \frac{g}{2} |\underline{m}^g|^2 \check{p}^2 - 2V_g \cos \check{\phi}, \quad \Omega_g = \sqrt{2|\underline{m}^g|^2 g |V_g|}, \quad (7.5)$$

where $\check{\phi} = \phi_{n_1^g} + \dots + \phi_{n_{N_g}^g} - \phi_{\bar{n}_1^g} - \dots - \phi_{\bar{n}_{N_g}^g}$ is the slow phase (pendulum coordinate), and \check{p} is the pendulum momentum (see Appendix D for the discussion of the kinetic energy term).

The resonance condition reads as

$$I_{n_1^g} + \dots + I_{n_{N_g}^g} - I_{\bar{n}_1^g} - \dots - I_{\bar{n}_{N_g}^g} = -\frac{\omega_{n_1^g} + \dots + \omega_{n_{N_g}^g} - \omega_{\bar{n}_1^g} - \dots - \omega_{\bar{n}_{N_g}^g}}{g} \equiv I_g^{\min}. \quad (7.6)$$

The right-hand side is positive, as we have imposed condition (6.23). Then the resonant configuration with the lowest activation barrier is obtained by setting to zero all $I_{\bar{n}}^g$'s, and all I_n^g 's except one, $I_{n_*^g}$, where n_*^g is the site having the largest multiplicity $m_{n_*^g}^g$, and if there are several such sites, the one with the smallest ω_n should be chosen. For this site one should set $I_{n_*^g} = I_g^{\min} / m_{n_*^g}^g$. This lowest activation barrier is given by

$$E_g = (\omega_{n_*^g} - \mu) \frac{I_g^{\min}}{m_{n_*^g}^g} + \frac{g}{2} \left(\frac{I_g^{\min}}{m_{n_*^g}^g} \right)^2. \quad (7.7)$$

The chaotic fraction $w_n^{(g)}$ corresponding to a given guiding resonance g is defined as

$$w_{n_*^g}^{(g)} = \left\langle |\underline{m}^g|^2 W_s \delta \left(I_{n_1^g} + \dots + I_{n_{N_g}^g} - I_{\bar{n}_1^g} - \dots - I_{\bar{n}_{N_g}^g} - I_g^{\min} \right) \right\rangle_T, \quad (7.8)$$

where the thermal average is defined in the usual way,

$$\langle \dots \rangle_T = \frac{\int (\dots) e^{(H - \mu I_{\text{tot}})/T} \prod_{n=-\infty}^{\infty} dI_n d\phi_n / 2\pi}{\int e^{(H - \mu I_{\text{tot}})/T} \prod_{n=-\infty}^{\infty} dI_n d\phi_n / 2\pi}. \quad (7.9)$$

The prefactor $|\underline{m}^g|^2 W_s$ in front of the δ -function in Eq. (7.8) represents the effective thickness of the resonant hyperplane defined by the δ -function, and is discussed in detail in Appendix D. W_s is the volume of the stochastic layer in the phase space of the effective pendulum. It is determined by the strength and the frequency mismatch of the layer resonance, so it depends on the actions of all oscillators involved in the layer resonance. The definitions and notations for the layer resonance are again as in Sec. 6.5, $r = \ell$. Then W_s can be found similarly to the case of a resonant pair, Eq. (5.19):

$$W_s = \frac{\Omega_g}{\pi |\underline{m}^g|^2 g} \frac{5 |V_\ell|}{2 |V_g|} \Lambda^2 \mathcal{A}_m(\Lambda) \ln \frac{2^{21/5} e |V_g| / |V_\ell|}{\Lambda^2 \mathcal{A}_m(\Lambda)}, \quad (7.10a)$$

where the Melnikov-Arnold integral is defined in Eq. (5.13), and its index and the argument are given by

$$m = 2 \frac{|(\underline{m}^g, \underline{m}^\ell)|}{|\underline{m}^g|^2}, \quad \Lambda = \frac{\tilde{\omega}_{n_1^\ell} + \dots + \tilde{\omega}_{n_{N_\ell}^\ell} - \tilde{\omega}_{\bar{n}_1^\ell} - \dots - \tilde{\omega}_{\bar{n}_{N_\ell}^\ell}}{\Omega_g} \equiv \frac{\varpi_\ell}{\Omega_g}. \quad (7.10b)$$

Definition (7.8) and expression (7.10a) are meaningful only when $\Lambda \gg 1$. When this is not the case, the two resonances should be treated on equal footing, so the situation is analogous to the case of the resonant triple. In particular, one arrives at a Hamiltonian similar to Eq. (5.28) with the kinetic energy given by $(g/2)|\underline{m}^g|^2 p_1^2 + g(\underline{m}^g, \underline{m}^\ell) p_1 p_2 + (g/2)|\underline{m}^\ell|^2 p_2^2$. In Eq. (7.8) the second δ -function should be introduced, and instead of $|\underline{m}^g|^2 W_s$ the prefactor should be $(|\underline{m}^g|^2 |\underline{m}^\ell|^2 - (\underline{m}^g, \underline{m}^\ell)^2) W_{ss}$, where W_{ss} is defined analogously to Eq. (5.30a). It will be seen below, however, that for those values of w which are important for the transport, $\Lambda \gg 1$ holds. Also, $\Lambda \gg m$ (indeed, m can grow at most linearly with N_g, N_ℓ , while Λ is exponential in N_g), so that the asymptotic expression (5.14) for the Melnikov-Arnold integral can be used.

Expression (7.10a) for W_s is already quite cumbersome for explicit analytical calculations. Hence, we will work with its upper and lower bounds,

$$10N_g \frac{\Delta}{g} \left(\frac{g|V_\ell|}{\Delta^2} \right) \frac{1}{(2N_\ell)!} e^{-\pi\Lambda/2} < |\underline{m}^g|^2 W_s < 20N_g^2 \frac{\Delta}{g} \left(\frac{g|V_\ell|}{\Delta^2} \right)^{1/\pi} \frac{(2\Lambda)^{(m+1)/\pi}}{[\Gamma(m)]^{1/\pi}} e^{-\Lambda/2}. \quad (7.11)$$

They can be obtained using the following inequalities, which are easy to check:

$$x \ln \frac{2^{21/5} e}{x} < 8x^{1/\pi}, \quad 2N_g \leq |\underline{m}^g|^2 < 2N_g^2, \quad \frac{1}{2N_g^2} \leq \frac{|(\underline{m}^g, \underline{m}^\ell)|}{|\underline{m}^g|^2} < N_\ell,$$

$$\Omega_g < \Delta \quad \Rightarrow \quad |V_g| < \frac{\Delta^2}{4gN_g}.$$

The upper bound for $|\underline{m}^g|^2 W_s$ can be further simplified by noting that large values of m are extremely inefficient. Indeed, if the guiding and the layer resonances have just one site in common, $m \sim 1/N_g$. To increase m to unity and beyond, about mN_g oscillators of the layer resonance should be restricted to overlap with the guiding resonance. According to the estimate (6.59), such a restriction would decrease the number of available layer resonances by a factor $\sim e^{mN_g}$, which would increase the typical smallest ϖ_ℓ by the same factor. Thus, we can estimate $\Lambda_m \sim \Lambda_0 e^{mN_g}$. The minimum of the function

$$\frac{(\Lambda_0 e^{mN_g})^{(m+1)/\pi}}{[\Gamma(m)]^{1/\pi}} \exp(-\Lambda_0 e^{mN_g}/2)$$

for $\Lambda_0 \gg 1$ is reached at small $m \rightarrow 0$. Using also the fact that $\Lambda^{1/\pi} e^{-\Lambda/2} < e^{-\Lambda/3}$, we obtain the following upper bound:

$$|\underline{m}^g|^2 W_s < 25N_g^3 \frac{\Delta}{g} \left(\frac{g|V_\ell|}{\Delta^2} \right)^{1/\pi} e^{-\Lambda/3}. \quad (7.12)$$

7.3. Thermal averaging

To integrate over the actions, it is convenient to resolve the δ -function in Eq. (7.8) with respect to $I_{n_*^g}$. As will be seen later, the typical value of action for oscillators with $n^g, \bar{n}^g, n^\ell, \bar{n}^\ell \neq n_*^g$, as well as the typical thermal value of the action, $T/|\mu|$, are much smaller than the typical value of I_g^{\min} :

$$I_n, \frac{T}{|\mu|} \ll I_g^{\min}. \quad (7.13)$$

Thus, we simply set $I_{n_*^g} = I_g^{\min}$.

7.3.1. Lower bound

In order to obtain the lower bound for w we write

$$\frac{\pi\Lambda}{2} < \frac{\pi\varpi_\ell}{4\sqrt{N_g g \mathcal{K}_g(I_g^{\min})^{m_{n_*^g}^g/2}} \prod_{n \neq n_*^g} \frac{1}{I_n^{|m_n^g|/4}}} < \frac{\pi\varpi_\ell}{4\sqrt{N_g g \mathcal{K}_g(T/|\mu|)^{m_{n_*^g}^g/2}} \prod_{n \neq n_*^g} \frac{1}{I_n^{|m_n^g|/4}}}, \quad (7.14)$$

while $|V_\ell|$ can be averaged over the thermal distribution independently. For the integral over the oscillators of the guiding resonance we use the inequality, derived in Appendix E for $A \gg 1$:

$$\int_0^\infty \exp\left[-A \prod_{n \neq n_*^g} \frac{1}{x_n^{|m_n^g|/4}}\right] \prod_{n \neq n_*^g} e^{-x_n} dx_n > \exp\left[-(2N_g - m_{n_*^g}^g + 4) \left(\frac{A}{4}\right)^{4/(2N_g - m_{n_*^g}^g + 4)}\right], \quad (7.15)$$

and simplify the argument of the exponential using

$$(2N_g - m_{n_*^g}^g + 4) \left(\frac{\pi}{16} \frac{1}{\sqrt{N_g}}\right)^{4/(2N_g - m_{n_*^g}^g + 4)} < 2N_g, \quad A^{4/(2N_g - m_{n_*^g}^g + 4)} < A^{4/N_g}, \quad (7.16)$$

while for the oscillators of the layer resonance we use the inequality

$$\int_0^\infty \prod_n x_n^{|m_n^\ell|/2} e^{-x_n} dx_n > e^{-N_\ell}, \quad (7.17)$$

following from the fact that $\Gamma(x+1) > e^{-x}$. As a result, the lower bound for w is

$$w^{(g,\ell)} > \frac{\mathcal{K}_\ell(T/e|\mu|)^{N_\ell-1}}{\Delta(2N_\ell)!} e^{-E_g/T} e^{-2N_g \Lambda_T^{4/N_g}}, \quad \Lambda_T \equiv \frac{\varpi_\ell}{\sqrt{g \mathcal{K}_g(T/|\mu|)^{N_g}}}. \quad (7.18)$$

7.3.2. Upper bound

Let us first average the actions of the oscillators belonging to the layer resonance, assuming it to have only one oscillator in common with the guiding resonance (see the discussion in the end of Sec. 7.2).

$$w^{(g,\ell)} < \frac{25N_g^3}{\Gamma(1/(2\pi) + 1)} \frac{|\mu|\Delta}{gT} \left[\sqrt{\frac{E_g}{T}} \frac{g\mathcal{K}_\ell}{\Delta^2} \left(\frac{T}{|\mu|} \right)^{N_\ell} \right]^{1/\pi} e^{-E_g/T} \langle e^{-\Lambda/3} \rangle_T \prod_{n=-\infty}^{\infty} \Gamma\left(\frac{|m_n^\ell|}{2\pi} + 1\right). \quad (7.19)$$

As in Sec. 7.2, this estimate can be simplified using the fact that large values of $|m_n^\ell|$ are inefficient. Indeed, suppose all $|m_n^\ell|$ are either equal to m or 0 ($1 \ll m < N_\ell$). Then the product of the gamma functions can be estimated as

$$[\Gamma(m/2\pi + 1)]^{2N_\ell/m} \sim \left(\frac{m}{2\pi e}\right)^{N_\ell/\pi}.$$

At the same time, this leads to an increase of Λ , $\Lambda \sim \Lambda_{m=1} e^{N_\ell} e^{-N_\ell/m}$. Clearly, the maximum of the function $m^{N_\ell/(2\pi)} e^{-\Lambda_1 e^{N_\ell} e^{-N_\ell/m}}$ is reached at the smallest $m = 1$. Analogously, one can show that restriction of one of the sites of the layer resonance to n_*^g again does more harm by increasing Λ by a factor of the order of 1, than help by introducing a factor E_g/T . Using $\Gamma(1/(2\pi) + 1) < 1$, we can simply replace all gamma functions by unity.

The average $\langle e^{-\Lambda/3} \rangle_T$ is sensitive to the multiplicities m_n^g . Again, large multiplicities are not efficient in lowering E_g , however, this fact is not obvious at this stage of the calculation, and it will be proven later, in Sec. 7.5.3. For the moment, we keep the typical multiplicity m^g as an additional degree of freedom and optimize with respect to it afterwards. The thermal average is estimated using the inequality

$$\int_0^\infty \exp\left[-x_1 - \dots - x_N - \frac{A}{(x_1 \dots x_N)^\alpha}\right] dx_1 \dots dx_N \leq N \left(\frac{8\pi}{e^2}\right)^{N/2} \exp\left[-\frac{N}{2} (\alpha A)^{1/(N\alpha+1)}\right], \quad (7.20)$$

proven in Appendix E. Let set $\alpha = m^g/4$, $N = (2N_g - m_{n_*^g}^g)/m^g$. In fact,

$$\begin{aligned} & \frac{2N_g - m_{n_*^g}^g}{m^g} \left(\frac{8\pi}{e^2}\right)^{(2N_g - m_{n_*^g}^g)/(2m^g)} \exp\left[-\frac{2N_g - m_{n_*^g}^g}{2m^g} (\alpha A)^{4/(2N_g - m_{n_*^g}^g + 4)}\right] \leq \\ & \leq 2N_g \left(\frac{8\pi}{e^2}\right)^{N_g/m^g} \exp\left[-\frac{N_g}{2m^g} (\alpha A)^{2/N_g}\right], \end{aligned}$$

where we denoted $m_{n_*^g}^g \equiv m_{n_*^g}^g$ for compactness. Thus, we arrive at the following upper

bound:

$$\begin{aligned}
w^{(g,\ell)} &< 50N_g^4 \frac{|\mu|\Delta}{gT} \left[\sqrt{\frac{E_g}{T}} \frac{g\mathcal{K}_\ell}{\Delta^2} \left(\frac{T}{|\mu|}\right)^{N_\ell} \right]^{1/\pi} \left(\frac{8\pi}{e^2}\right)^{N_g/m^g} e^{-E_g/T} \times \\
&\times \exp \left[-\left(\frac{N_g}{2m^g}\right)^{1-2/N_g} \left(\frac{T}{E_g}\right)^{m_g^g/(2N_g)} \left(\frac{\Lambda_T}{12}\right)^{2/N_g} \right], \quad (7.21) \\
\Lambda_T &\equiv \frac{\varpi_\ell}{\sqrt{g\mathcal{K}_g(T/|\mu|)^{N_g}}}.
\end{aligned}$$

7.4. Summation over layer resonances

The previous subsection was dedicated to the estimation of the contribution to the chaotic fraction $w^{(g,\ell)}$ due to a given pair of guiding and layer resonances (g, ℓ) . Here we are going to perform the summation over ℓ in Eq. (7.2):

$$S_g(\lambda) = \sum_{\ell} \mathcal{P} \{ w^{(g,\ell)} > e^{-\lambda} \} \quad (7.22)$$

Since afterwards this quantity will be summed over the guiding resonances, we are interested in those λ for which $S_g \ll 1$. In Sec. 7.3 upper and lower bounds for $w^{(g,\ell)}$ were given, $w_{<}^{(g,\ell)} < w^{(g,\ell)} < w_{>}^{(g,\ell)}$. Then, S_g can be estimated as

$$\sum_{\ell} \overline{\theta \left(\lambda - \ln \frac{1}{w_{<}^{(g,\ell)}} \right)} < S_g(\lambda) < \sum_{\ell} \overline{\theta \left(\lambda - \ln \frac{1}{w_{>}^{(g,\ell)}} \right)}, \quad (7.23)$$

where the averaging is performed over the frequencies involved in the layer resonance.

7.4.1. Lower bound

The lower bound, $w_{<}^{(g,\ell)}$, depends on the frequencies through two quantities: the frequency mismatch ϖ_ℓ and the coupling \mathcal{K}_ℓ . For the former we simply use the central limit theorem, Eq. (6.33). Moreover, since we are interested in very small ϖ_ℓ , the Gaussian exponential can be omitted. Then we obtain

$$S_g > \sqrt{\frac{g\mathcal{K}_g(T/|\mu|)^{N_g}}{\Delta^2}} \frac{1}{(2N_g)^{N_g/4}} \sum_{\ell} \frac{1}{N_\ell} \left[\lambda - \frac{E_g}{T} - \ln \frac{(2N_\ell)!}{(\rho/e)^{N_\ell-1}} - \ln \frac{g^{N_\ell-1}}{\Delta^{N_\ell-2}\mathcal{K}_\ell} \right]^{N_g/4}, \quad (7.24)$$

where $\rho \equiv gT/(|\mu|\Delta)$, and where $[x] \equiv x\theta(x)$, i. e., $[x] = x$ for $x > 0$ and $[x] = 0$ otherwise.

To average over \mathcal{K}_ℓ , we use the left inequality in Eq. (6.52):

$$S_g > \sqrt{\frac{g\mathcal{K}_g(T/|\mu|)^{N_g}}{\Delta^2}} \frac{1}{(2N_g)^{N_g/4}} \sum_\ell \frac{1}{N_\ell} \times \left[\lambda - \ln \frac{\sqrt{2\pi N_\ell \rho}}{4e} - \frac{E_g}{T} - N_\ell \ln \left(\frac{4N_\ell^2}{e\rho} + 2 \right) - L_\ell \ln \frac{2N_\ell}{\tau} \right]^{N_g/4}. \quad (7.25)$$

We sum over L_ℓ, N_ℓ using the left inequality (6.59):

$$S_g > \sqrt{\frac{g\mathcal{K}_g(T/|\mu|)^{N_g}}{\Delta^2}} \frac{1}{(2N_g)^{N_g/4}} \sum_{N_\ell} \frac{(e/N_\ell)^{N_\ell}}{\sqrt{2\pi N_\ell}} \times \sum_{L_\ell} \left[\lambda - \ln \frac{\sqrt{2\pi N_\ell \rho}}{4e} - \frac{E_g}{T} - N_\ell \ln \left(\frac{4N_\ell^2}{e\rho} + 2 \right) - L_\ell \ln \frac{2N_\ell}{\tau} \right]^{N_g/4} [L_\ell - 3N_\ell]^{N_\ell}. \quad (7.26)$$

The sum over L_ℓ is estimated from below by its largest term,

$$L_\ell - 3N_\ell = \frac{N_\ell}{N_g/4 + N_\ell} \frac{\lambda - E_g/T - \ln(\sqrt{2\pi N_\ell \rho}/4e) - N_\ell \ln[32N_\ell^5/(e\tau^3\rho)]}{\ln(2N_\ell/\tau)}, \quad (7.27a)$$

$$S_g > \sqrt{\frac{g\mathcal{K}_g(T/|\mu|)^{N_g}}{\Delta^2}} \frac{1}{2^{3N_g/4}} \sum_{N_\ell} \frac{1}{\sqrt{2\pi N_\ell}} \left[\frac{e}{\ln(2N_\ell/\tau)} \right]^{N_\ell} \frac{1}{(N_\ell + N_g/4)^{N_\ell + N_g/4}} \times \left[\lambda - \ln \frac{\sqrt{2\pi N_\ell \rho}}{4e} - \frac{E_g}{T} - N_\ell \ln \frac{32N_\ell^5}{e\tau^3\rho} \right]^{N_\ell + N_g/4}. \quad (7.27b)$$

Again, we estimate the sum over N_ℓ from below by its largest term. It is easy to show that

$$\max_N \left(\frac{A}{N} - a \right)^N = e^{(A/a)F(a)}, \quad N_{max} = \frac{A/a}{1 + 1/F(a)}, \quad (7.28a)$$

where the function $F(a)$ is defined as the solution of the equation

$$\ln \frac{a}{F} = 1 + F. \quad (7.28b)$$

We note that $F(a \rightarrow 0) = a/e + O(a^2)$, $F(e^2) = 1$, $F(a \rightarrow \infty) \sim \ln a$, and

$$\frac{1}{2} \ln a \leq F(a) < \ln(2a), \quad a \geq 1. \quad (7.28c)$$

As will be seen later, the values of λ which are important for the transport correspond to N_g, N_ℓ satisfying the inequalities

$$N_g \ll N_\ell \ll \frac{1}{\tau}, \frac{1}{\rho}. \quad (7.29)$$

Thus, with logarithmic precision we approximate

$$\ln \frac{32N_\ell^5}{e\tau^3\rho} \approx \ln \frac{1}{\tau^3\rho}, \quad \ln \frac{4e}{\sqrt{2\pi N_\ell\rho}} \approx \ln \frac{1}{\rho} \quad (7.30)$$

so we arrive at the following bound

$$S_g > \frac{1}{\sqrt{2\pi}} \sqrt{\frac{g\mathcal{K}_g(T/|\mu|)^{N_g}}{\Delta^2}} \left(\frac{1}{8e} \ln \frac{1}{\tau^3\rho} \right)^{N_g/4} \left[\frac{\lambda + \ln(1/\rho) - E_g/T}{\ln(1/\tau^3\rho)} + \frac{N_g}{4} \right]^{-1/2} \times \quad (7.31)$$

$$\times \exp \left\{ \left[\frac{\lambda + \ln(1/\rho) - E_g/T}{\ln(1/\tau^3\rho)} + \frac{N_g}{4} \right] F \left(\frac{e \ln(1/\tau^3\rho)}{\ln(1/\tau)} \right) \right\}.$$

7.4.2. Upper bound

The procedure is not very different from that for the lower bound. After using the central limit theorem for ϖ_ℓ and averaging over \mathcal{K}_ℓ with the help of the right inequality in Eq. (6.52), we obtain

$$S_g < 24 \left(\frac{E_g}{T} \right)^{m_g^s/4} \sqrt{\frac{g\mathcal{K}_g(T/|\mu|)^{N_g}}{\Delta^2}} \left(\frac{2m_g^s}{N_g} \right)^{N_g/2-1} \times$$

$$\times \sum_\ell \left[\lambda - \frac{E_g}{T} - \ln \left(\frac{\rho}{50N_g} \left[\frac{T}{16E_g} \right]^{1/2\pi} \left[\frac{e^2}{8\pi} \right]^{N_g/m_g^s} \right) - \frac{N_\ell}{\pi} \ln \frac{2}{e^3\rho} - \frac{L_\ell}{\pi} \ln \frac{2}{e^3\tau} \right]^{N_g/2}. \quad (7.32)$$

We sum over L_ℓ, N_ℓ using the right inequality (6.59). The sum over L_ℓ is estimated from above by its largest term, which corresponds to

$$L_\ell - \frac{N_\ell}{2} = \frac{3N_\ell}{N_g/2 + 3N_\ell} \frac{\pi}{\ln(2e^{-3}/\tau)} \times$$

$$\times \left[\lambda - \frac{E_g}{T} - \ln \left(\frac{\rho}{50N_g} \left[\frac{T}{16E_g} \right]^{1/2\pi} \left[\frac{e^2}{8\pi} \right]^{N_g/m_g^s} \right) - \frac{N_\ell}{2\pi} \ln \frac{8}{e^9\rho^2\tau} \right],$$

multiplied by the number of terms,

$$\frac{\pi}{\ln(2e^{-3}/\tau)} \left[\lambda - \frac{E_g}{T} - \ln \left(\frac{\rho}{50N_g} \left[\frac{T}{16E_g} \right]^{1/2\pi} \left[\frac{e^2}{8\pi} \right]^{N_g/m_g^s} \right) - \frac{N_\ell}{2\pi} \ln \frac{8}{e^9\rho^2\tau} \right].$$

This gives

$$\begin{aligned}
S_g &< \frac{N_g}{2m^g} \left(\frac{E_g}{T} \right)^{m_*^g/4} \sqrt{\frac{g\mathcal{K}_g(T/|\mu|)^{N_g}}{\Delta^2}} (2m^g)^{N_g/2} \times \\
&\times \sum_{N_\ell} \left(\frac{24\pi}{\ln(2e^{-3}/\tau)} \right)^{3N_\ell+1} \frac{1}{(6N_\ell + N_g)^{N_g/2+3N_\ell}} \times \\
&\times \left[\lambda - \frac{E_g}{T} - \ln \left(\frac{\rho}{50N_g} \left[\frac{T}{16E_g} \right]^{1/2\pi} \left[\frac{e^2}{8\pi} \right]^{N_g/m^g} \right) - \frac{N_\ell}{2\pi} \ln \frac{8}{e^9\tau\rho^2} \right]^{N_g/2+3N_\ell+1}.
\end{aligned} \tag{7.33}$$

The sum over N_ℓ is again estimated from above by its largest term multiplied by the number of terms using Eqs. (7.28a)–(7.28c) and Eq. (7.29). Also, we estimate $E_g/T < N_g/(m_*^g\rho)$ in the prefactor and under the logarithm, where we replaced the Gaussian distribution (6.33) for the frequency difference in Eq. (7.6) by a box distribution. This gives

$$\begin{aligned}
S_g &< \frac{3N_g}{m^g} \left(\frac{N_g}{m_*^g\rho} \right)^{m_*^g/4} \sqrt{\frac{g\mathcal{K}_g(T/|\mu|)^{N_g}}{\Delta^2}} \left(\frac{m^g}{12\pi} \ln \frac{1}{\tau} \right)^{N_g/2} \times \\
&\times \left[\frac{6\pi(\lambda - \lambda_1^> - E_g/T)}{\ln(1/\tau\rho^2)} + \frac{6\pi \ln(8\pi/e^2)}{\ln(1/\tau\rho^2)} \frac{N_g}{m^g} + \frac{N_g}{2} \right]^2 \times \\
&\times \exp \left\{ \left[\frac{6\pi(\lambda - \lambda_1^> - E_g/T)}{\ln(1/\tau\rho^2)} + \frac{6\pi \ln(8\pi/e^2)}{\ln(1/\tau\rho^2)} \frac{N_g}{m^g} + \frac{N_g}{2} \right] F \left(\frac{2 \ln(1/\tau\rho^2)}{\ln(1/\tau)} \right) \right\}, \\
\lambda_1^> &= \ln \left[\frac{\rho}{50N_g} \left(\frac{e^9\tau\rho^2}{8} \right)^{1/6\pi} \left(\frac{m_*^g\rho}{16N_g} \right)^{1/2\pi} \right].
\end{aligned} \tag{7.34}$$

7.5. Summation over guiding resonances

7.5.1. Toy calculation

Before proceeding with the main calculation, let us illustrate the difference between two ways of calculation of S from S_g , mentioned in Sec. 7.1, namely,

$$S = \sum_g \overline{S_g} \tag{7.35}$$

and

$$S = \sum_g \overline{(1 - e^{-S_g})}, \tag{7.36}$$

using a simplified “toy” expression, which nevertheless captures the essential features of the results obtained in Sec. 7.4:

$$S_g = (\tau^p\rho)^{N_g} \exp \left(\frac{\lambda - x_g/\rho}{\ln(1/\tau^p\rho)} \right). \tag{7.37}$$

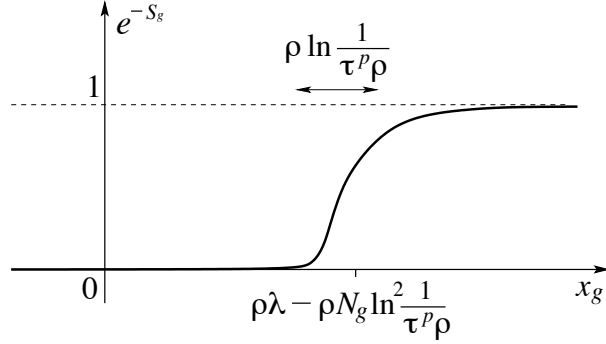


Figure 10: A schematic plot of e^{-S_g} as a function of x_g , as determined by Eq. (7.37).

Here x_g is a random variable uniformly distributed on $0 \leq x_g \leq 1$, ascribed to each guiding resonance. The number of resonances corresponding to a given N_g will be taken to be simply 2^{N_g} just for this toy calculation.

The first calculation is straightforward:

$$\begin{aligned} \sum_g \overline{S_g} &= \sum_{N_g=1}^{\infty} (2\tau^p \rho)^{N_g} \left\{ \theta(1 - \lambda \rho) \left[\left(e^{\lambda / \ln(1/\tau^p \rho)} - 1 \right) \rho \ln \frac{1}{\tau^p \rho} + 1 - \lambda \rho \right] + \right. \\ &\quad \left. + \theta(\lambda \rho - 1) e^{\lambda / \ln(1/\tau^p \rho)} \left(1 - e^{-1/\rho \ln(1/\tau^p \rho)} \right) \rho \ln \frac{1}{\tau^p \rho} \right\} \approx \\ &\approx \left(e \tau^p \rho^2 \ln \frac{1}{\tau^p \rho} \right) e^{\lambda / \ln(1/\tau^p \rho)}. \end{aligned} \quad (7.38)$$

The sum is dominated by $N_g = 1$, which corresponds to resonant pairs. This means that only two resonances (i. e., 2^{N_g} as mentioned in the previous paragraph, taken at $N_g = 1$) effectively contribute. Thus the whole calculation is meaningless, the correct one being

$$e^{-S} = \prod_g \mathcal{P} \left\{ w^{(g)} < e^{-\lambda} \right\} = \prod_g \overline{e^{-S_g}}. \quad (7.39)$$

When $1 - \overline{e^{-S_g}} \ll 1$, this is equivalent to Eq. (7.36).

The plot of e^{-S_g} as a function of x_g is schematically shown in Fig. 10. It can be viewed as a step function with a width of the order of $\rho \ln(1/\tau^p \rho)$. As long as this width is smaller than the offset, $x_g = \lambda \rho - \rho N_g \ln^2(1/\tau^p \rho)$, defined as the point where $S_g = 1$, we can simply approximate it by the Heaviside function. Then

$$\overline{e^{-S_g}} = 1 - \rho \left[\lambda - N_g \ln^2 \frac{1}{\tau^p \rho} \right] \quad (7.40)$$

(we remind that $\lfloor x \rfloor = x$ for $x > 0$ and $\lfloor x \rfloor = 0$ otherwise), which gives

$$S = \rho \sum_{N_g=1}^{\lambda/\ln^2(1/\tau^p\rho)} 2^{N_g} \left(\lambda - N_g \ln^2 \frac{1}{\tau^p\rho} \right) = \rho \left(\ln \frac{1}{\tau^p\rho} \right)^2 \left(\sum_{N=1}^{\infty} 2^{-N} N \right) e^{\lambda \ln 2 / \ln^2(1/\tau^p\rho)}. \quad (7.41)$$

Note that the typical value of the offset, $\lambda\rho - \rho N_g \ln^2(1/\tau^p\rho) \sim \rho \ln^2(1/\tau^p\rho)$, which is indeed greater than the width, $\rho \ln(1/\tau^p\rho)$.

7.5.2. Lower bound

As discussed above, from estimate (7.31) for S_g we pass to the estimate for S :

$$S > \sum_g \overline{\left[1 - \exp(-e^{\lambda_g}) \right]},$$

$$\lambda_g = \left(\frac{\lambda - \ln \rho - E_g/T}{\ln(1/\tau^3\rho)} + \frac{N_g}{4} \right) F \left(\frac{e \ln(1/\tau^3\rho)}{\ln(1/\tau)} \right) - \frac{1}{2} \ln \left(\frac{\lambda - \ln \rho - E_g/T}{\ln(1/\tau^3\rho)} + \frac{N_g}{4} \right) +$$

$$+ \frac{N_g}{4} \ln \left(\frac{1}{8e} \ln \frac{1}{\tau^3\rho} \right) - \frac{1}{2} \ln \frac{2\pi\Delta^2}{g\mathcal{K}_g(T/|\mu|)^{N_g}}. \quad (7.42)$$

To perform the averaging, we replace $\exp(-e^{\lambda_g}) \rightarrow \theta(-\lambda_g)$, due to the abrupt cutoff at $\lambda_g > 0$. To transform the lower bound on λ_g into an upper bound on E_g , we note that the solution of the equation $\alpha x - \ln \sqrt{x} = A$ is smaller than $(2/\alpha)A$ for $A \gg 1$, $\alpha \sim 1$. This makes the restriction on E_g tighter, so using the central limit theorem, Eq. (6.33), to average over E_g which for the lower bound can be approximated as $E_g = |\mu|\varpi_g/g$, and the left inequality (6.52) to average over \mathcal{K}_g , we obtain

$$S > \sum_g \frac{2\rho}{N_g} \left[\lambda + \ln \frac{1}{\rho} - \right.$$

$$\left. - \ln \frac{1}{\tau^3\rho} \left[F \left(\frac{e \ln(1/\tau^3\rho)}{\ln(1/\tau)} \right) \right]^{-1} \left(\ln \frac{\pi}{2} + N_g \ln \frac{4 \ln^{1/4}(1/\tau^e)}{\rho \ln^{3/4}(1/\tau^3\rho)} + L_g \ln \frac{2N_g}{\tau} \right) \right]. \quad (7.43)$$

The sum over L_g, N_g is treated in full analogy with Sec. 7.4.1, to give

$$S > \frac{1}{2\sqrt{\pi e}} \ln^4 \frac{1}{\tau^3\rho} \ln \frac{1}{\tau} \left[F \left(\frac{e \ln(1/\tau^3\rho)}{\ln(1/\tau)} \right) \right]^{-5/2} \times$$

$$\times \frac{\rho}{\lambda^{3/2}} \exp \left\{ \frac{\lambda}{\ln^2(1/\tau^3\rho)} \left[F \left(\frac{e \ln(1/\tau^3\rho)}{\ln(1/\tau)} \right) \right]^2 \right\}. \quad (7.44)$$

7.5.3. Upper bound

Analogously to the lower bound, we write the upper bound for S in the form

$$\begin{aligned}
S &< \sum_g \overline{[1 - \exp(-e^{\lambda_g})]}, \\
\lambda_g &= \lambda_{gg} F\left(\frac{2 \ln(1/\tau\rho^2)}{\ln(1/\tau)}\right) + 2 \ln \lambda_{gg} - \frac{1}{2} \ln \frac{\Delta^2}{g^g \mathcal{K}_g(T/|\mu|)^{N_g}} + \\
&\quad + \frac{N_g}{2} \ln\left(\frac{m^g}{24\pi} \ln \frac{1}{\tau}\right) + \frac{m_*^g}{4} \ln \frac{N_g}{m_*^g \rho} + \ln \frac{3N_g}{m^g}, \\
\lambda_{gg} &= \frac{6\pi(\lambda - \lambda_1^> - E_g/T)}{\ln(1/\tau\rho^2)} + \frac{6\pi \ln(8\pi/e^2)}{\ln(1/\tau\rho^2)} \frac{N_g}{m^g} + \frac{N_g}{2}.
\end{aligned} \tag{7.45}$$

To perform the averaging, we again replace $\exp(-e^{\lambda_g}) \rightarrow \theta(-\lambda_g)$ and transform the lower bound on λ_g into an upper bound on E_g , noting that the solution of the equation $\alpha x + 2 \ln x = A$ is greater than $A/(2\alpha)$ for $A \gg 1$, $\alpha \sim 1$. This makes the restriction on E_g looser, so using the central limit theorem, Eq. (6.33), to average over E_g which can be approximated as $E_g = |\mu|\varpi_g/(m_*^g g)$, and the right inequality (6.52) to average over $\tilde{\mathcal{K}}_g$, we obtain

$$\begin{aligned}
S &< \sum_g \frac{2m_*^g \rho}{\sqrt{N_g}} \left[\lambda - \lambda_1^> + \frac{N_g}{m^g} \ln \frac{8\pi}{e^2} + \frac{1}{6\pi} \ln \frac{1}{\tau\rho^2} \left[F\left(\frac{2 \ln(1/\tau\rho^2)}{\ln(1/\tau)}\right) \right]^{-1} \times \right. \\
&\quad \times \left[-N_g \ln \frac{2}{e^3 \rho} + N_g \ln\left(\frac{m^g}{24\pi} \ln \frac{1}{\tau}\right) + \frac{N_g}{2} F\left(\frac{2 \ln(1/\tau\rho^2)}{\ln(1/\tau)}\right) - \right. \\
&\quad \left. \left. - L_g \ln \frac{2}{e^3 \tau} + \frac{m_*^g}{2} \ln \frac{N_g}{m_*^g \rho} + \ln \frac{12N_g}{m^g} \right] \right].
\end{aligned} \tag{7.46}$$

To sum over the resonances we use a generalized version of Eq. (6.60) to include m_*^g :

$$\sum_g \rightarrow \sum_{m^g, m_*^g < N_g < 2L_g} 64^{(N_g - m_*^g/2)/m_g} \left[\frac{L_g}{N_g} - \frac{1}{2} \right]^{3(N_g - m_*^g/2)/m_g}. \tag{7.47}$$

The sum over L_g is estimated by the largest term multiplied by the number of terms:

$$\begin{aligned}
S < \sum_{m^g, m_*^g < N_g} \frac{m_*^g m^g \sqrt{N_g} \rho}{72\pi e} \ln \frac{1}{\tau \rho^2} \ln \frac{1}{\tau} \left[F \left(\frac{2 \ln(1/\tau \rho^2)}{\ln(1/\tau)} \right) \right]^{-1} \times \\
& \times \left\{ \frac{12\pi}{N_g \ln(1/\tau)} \left[\frac{\lambda - \lambda_1^> + (N_g/m^g) \ln(8\pi/e^2)}{\ln(1/\tau \rho^2)} 2F \left(\frac{2 \ln(1/\tau \rho^2)}{\ln(1/\tau)} \right) + \right. \right. \\
& \quad \left. \left. + \ln \frac{12N_g}{m^g} + \frac{m_*^g}{2} \ln \frac{N_g}{m_*^g \rho} - \frac{N_g}{2} \ln \frac{1}{\tau \rho^2} + N_g \ln \left(\frac{m^g}{24\pi} \ln \frac{1}{\tau} \right) + \frac{N_g}{2} F \left(\frac{2 \ln(1/\tau \rho^2)}{\ln(1/\tau)} \right) \right] \right\}^{2+3(N_g-m_*^g/2)/m_g}.
\end{aligned} \tag{7.48}$$

Now we can optimize with respect to m^g . The main competition is between the exponent $\sim N_g/m^g$, which is decreased upon increasing m^g , and the term $N_g \ln m^g$ which increases the base. The sum over N_g has a finite range, $1 \leq N_g \leq N_g^{max}$. Note that N_g^{max} is almost the same for $m^g = 1$ and $m^g = N_g$, since the term $N_g \ln m^g$ gives only a small correction to the term $-(N_g/2) \ln(1/\tau \rho^2)$, due to Eq. (7.29). This means that when we fix $1 \leq m^g \leq N_g^{max}$, and sum over N_g , analogously to the preceding subsections, the result of the summation has a form a^{N_g/m^g} , where $N_g \gg 1$ corresponds to the maximum of the whole expression and $a > 1$. This maximum is determined by the balance of different terms which enter a , and thus also only weakly depends on m^g . Thus, already as m^g is increased from 1 to 2, $a^{N_g} \gg a^{N_g/2}$. Hence, the sum is strongly dominated by $m^g = 1$.

The situation with m_*^g is less obvious, as the sum is effectively contributed by a few $m_*^g \sim 1$. To see this, let us fix m_*^g and sum over N_g . With logarithmic precision we approximate

$$\begin{aligned}
& - \frac{N_g}{2} \ln \frac{1}{\tau \rho^2} + N_g \ln \left(\frac{m^g}{24\pi} \ln \frac{1}{\tau} \right) + \frac{N_g}{2} F \left(\frac{2 \ln(1/\tau \rho^2)}{\ln(1/\tau)} \right) + \frac{m_*^g}{2} \ln \frac{N_g}{m_*^g \rho} \approx \\
& \approx - \frac{2 + 3(N_g - m_*^g/2)}{6} \ln \frac{1}{\tau \rho^2} - \frac{m_*^g}{2} \ln \frac{1}{\tau} + \frac{1}{3} \ln \frac{1}{\tau \rho^2},
\end{aligned} \tag{7.49a}$$

$$\frac{1}{N_g^{2+3(N_g-m_*^g/2)}} \approx \left(\frac{3}{2 + 3(N_g - m_*^g/2)} \right)^{2+3(N_g-m_*^g/2)} e^{2-3m_*^g/2}. \tag{7.49b}$$

The sum over N_g is treated in full analogy with Sec. 7.4.2, to give

$$\begin{aligned}
S < \left(\sum_{m_*^g=1}^{\infty} \frac{m_*^g e^{-3m_*^g/2}}{9\pi/e} \right) \left(\ln \frac{1}{\tau \rho^2} \right)^{-1/2} \ln \frac{1}{\tau} \left[F \left(\frac{2 \ln(1/\tau \rho^2)}{\ln(1/\tau)} \right) \right]^{1/2} \times \\
& \times \rho \lambda^{3/2} \exp \left\{ \frac{12\lambda}{\ln^2(1/\tau \rho^2)} F \left(\frac{2 \ln(1/\tau \rho^2)}{\ln(1/\tau)} \right) F \left(\frac{6\pi \ln(1/\tau \rho^2)}{\ln(1/\tau)} \right) \right\},
\end{aligned} \tag{7.50}$$

where the sum over m_*^g converges at $m_*^g \sim 1$ and can be estimated as $1/28$.

7.6. Summary

We have arrived at the following expression for $S(\lambda) = -\ln \mathcal{P}\{w < e^{-\lambda}\}$:

$$S(\lambda) = C_1 \lambda^{p_1} \rho \exp \left[\frac{\lambda}{C \ln^2(1/\tau^p \rho)} \right], \quad \frac{1}{2} \leq p \leq 3, \quad -\frac{3}{2} \leq p_1 \leq \frac{3}{2}. \quad (7.51a)$$

$C = C(\ln \rho / \ln \tau)$ is a slow function of the ratio of two logarithms. It can be bounded by estimating the argument of the exponential in Eq. (7.44) from below, and that in Eq. (7.50) from above:

$$\frac{1}{4} [1 + \ln(1+x)]^2 \leq \frac{1}{C(x)} \leq 3[1 + \ln(1+x)]^2. \quad (7.51b)$$

$C_1 = C_1(\ln(1/\tau), \ln(1/\rho))$ is a power-law function of $\ln(1/\tau)$ and $\ln(1/\rho)$ whose explicit form does not enter the final result within our precision. Note that the power p is inherited directly from the value of the lower cutoff of L_r , $\min(L_r/N_r)$, appearing in the expression (6.59) for the number of resonances, while the exponential asymptotics of this expression contributes to C .

From Sec. 7.5 it is seen that the sum over the guiding resonances is mostly contributed by

$$N_g \sim \frac{\lambda}{\ln^2(1/\tau^p \rho)}, \quad \frac{E_g}{T} \sim \lambda, \quad (7.52)$$

while the values of L_g are those close to the lower cutoff. Similarly, from Sec. 7.4 we obtain

$$N_\ell \sim \frac{\lambda}{\ln(1/\tau^p \rho)}, \quad \Lambda_T \sim \left(\frac{\lambda}{N_g} \right)^{N_g/2}, \quad \ln \frac{\Delta}{\varpi_\ell} \sim N_g \ln \left[\frac{1}{\tau^p \rho \ln^2(1/\tau^p \rho)} \right], \quad (7.53)$$

the values of L_ℓ again close to the lower cutoff. Then, from Sec. 7.3 we obtain

$$\Lambda \sim N_g \Lambda_T^{2/N_g} \sim \lambda, \quad I_{n^g \neq n_*^g} \sim \frac{T}{|\mu|} \left(\frac{\Lambda_T}{\Lambda} \right)^{2/N_g} \sim \frac{T}{|\mu|} \ln^2 \frac{1}{\tau^p \rho}. \quad (7.54)$$

The inequality $\lambda - L_\ell \ln N_\ell \gg N_g$, necessary to use the first regime of Eq. (6.50), becomes evident at this point. As a result, the long calculations of Sec. 7 can be summarized in very simple terms: the chaotic fraction can be written as the product of three factors

$$w \sim \left\langle \frac{g|V_\ell|}{\Delta^2} \right\rangle \left\langle e^{-\varpi_\ell/\Omega_g} \right\rangle e^{-E_g/T}, \quad (7.55)$$

where the prefactors containing τ, ρ in powers ~ 1 are neglected, and the most important configurations determining to $\mathcal{P}\{w < e^{-\lambda}\}$ correspond to the logarithms of each of the three factors being of the same order, $-\lambda$.

It may be interesting to compare the contributions to the stochastic layer width from the layer resonance and from the next best candidate. For the latter the orders in τ, g are likely to be the same, $L_r = L_\ell, N_r = N_\ell$, while the frequency mismatch, ϖ_r , is greater than that for the layer resonance, ϖ_ℓ , by a factor ~ 1 . Thus, we set $\varpi_r = 2\varpi_\ell$ for an estimate, so that Λ_T is twice greater for the second resonance, and focus on the ratio between the values of the Melnikov-Arnold exponentials,

$$\frac{\langle e^{-\varpi_r/\Omega_g} \rangle}{\langle e^{-\varpi_\ell/\Omega_g} \rangle} \sim \exp\left[-(2^{2/N_g} - 1)\Lambda\right] \sim e^{-\ln^2(1/\tau^p\rho)}. \quad (7.56)$$

Thus, the contribution of the next best resonance to the stochastic layer width is parametrically smaller.

Finally, to justify inequalities (7.29), $N_g \ll N_\ell \ll 1/\tau, 1/\rho$, as well as assumption (7.13), $T/|\mu| \ll I_{ng} \ll I_g^{\min}$, we have to specify λ . The typical values of λ are those for which $S(\lambda) \sim 1$, i. e. $\lambda \sim \ln(1/\rho) \ln^2(1/\tau^p\rho)$, so inequalities (7.29), (7.13) are indeed satisfied. As we will see in Sec. 9, the transport is dominated by regions with anomalously small w , i. e. with larger λ , so that Eq. (7.51a) works. It ceases to be valid for $\lambda \lesssim \ln^2(1/\tau^p\rho)$, so it is not suitable to find the average value of w , which is dominated by rare resonant configurations (triples). Moreover, for $\lambda \gg \ln^2(1/\tau^p\rho)$ the typical strength of the guiding resonance V_g , which scales as $(\tau^p\rho)^{N_g}$, is smaller than ρ even at $\rho \ll \tau$, so that the range of validity of the pendulum approximation coincides with that of Eq. (7.51a). The relation between τ and ρ becomes important in determining the nature of the rare resonant configurations (whether they correspond to nearest-neighbor triples, or spatially separated ones).

8. Stochastic pump and Arnold diffusion

The standard description of Arnold diffusion in multidimensional dynamical systems is based on the stochastic pump model [54, 55]. Namely, motion of the oscillators participating in the guiding resonance (the chaotic spot) is assumed to have a stochastic component with a continuous frequency spectrum. The continuous spectrum arises because the motion corresponds to successive passages of the separatrix of the effective pendulum at random instants of time and is analyzed in detail in Sec. 8.1. These oscillators of the chaotic spot are coupled to all other oscillators in the system (typically, in a high order of the perturbation theory). The combination of the two ingredients (coupling and continuous spectrum) results in energy and action exchange between the chaotic spot and the surrounding oscillators. This exchange occurs by small random amounts, which corresponds to diffusion. The corresponding diffusion equation is written in Sec. 8.2, and its consequences are analyzed in subsequent subsections.

8.1. Stochastic pump spectrum

Let us assume the general form of the guiding resonance, as defined in Sec. 6.5:

$$\sum_n m_n^g \tilde{\omega}_n = 0, \quad (8.1)$$

where $\tilde{\omega}_n(I_n) = \omega_n + gI_n$, and the integer numbers $\{m_n^g\}$ satisfy Eq. (6.25). If the dynamics of the guiding resonance can be described by an effective pendulum Hamiltonian, and the stochastic layer around the separatrix is thin, for each oscillator participating in the guiding resonance its phase ϕ_n can be written as

$$\phi_n(t) = \tilde{\omega}_n t + \frac{m_n^g}{|\underline{m}^g|^2} \check{\phi}(t), \quad (8.2)$$

where

$$\check{\phi}(t) = \sum_n m_n^g \phi_n(t) \quad (8.3)$$

is the slow phase which represents the coordinate of the effective pendulum (see Appendix D for details). For rotation and oscillation of the pendulum, corresponding to the pendulum energy being above or below the separatrix energy, respectively, $\check{\phi}(t)$ can be represented in the following form (see also Fig. 11):

$$\check{\phi}(t) = \sum_{j=-\infty}^{\infty} \begin{cases} 4 \arctan e^{\Omega_g(t-t_j)} - \pi, & \text{rotation,} \\ [4 \arctan e^{\Omega_g(t-t_j)} - \pi] - [4 \arctan e^{\Omega_g(t-t_j/2-t_{j+1}/2)} - \pi], & \text{oscillation.} \end{cases} \quad (8.4)$$

Here Ω_g is the effective pendulum frequency, see Eq. (7.5). The instants of time t_j , which are determined by the separatrix mapping [Eqs. (5.16a), (5.16b) with $t = \theta/(\Lambda\Omega_g)$], represent the random ingredient of the problem. Assuming the typical interval $t_{j+1} - t_j \gg 1/\Omega_g$, we can represent the Fourier transform as a sum of independent contributions:

$$\int_{-\infty}^{\infty} e^{-i(m/2)\check{\phi}(t)} e^{i\omega t} dt = \frac{1}{\Omega_g} \sum_{j=-\infty}^{\infty} \begin{cases} \mathcal{A}_m(\omega/\Omega_g) e^{i\omega t_j}, \\ \mathcal{A}_m(\omega/\Omega_g) e^{i\omega t_j} + \mathcal{A}_m(-\omega/\Omega_g) e^{i\omega(t_j+t_{j+1})/2}. \end{cases} \quad (8.5)$$

The Melnikov-Arnold integral $\mathcal{A}_m(\Lambda)$ is defined in Eq. (5.13), and here we use the standard notation for its index $m = 2m_n^g/|\underline{m}^g|^2$, which is not necessarily an integer. If the times t_j are assumed random and uncorrelated, the power spectrum is given by

$$\begin{aligned} \nu_{mm'}(\omega) &= \int_{-\infty}^{\infty} \left\langle e^{-i(m/2)\check{\phi}(t)+i(m'/2)\check{\phi}(t')} \right\rangle_t e^{i\omega(t-t')} d(t-t') = \\ &= \frac{\langle \delta t^{-1} \rangle_t}{2\Omega_g^2} \begin{cases} 2 \mathcal{A}_m(\omega/\Omega_g) \mathcal{A}_{m'}(\omega/\Omega_g), \\ \mathcal{A}_m(\omega/\Omega_g) \mathcal{A}_{m'}(\omega/\Omega_g) + \mathcal{A}_m(-\omega/\Omega_g) \mathcal{A}_{m'}(-\omega/\Omega_g). \end{cases} \end{aligned} \quad (8.6)$$

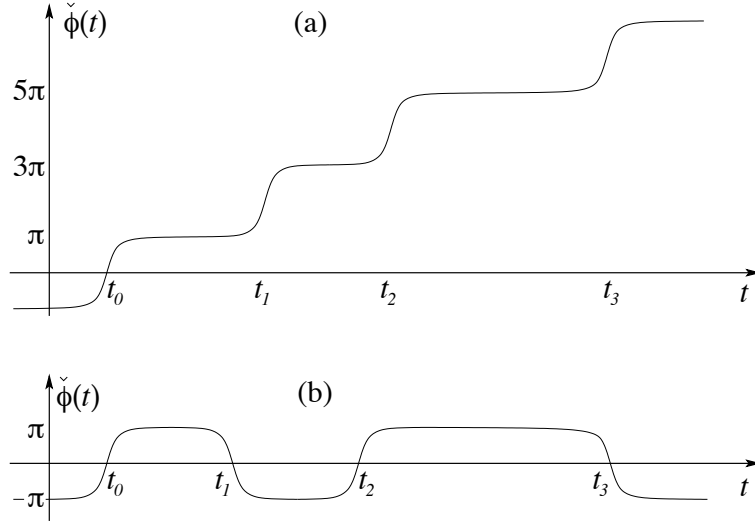


Figure 11: Schematic representation of the behavior of the slow phase $\check{\phi}(t)$, corresponding to rotation (a) and oscillation (b) of the effective pendulum. The flat regions around odd multiples of π correspond to long intervals of time spent in the vicinity of the unstable equilibrium of the pendulum, while the steps correspond to passages through the stable equilibrium at random instants of time t_j .

Here $\langle \delta t^{-1} \rangle_t$ is the average repetition rate of t_j 's for rotation, and the double repetition rate for oscillation. Note that $\langle \delta t^{-1} \rangle_t \sim \Omega_g$, up to a logarithmic factor. The angular brackets here correspond to the average over the dynamics:

$$\langle f(t_1, \dots, t_N) \rangle_t = \lim_{t \rightarrow \infty} \int_0^t \frac{dt'}{t} f(t_1 + t', \dots, t_N + t'). \quad (8.7)$$

The assumption of random and uncorrelated t_j is not fully correct. Small residual correlations in the phase found in Ref. [67] for the standard mapping translate in correlations between different t_j 's. These residual correlations are usually explained by the system sticking to various structures inside the chaotic region, such as stability islands where the diffusion is anomalously slow, or accelerator modes, where the diffusion is anomalously fast. When dealing with the standard mapping, one often introduces a small amount of external noise which prevents the system from sticking [81, 67]. The present problem, however, is more complex than the standard mapping, as we already discussed in the end of Sec. 5.2. In addition to that discussion, we note that the resonant triple is not isolated, but it is subject to perturbations from surrounding oscillators. Even though these perturbations are not truly random, it is quite plausible to assume that they are sufficient to prevent the triple from sticking, and thus effectively fulfill the role of the external noise.

As we have seen in Sec. 5.4, a chaotic spot is not always described by an effective pendulum with a thin stochastic layer around the separatrix, and the guiding and the layer resonances are not always distinguishable, so that above expressions are not always applicable. Still, for any oscillator n , belonging to the chaotic spot ($n \in \text{chaotic}$), we can write

$$\psi_n(t) = \sqrt{I_n} e^{-i\tilde{\omega}_n t} \xi_n(t), \quad (8.8)$$

where $\xi(t)$ is a certain random process. Its statistical properties cannot be determined precisely. Still, one can assume $\langle \xi_n(t) \rangle_t = 0$. Also, for any set of integer numbers $\underline{m} \equiv \{m_n\}$ the two-time correlator and the corresponding spectral density can be defined:

$$\begin{aligned} \langle \Xi_{\underline{m}}(t_1) \Xi_{\underline{m}}^*(t_2) \rangle_t &= \int \frac{d\omega}{2\pi} \nu_{\underline{m}}(\omega) e^{-i\omega(t_1-t_2)}, \\ \Xi_{\underline{m}}(t) &= \prod_{n \in \text{chaotic}} \begin{cases} \xi_n^{m_n}(t), & m_n \geq 0, \\ [\xi_n^*(t)]^{|m_n|}, & m_n < 0. \end{cases} \end{aligned} \quad (8.9)$$

When the guiding and the layer resonances are not distinguishable, the chaotic dynamics has only one characteristic frequency scale, Ω_g . Then, the leading exponential in the high-frequency asymptotics $|\omega| \gg \Omega_g$, can be estimated as

$$\nu_{\underline{m}}(\omega) \sim \frac{1}{\Omega_g} e^{-\pi|\omega|/(2\Omega_g)}. \quad (8.10)$$

For a resonant triple, considered in Sec. 5.4, $\Omega_g \sim \sqrt{\tau\rho}\Delta$, which is valid at $\tau \ll \rho$. As discussed in Sec. 6.7, in the opposite limiting case, $\tau \gg \rho$, one should effectively replace τ by ρ , so $\Omega_g \sim \rho\Delta$.

8.2. Diffusion equation

Let us now consider the dynamics of oscillators, surrounding the chaotic spot. The latter is assumed to be described by the Hamiltonian

$$H = \sum_n \left(\omega_n I_n + \frac{g}{2} I_n^2 \right) - 2V_g \cos \left(\sum_n m_n^g \phi_n \right). \quad (8.11)$$

Other oscillators are coupled to those of the guiding resonance by the Hamiltonian of the form

$$V = - \sum_r 2V_r \cos \left(\sum_n m_n^r \phi_n \right), \quad (8.12)$$

where the integer vectors \underline{m}^g and \underline{m}^r have a nonzero overlap. They satisfy the constraints imposed by the total action conservation, Eq. (6.25). Generally speaking, V_g and V_r depend on the actions of the participating oscillators. For the moment we assume the effective pendulum description of the guiding resonance to be valid, so we take V_g and V_r exactly at resonance (the opposite case is considered in the end of this subsection).

Let us restrict our attention to a finite number $N > N_g$ of oscillators. To separate the slow phase of the guiding resonance, we perform a canonical transformation (see also Appendix D):

$$\begin{aligned} \check{\phi} &= \sum_{n=1}^N m_n^g \phi_n \equiv (\underline{m}^g, \underline{\phi}), \quad \phi'_k = \sum_{n=1}^N u_{kn} \phi_n \equiv (\underline{u}_k, \underline{\phi}), \quad k = 2, \dots, N, \\ I_n &= m_n^g p_1 + \sum_{k=2}^N p_k u_{kn}, \quad \check{p} = p_1 + \frac{(m^g, \omega)}{g|\underline{m}^g|^2}, \quad \underline{\omega} = (\omega_1, \dots, \omega_N). \end{aligned} \quad (8.13)$$

Here \check{p} is the momentum, conjugate to the slow phase, and counted from the point of the exact resonance. u_{kn} is some constant matrix satisfying the appropriate orthogonality relations:

$$(\underline{u}_{k>1}, \underline{u}_{k'>1}) = \delta_{kk'}, \quad (\underline{u}_{k>1}, \underline{m}^g) = 0, \quad (u^{-1})_{nk} = \begin{cases} m_n^g/|\underline{m}^g|^2, & k = 1, \\ u_{kn}, & k > 1. \end{cases} \quad (8.14)$$

For oscillators not participating in the guiding resonance one can set $u_{kn} = \delta_{kn}$, i. e., $p_k = I_k$. It is also convenient to introduce the vector \underline{u}^I with all components $u_n^I = 1$, which corresponds to the total action:

$$I_{tot} = \sum_{n=1}^N I_n = \sum_{k=2}^N p_k (\underline{u}_k, \underline{u}^I), \quad (\underline{m}^g, \underline{u}^I) = (\underline{m}^r, \underline{u}^I) = 0. \quad (8.15)$$

In the absence of the couplings V_r the hamiltonian is given by

$$H = \sum_{k=2}^N \left[(\underline{\omega}, \underline{u}_k) p_k + \frac{g}{2} p_k^2 \right] - \frac{(m^g, \omega)^2}{2g|\underline{m}^g|^2} + \check{H}_g, \quad \check{H}_g = \frac{g|\underline{m}^g|^2}{2} \check{p}^2 - 2V_g \cos \check{\phi}, \quad (8.16)$$

so the actions p_2, \dots, p_N , as well as the pendulum Hamiltonian \check{H}_g , are conserved. When the couplings V_r are switched on, the change in the actions between two moments $t_1 < t_2$ is determined from the Hamilton's equations, $dp_k/dt = -\partial V/\partial \phi'_k$, and the change in \check{H}_g is found from $d\check{H}_g/dt = -(\partial V/\partial \check{\phi})(\partial \check{H}/\partial \check{p})$:

$$\delta p_{k>1} = -i \sum_r V_r(\underline{m}^r, \underline{u}_k) \int_{t_1}^{t_2} dt' \exp \left[i\varpi_r t' + i \frac{(m^r, m^g)}{|\underline{m}^g|^2} \check{\phi}(t') \right] + \text{c. c.}, \quad (8.17a)$$

$$\delta \check{H}_g = -i \sum_r V_r \frac{(m^r, m_g)}{|\underline{m}^g|^2} \int_{t_1}^{t_2} dt' \frac{d\check{\phi}(t')}{dt'} \exp \left[i\varpi_r t' + i \frac{(m^r, m^g)}{|\underline{m}^g|^2} \check{\phi}(t') \right] + \text{c. c.}, \quad (8.17b)$$

where “c. c.” stands for the complex conjugate and $\varpi_r = \sum_n m_n^r \tilde{\omega}_n = (\underline{m}^r, \underline{\tilde{\omega}})$. Note the relations

$$\sum_{k=2}^N \delta p_k(\underline{u}_k, \underline{u}^I) = 0, \quad (8.18a)$$

$$\sum_{k=2}^N \delta p_k(\underline{u}_k, \underline{\tilde{\omega}}) + \delta \check{H} = V(0) - V(t). \quad (8.18b)$$

The first relation follows from the orthogonality relations and represents the total action conservation. The second relation is obtained by integrating by parts and represents the total energy conservation. In fact, these relations hold separately for each given term r of the perturbation.

The integrand in Eqs. (8.17a), (8.17b) is randomly oscillating due to the chaotic dynamics of $\check{\phi}(t)$, so $\langle \delta p_k \rangle$ remains bounded even for large $t_2 - t_1$. In contrast, the average of the product $\langle \delta p_k \delta p_{k'} \rangle_t$ has a contribution growing linearly with time $t_2 - t_1$:

$$\langle \delta p_k \delta p_{k'} \rangle_t = 2(t_2 - t_1) \sum_r V_r^2 v_{\underline{m}^r}(\varpi_r) (\underline{m}^r, \underline{u}_k) (\underline{m}^r, \underline{u}_{k'}), \quad (8.19)$$

where the stochastic pump spectral density is defined analogously to Eq. (8.6):

$$v_{\underline{m}^r}(\omega) = \int_{-\infty}^{\infty} \langle e^{i[\check{\phi}(t_1) - \check{\phi}(t_2)](\underline{m}^r, \underline{m}^s)/|\underline{m}^s|^2} \rangle_t e^{i\omega(t_1 - t_2)} d(t_1 - t_2). \quad (8.20)$$

The interference terms with $r \neq r'$ give a contribution which does not grow with time and thus are neglected. Using Eq. (8.18b), we can also write

$$\frac{\langle \delta p_k \delta \check{H}_g \rangle_t}{t_2 - t_1} = - \sum_{k'=2}^N \frac{\langle \delta p_k \delta p_{k'} \rangle_t}{t_2 - t_1} (\underline{u}_k, \underline{\tilde{\omega}}), \quad \frac{\langle (\delta \check{H}_g)^2 \rangle_t}{t_2 - t_1} = \sum_{k, k'=2}^N \frac{\langle \delta p_k \delta p_{k'} \rangle_t}{t_2 - t_1} (\underline{u}_k, \underline{\tilde{\omega}}) (\underline{u}_{k'}, \underline{\tilde{\omega}}). \quad (8.21)$$

To write the diffusion equation, it is convenient to pass from the pendulum energy \check{H}_g , Eq. (7.5), to the pendulum action W using the standard expression in terms of the complete elliptic integrals $K(\kappa)$ and $E(\kappa)$,

$$W = \frac{8}{\pi} \sqrt{\frac{2V_g}{g|\underline{m}^s|^2}} \begin{cases} E(\kappa) - (1 - \kappa^2)K(\kappa) & \kappa < 1, \\ (\kappa/2)E(1/\kappa) + 1/2 & \kappa > 1, \end{cases} \quad \kappa = \sqrt{\frac{\check{H}_g + 2V_g}{4V_g}}. \quad (8.22)$$

Since transformation (8.13) is canonical, the volume element in the phase space is preserved:

$$\frac{dW d\check{\phi}}{2\pi} \prod_{k=2}^N \frac{dp_k d\phi'_k}{2\pi} = \prod_{n=1}^N \frac{dI_n d\phi_n}{2\pi}. \quad (8.23)$$

Not being interested in the oscillating phases, we introduce the distribution function \hat{f} in the action space, so that the probability to find the system in an infinitesimal volume element is given by

$$dP = \hat{f}(W, p_2, \dots, p_n) dW dp_2 \dots dp_n. \quad (8.24)$$

It is the flatness of the phase space measure appearing here that was the main purpose of passing from \check{H}_g to W .

Now, from Eqs. (8.19) and (8.21) we can immediately pass to the diffusion equation

$$\frac{\partial \hat{f}}{\partial t} = \frac{\partial}{\partial W} \left[\hat{D}_{WW} \frac{\partial \hat{f}}{\partial W} + \hat{D}_{Wk} \frac{\partial \hat{f}}{\partial p_k} \right] + \frac{\partial}{\partial p_k} \left[\hat{D}_{kW} \frac{\partial \hat{f}}{\partial W} + \hat{D}_{kk'} \frac{\partial \hat{f}}{\partial p_{k'}} \right], \quad (8.25a)$$

$$\hat{D}_{kk'} = \sum_r V_r^2(\underline{m}^r, \underline{u}_k)(\underline{m}^r, \underline{u}_{k'}) \nu_{-2(\underline{m}^r, \underline{m}^s)/|\underline{m}^s|^2}(\underline{\omega}_r), \quad (8.25b)$$

$$\hat{D}_{kW} = \hat{D}_{Wk} = -\hat{D}_{kk'}(\underline{u}_{k'}, \underline{\omega}) \frac{dW}{d\check{H}_g}, \quad (8.25c)$$

$$\hat{D}_{WW} = \hat{D}_{kk'}(\underline{u}_k, \underline{\omega})(\underline{u}_{k'}, \underline{\omega}) \left(\frac{dW}{d\check{H}_g} \right)^2, \quad (8.25d)$$

where summation over repeating indices $k, k' = 2, \dots, N$ is assumed.

Diffusion in W is confined to the narrow stochastic layer of the width W_s , given by Eq. (7.10a). At times longer than the diffusion time across the layer we can assume the distribution function to be independent on W , and write the probability (8.24) as

$$dP = f(p_2, \dots, p_n) W_s dp_2 \dots dp_n. \quad (8.26)$$

As discussed in detail in Appendix F, projection of the full diffusion equation on the layer leads to a closed equation for f :

$$W_s \frac{\partial f}{\partial t} = \sum_{k,k'=2}^N \frac{\partial}{\partial p_k} W_s D_{kk'} \frac{\partial f}{\partial p_{k'}}, \quad (8.27)$$

which describes the Arnold diffusion in the space of the variables p_2, \dots, p_n . The diffusion coefficient is given by

$$D_{kk'} = D_{k'k} = \int_{\text{layer}} \frac{dW}{W_s} \left[(u_k, \underline{D}, u_{k'}) - \frac{(u_k, \underline{D}, \underline{\omega})(\underline{\omega}, \underline{D}, u_{k'})}{(\underline{\omega}, \underline{D}, \underline{\omega})} \right], \quad (8.28a)$$

$$\underline{D} = \sum_r [\underline{m}^r \otimes \underline{m}^r] V_r^2 \nu_{\underline{m}^r}(\underline{\omega}_r), \quad (8.28b)$$

and we use obvious tensor notations,

$$(\underline{u}, [\underline{m}^r \otimes \underline{m}^r], \underline{u}') \equiv (\underline{u}, \underline{m}^r)(\underline{m}^r, \underline{u}'), \quad ([\underline{m}^r \otimes \underline{m}^r], \underline{u}') \equiv \underline{m}^r(\underline{m}^r, \underline{u}'). \quad (8.29)$$

As seen from Eq. (8.28a), the diffusion coefficient vanishes if the tensor \underline{D} is separable. This would be the case if the sum over r involved only one term. If the sum involves terms of very different strength, the contribution of the strongest one is eliminated. This corresponds to the situation discussed in Ref. [54]: the strongest perturbation of the guiding resonance effectively determines the stochastic layer width W_s , but does not contribute to the Arnold diffusion. This strongest term is called the layer resonance, $r = \ell$. Also, the diffusion coefficient (8.28a) vanishes identically for the directions corresponding to the change of the total action and of the total energy:

$$\sum_{k'=2}^N D_{kk'}(\underline{u}_{k'}, \underline{u}^I) = 0, \quad \sum_{k'=2}^N D_{kk'}(\underline{u}_{k'}, \underline{\tilde{\omega}}) = 0. \quad (8.30)$$

Thus, the minimal number of oscillators, necessary to produce the Arnold diffusion, is $N = 4$ in a system with two conserved quantities.

Constraints (8.30) ensure that any distribution function f which depends on p_k only via the combinations

$$I_{tot}(p_2, \dots, p_N) = \sum_{k=2}^N p_k(\underline{u}_k, \underline{u}^I), \quad H_{tot}(p_2, \dots, p_N) = \sum_{k=2}^N \left[(\underline{\omega}, \underline{u}_k) p_k + \frac{g}{2} p_k^2 \right], \quad (8.31)$$

is a stationary solution of Eq. (8.27). Two specific distributions are particularly important. One is the microcanonical distribution, determined by two parameters I_{tot}^0, H_{tot}^0 :

$$f_{I_{tot}^0, H_{tot}^0}(p_2, \dots, p_N) = e^{-S} \delta(H_{tot}(p_2, \dots, p_N) - H_{tot}^0) \delta(I_{tot}(p_2, \dots, p_N) - I_{tot}^0), \quad (8.32a)$$

where e^{-S} is the normalization factor, determined from

$$e^S = \int \delta(H_{tot}(p_2, \dots, p_N) - H_{tot}^0) \delta(I_{tot}(p_2, \dots, p_N) - I_{tot}^0) W_s dp_2 \dots dp_N. \quad (8.32b)$$

Thus defined $S = S(I_{tot}^0, H_{tot}^0)$ is nothing else than the entropy. The microcanonical distribution is the one to which N oscillators relax after having started from an initial condition characterized by some values of $I_{tot}(p_2, \dots, p_N) = I_{tot}^0$ and $H_{tot}(p_2, \dots, p_N) = H_{tot}^0$, provided that these N oscillators are *isolated* from the rest of the chain. Indeed, the microcanonical distribution (8.32a) is the only one which (i) is a stationary solution of the diffusion equation (8.27), and (ii) has definite values of I_{tot} and H_{tot} . In other words, the diffusion equation makes any initial distribution evolve towards the flat one on the allowed manifold, which is precisely the microcanonical distribution (8.32a).

The other important distribution is the grand canonical distribution, determined by two parameters $\beta \equiv 1/T$ (the inverse temperature) and μ (the chemical potential):

$$f_{\beta, \mu}(p_2, \dots, p_N) = e^{\beta F - \beta [H_{tot}(p_2, \dots, p_N) - \mu I_{tot}(p_2, \dots, p_N)]}, \quad (8.33a)$$

where $e^{\beta F}$ is the normalization factor, determined from

$$e^{-\beta F} = \int e^{-\beta[H_{\text{tot}}(p_2, \dots, p_N) - \mu I_{\text{tr}}(p_2, \dots, p_N)]} W_s dp_2 \dots dp_N = 1. \quad (8.33b)$$

Thus defined $F = F(\beta, \mu)$ is the free energy (more precisely, the grand canonical thermodynamic potential). The grand canonical distribution (8.33a) is established on a finite segment of the chain, considered to be a part of a larger segment, upon relaxation of this larger segment to equilibrium. This larger segment may be considered isolated, then the grand canonical distribution for the smaller segment can be derived from the microcanonical distribution for the larger segment using the standard argumentation of statistical physics [82].

In the region of the phase space where the guiding and the layer resonances cannot be easily distinguished, the above considerations should be slightly modified. Let us consider a resonant triple occupying the sites $n = 1, 2, 3$, and other oscillators on the sites $n = 4, \dots, N$. As discussed in Sec. 5.4, the internal chaotic dynamics of the triple cannot be described in the diffusion approximation. The relevant information about this dynamics is contained in the spectral density $\nu_{m^r}(\omega)$, defined in Eq. (8.9). Besides, the isolated triple can be characterized by the values of its total action I_{tr} and the total energy, which are conserved. The Hamiltonian of the triple is given by Eq. (5.28), which we write as $H_{\text{tr}}(I_{\text{tr}}) + \check{H}$.

Under the action of the perturbation, $I_n, I_{\text{tr}}, \check{H}$ acquire the increments

$$\delta I_{n>3} = -i \sum_r V_r m_n^r \int_0^\infty dt' e^{i\tilde{\omega}_r t'} \Xi_{m^r}(t') + \text{c. c.}, \quad (8.34a)$$

$$\sum_{n=4}^N \delta I_n + \delta I_{\text{tr}} = 0, \quad (8.34b)$$

$$\sum_{n=4}^N \tilde{\omega}_n \delta I_n + \tilde{\omega}_{\text{tr}} \delta I_{\text{tr}} + \delta \check{H} = V(0) - V(t), \quad (8.34c)$$

where $\tilde{\omega}_{\text{tr}} = \partial H_{\text{tr}} / \partial I_{\text{tr}}$, and $\Xi_{m^r}(t)$ was defined in Eq. (8.9). As discussed in Sec. 5.4, the excursion in \check{H} is limited to the chaotic region of a finite phase volume, so the Arnold diffusion occurs in the space of $(I_{\text{tr}}, I_4, I_5, \dots, I_N)$. Thus, we introduce the distribution function f , such that the probability for the system to be in an elementary volume of this space is

$$dP = f(I_{\text{tr}}, I_4, \dots, I_N) W_{ss} dI_{\text{tr}} dI_4 \dots dI_N, \quad (8.35)$$

where W_{ss} is the chaotic phase volume in the space (I_1, I_2, I_3) at fixed $I_{\text{tr}} = I_1 + I_2 + I_3$, as defined in Eq. (5.30a). If we let the index k assume the values $\text{tr}, 4, 5, \dots, N$ and define the vectors \underline{u}_k as

$$\underline{u}_{kn} = \begin{cases} \delta_{1n} + \delta_{2n} + \delta_{3n}, & k = \text{tr}, \\ \delta_{kn}, & k = 4, \dots, N, \end{cases} \quad (8.36)$$

then the diffusion equation for distribution equation has the same form as Eq. (8.27) with the only replacement $W_s \rightarrow W_{ss}$, and the diffusion coefficient is again given by Eq. (8.28a).

8.3. Relaxation of remote oscillators

Here we apply the diffusion equation from Sec. 8.2, Eq. (8.27), to study thermalization of an oscillator which is sufficiently far away from the chaotic spot. In particular, we find the thermalization time.

Let the N th oscillator have the weakest coupling to the chaotic spot, i. e., $D_{kN}, D_{NN} \ll D_{kk'}$ for $k, k' < N$. Then the first $N - 1$ oscillators equilibrate among themselves much faster than with the N th one. In this situation, equilibration of the N th oscillator can be described by seeking the distribution function in the form

$$f(\vec{p}, I_N; t) = f_{\beta, \mu}^{\perp}(\vec{p}) f^{\parallel}(I_N; t) + \delta f(\vec{p}, I_N; t), \quad (8.37)$$

where we have denoted $\vec{p} \equiv (p_2, \dots, p_{N-1})$. Being sufficiently far away, the N th oscillator is not involved in the guiding or layer resonances, so $p_N = I_N$, and W_s is assumed to be independent of I_N . In the first term, $f_{\beta, \mu}^{\perp}$ is the grand canonical distribution function, Eq. (8.33a), for the first $N - 1$ oscillators. Finally, δf is the small correction, $O(D_{NN}/D_{kk'})$, whose component along $f_{\beta, \mu}^{\perp}$ in the space of functions of \vec{p} is fixed by

$$\int \delta f W_s dp_2 \dots dp_{N-1} = 0. \quad (8.38)$$

Neglecting terms of the second order in D_{NN} and using constraints (8.30), we write Eq. (8.27) as

$$\begin{aligned} W_s f_{\beta, \mu}^{\perp} \frac{\partial f^{\parallel}}{\partial t} &= f_{\beta, \mu}^{\perp} b_N \left[\frac{\partial}{\partial I_N} + \beta(\tilde{\omega}_N - \mu) \right] f^{\parallel} + f_{\beta, \mu}^{\perp} W_s D_{NN} \left[\frac{\partial}{\partial I_N} + \beta(\tilde{\omega}_N - \mu) \right]^2 f^{\parallel} + \\ &+ \sum_{k, k'=2}^{N-1} \frac{\partial}{\partial p_k} W_s D_{kk'} \frac{\partial \delta f}{\partial p_{k'}}, \end{aligned} \quad (8.39)$$

where we denoted

$$b_N \equiv \sum_{k=2}^{N-1} \frac{\partial(W_s D_{kN})}{\partial p_k}. \quad (8.40)$$

Note that the last term in Eq. (8.39) is of the same order as others; its role is to compensate the dependence of W_s, b_N, D_{NN} on \vec{p} . However, being a total derivative, it vanishes when integrated over p_2, \dots, p_{N-1} . Thus, integrating Eq. (8.39) over p_2, \dots, p_{N-1} , denoting

$$\langle \dots \rangle_{\perp} = \int (\dots) f_{\beta, \mu}^{\perp} W_s dp_2 \dots dp_{N-1}, \quad (8.41)$$

and noting that

$$\int b_N f_{\beta,\mu}^\perp dp_2 \dots dp_{N-1} = \frac{\partial \langle D_{NN} \rangle_\perp}{\partial I_N} - \beta(\tilde{\omega}_N - \mu) \langle D_{NN} \rangle_\perp, \quad (8.42)$$

we obtain a closed equation for $f^\parallel(I_N)$:

$$\frac{\partial f^\parallel}{\partial t} = \frac{\partial}{\partial I_N} \langle D_{NN} \rangle_\perp \left[\frac{\partial}{\partial I_N} + \beta(\tilde{\omega}_N - \mu) \right] f^\parallel. \quad (8.43)$$

Solution of this equation is not trivial since both $\langle D_{NN} \rangle_\perp$ and $\tilde{\omega}_N$ depend on I_N : $\tilde{\omega}_N = \omega_N + gI_N$, and $\langle D_{NN} \rangle_\perp \propto I_N$, as discussed in Sec. 8.4. Still, its stationary solution is readily found to be given by $f_{\beta,\mu}(I_N)$.

An analytical solution of Eq. (8.43) describing the relaxation dynamics can be obtained when $gI_N \ll \omega_N - \mu$, so we replace $\tilde{\omega}_N \rightarrow \omega_N$. After rescaling the action and time variables, we can rewrite Eq. (8.43) as

$$\begin{aligned} \partial_{t'} u &= \partial_x [x(\partial_x + 1)u], \\ x &\equiv \beta(\omega_N - \mu)I_N, \quad t' \equiv \beta(\omega_N - \mu) \frac{\partial \langle D_{NN} \rangle_\perp}{\partial I_N} t \equiv \Gamma t. \end{aligned} \quad (8.44)$$

Seeking the solutions $\propto e^{-\lambda t'}$, and performing the Laplace transform,

$$\tilde{u}(s) = \int_0^\infty u(x) e^{-sx} dx, \quad (8.45)$$

we obtain

$$s \frac{d}{ds} [(s+1)\tilde{u}] = \lambda \tilde{u} \quad \Rightarrow \quad \tilde{u}_\lambda(s) = \frac{s^\lambda}{(s+1)^{\lambda+1}}. \quad (8.46)$$

The inverse Laplace transform takes especially simple form when λ is integer:

$$u_n(x) = \frac{1}{n!} \frac{d^n (x^n e^{-x})}{dx^n} = L_n(x) e^{-x}, \quad (8.47)$$

where $L_n(x)$ are the Laguerre polynomials, which form a complete and orthonormal set of functions on $0 < x < \infty$ with the weight e^{-x} :

$$\int_0^\infty L_n(x) L_{n'}(x) e^{-x} dx = \delta_{nn'}, \quad \sum_{n=0}^\infty L_n(x_0) L_n(x) e^{-x} = \delta(x - x_0), \quad x, x_0 > 0. \quad (8.48)$$

The eigenfunction $u_0(x) = e^{-x}$ with zero relaxation rate corresponds to the equilibrium distribution,

$$f_{\beta,\mu}^\parallel(I_N) = \beta(\omega_N - \mu) e^{-\beta(\omega_N - \mu)I_N}. \quad (8.49)$$

The eigenfunction $u_1(x) = (1-x)e^{-x}$ corresponds to a small mismatch in the temperature [or in the chemical potential, as they enter in one combination, $\beta(\omega_N - \mu)$]:

$$\frac{\partial f_{\beta,\mu}^{\parallel}(I_N)}{\partial \beta} \delta\beta = \delta\beta (\omega_N - \mu) [1 - \beta(\omega_N - \mu)I_N] e^{-\beta(\omega_N - \mu)I_N}. \quad (8.50)$$

Since the components of the distribution function, proportional to eigenfunctions $u_{n>0}$, decay as $e^{-n\Gamma t}$, the typical action (or energy) relaxation time of the oscillator can be estimated as $\Gamma^{-1} \sim (T/|\mu|)^2 \langle D_{NN} \rangle_{\perp}^{-1}$.

From Eq. (8.43) one can easily obtain the fluctuation-dissipation theorem – a relation between dynamical fluctuations of the system in equilibrium and the system's dynamical response to an external perturbing force [83]. First, let us find the power spectrum of the fluctuations of the action,

$$S_N(\omega) \equiv \int_{-\infty}^{\infty} [\langle I_N(t) I_N(0) \rangle - \langle I_N \rangle^2] e^{i\omega t} dt. \quad (8.51)$$

The average can be written as

$$\langle I_N(t) I_N(0) \rangle = \int I_N^0 f_{\beta,\mu}^{\parallel}(I_N^0) dI_N^0 \int I_N G(I_N, t | I_N^0) dI_N, \quad (8.52)$$

where the first integral represents the averaging over the initial conditions $I_N(0) = I_N^0$, and in the second integral we introduced the conditional probability $G(I_N, t | I_N^0)$ – the probability distribution of I_N at time t , given that at $t = 0$ it had a fixed value $I_N = I_N^0$. Thus, $G(I_N, t | I_N^0)$ is given by the solution of Eq. (8.43) with the initial condition $f^{\parallel}(I_N) = \delta(I_N - I_N^0)$. This solution is easily found using the second of the equations (8.48):

$$G(I_N, t | I_N^0) = \beta(\omega_N - \mu) \sum_{n=0}^{\infty} L_n(\beta(\omega_N - \mu)I_N^0) L_n(\beta(\omega_N - \mu)I_N) e^{-\beta(\omega_N - \mu)I_N - n\Gamma t}. \quad (8.53)$$

This immediately gives

$$\langle I_N(t) I_N(0) \rangle = \frac{1 + e^{-\Gamma|t|}}{\beta^2(\omega_N - \mu)^2}, \quad S_N(\omega) = \frac{1}{\beta^2(\omega_N - \mu)^2} \frac{2}{1 + \omega^2/\Gamma^2}. \quad (8.54)$$

Let us now find the susceptibility $\chi_N(\omega)$ which determines the response of I_N to a periodic perturbation of the system's Hamiltonian,

$$\delta H = - (F_{\omega} e^{-i\omega t} + F_{\omega}^* e^{i\omega t}) I_N, \quad (8.55)$$

where F_{ω} is the generalized force corresponding to I_N . It has the dimensionality of a frequency, so it can be viewed as a periodic modulation of the frequency ω_N . This

modulation produces a periodic deviation of the action I_N from its equilibrium average value; by definition,

$$\langle I_N \rangle = \langle I_N \rangle|_{F_\omega=0} + \chi_N(\omega) F_\omega e^{-i\omega t} + \chi_N^*(\omega) F_\omega e^{i\omega t} + O(F_\omega^2). \quad (8.56)$$

The average of I_N on the left-hand side is performed over the perturbed distribution function,

$$f^\parallel(I_N) = f_{\beta,\mu}^\parallel(I_N) + \delta f_\omega^\parallel(I_N) e^{-i\omega t} + [\delta f_\omega^\parallel(I_N)]^* e^{i\omega t} + O(F_\omega^2), \quad (8.57)$$

which should be found from the perturbed Eq. (8.43). The frequency ω_N enters Eq. (8.43) in two places: first, explicitly in the square brackets; second, through $\langle D_{NN} \rangle_\perp$. Note, however, that the modulation of $\langle D_{NN} \rangle_\perp$ does not produce any correction to the equilibrium distribution function: $e^{-\beta(\omega_N - \mu)I_N}$ is a stationary solution of the equation no matter what happens to $\langle D_{NN} \rangle_\perp$. Thus, to find the linear in F_ω correction to $f^\parallel(I_N)$, we should only include the modulation of ω_N in the square brackets Eq. (8.43). As a result, $\delta f_\omega^\parallel(I_N)$ can be found from the equation

$$\left\{ i\omega + \frac{\partial}{\partial I_N} \langle D_{NN} \rangle_\perp \left[\frac{\partial}{\partial I_N} + \beta(\omega_N - \mu) \right] \right\} \delta f_\omega^\parallel(I_N) = \beta F_\omega \frac{\partial}{\partial I_N} \frac{\langle D_{NN} \rangle_\perp e^{-\beta(\omega_N - \mu)I_N}}{\beta(\omega_N - \mu)}. \quad (8.58)$$

Noting that the right-hand side of this equation is proportional to the eigenfunction $u_1(x)$, we easily find $\delta f_\omega^\parallel$ and the susceptibility:

$$\chi_N(\omega) = \frac{1}{1 - i\omega/\Gamma} \frac{1}{\beta(\omega_N - \mu)^2}. \quad (8.59)$$

Comparing this with the expression for $S_N(\omega)$, Eq. (8.54), we obtain the relation

$$S_N(\omega) = \frac{2}{\beta\omega} \text{Im} \chi_N(\omega), \quad (8.60)$$

which is precisely the classical form of the fluctuation-dissipation theorem [82].

8.4. Coupling to remote oscillators

Here we analyze the perturbation theory terms which determine the diffusion in action of an oscillator which is sufficiently far away from the chaotic spot. Let the rightmost oscillator of the guiding resonance be on the site $n = 0$, and let us focus on the oscillator at $n = L$, assuming it to be further away than the oscillators of the layer resonance, i. e. $L \gg L_\ell$. As we have seen in Sec. 8.3, relaxation of this oscillator is determined by the diagonal element D_{LL} of the diffusion coefficient. The latter, in turn, is given by Eq. (8.28a) where the second term can be neglected as its denominator is determined by oscillators with $|n| \sim L_\ell \ll L$, and thus is large.

To describe the coupling between the oscillators at $n = 0$ and $n = L$ for large enough L , it is sufficient to consider perturbation terms whose spatial structure is described by

diagrams of the kind shown in Fig. 12. First, consider Fig. 12(a). Namely, $N_r - 1$ nonlinear vertices are placed on some sites n'_1, \dots, n'_{N_r-1} between 0 and L , and each of these sites has $m_{n'_k}^r = 2(-1)^k$, while $m_0^r = 1$, $m_L^r = (-1)^{N_r}$, and the rest of $m_n^r = 0$. Indeed, $V_r \propto \tau^L$ which is clearly the lowest possible order in τ . The number of resonances grows as

$$\mathcal{R} = \frac{(L-1)!}{(N_r-1)!(L-N_r)!} \approx \sqrt{\frac{N_r}{2\pi L^2}} \left(\frac{e^{1+O(N_r/L)} L}{N_r} \right)^{N_r}, \quad N_r \ll L. \quad (8.61a)$$

Next order in τ is obtained by putting two oscillators at neighboring sites near one of the $N_r - 1$ nonlinear vertices, so it introduces a factor $\sim N_r$ in the number of resonances. Higher orders in τ can be obtained if one separates the two ends of the solid lines near the k th nonlinear vertex by a distance l_k . Assuming $l_k \ll L/N_r$, which is equivalent to $L_r - L \ll L$, we can represent the number of resonances corresponding to such configurations as

$$\begin{aligned} \mathcal{R} &= \frac{(L-1)!}{(N_r-1)!(L-N_r)!} \sum_{l_1, \dots, l_{N_r-1} \geq 0} \delta_{l_1 + \dots + l_{N_r-1}, L_r - L} = \\ &= \frac{(L-1)!}{(N_r-1)!(L-N_r)!} \frac{(L_r - L + N_r - 2)!}{(L_r - L)!(N_r - 2)!}. \end{aligned} \quad (8.61b)$$

This expression does not take into account changing the direction of the solid lines, shown in Fig. 12(b), which can be done at those nonlinear vertices where $l_k > 0$. Thus, Eq. (8.61b) gives a lower bound for the number of resonances, while the upper bound is obtained by multiplying it by 2^{N_r} for the two possible directions of each solid line. The number of terms of the perturbation theory which have the same order in τ, ρ and contribute to the same resonance, is given by the product $\mathcal{N} = (l_1 + 1) \dots (l_{N_r-1} + 1)$. Note that Eqs. (8.61a), (8.61b) do not fit in the discussion of Sec. 6.6, as an extra constraint is imposed (two sites of the resonance, $n = 0$ and $n = L$, are fixed).

It is not always necessary to invoke terms shown in Fig. 12(b), as they bring an additional smallness $\tau^{2(L_r-L)}$ to $\langle D_{LL} \rangle$, while the resonances counted in Eq. (8.61a) which correspond to Fig. 12(a) may already be sufficient to remove the smallness of the Melnikov-Arnold exponential, especially for very large L . Thus, at $L \gtrsim L_\ell$ one can write the following bounds:

$$\frac{\Delta^3}{g^2} w e^{-C_3 \ln^2(1/\tau^p \rho)} \tau^{2(L-L_\ell)} (\zeta_1^2 + \dots + \zeta_N^2) < \langle D_{LL} \rangle < \frac{\Delta^3}{g^2} \tau^{2L} (\zeta_1^2 + \dots + \zeta_N^2). \quad (8.62)$$

Here each ζ_k is a product of random denominators, discussed in Appendix C. The upper bound is obtained by simply setting $L_r = L$, $N_r = 0$, and the Melnikov-Arnold exponential to unity. The lower bound is written by noting that if the optimal resonance is sought not on the full segment of the length L , but on a shorter one of the length L_ℓ , it will be similar to the layer resonance, so the corresponding factors are the same as those determining the chaotic fraction, w , except that instead of the layer resonance one should take

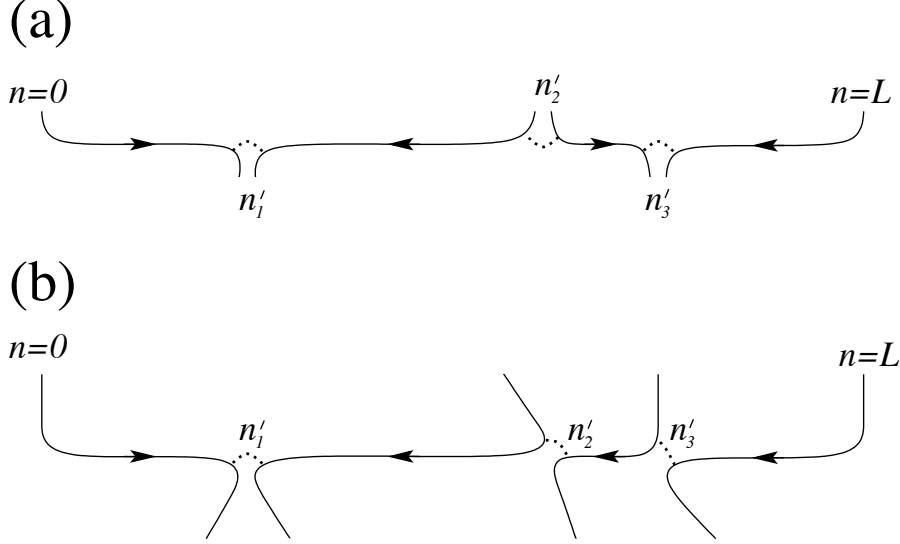


Figure 12: Examples of diagrams describing the coupling between the chaotic spot and a remote oscillator with $N_r = 4$.

the next best driving resonance, hence the factor $e^{-C_3 \ln^2(1/\tau^p \rho)}$ with $C_3 \sim 1$, as discussed in the end of Sec. 7.6. Also, w contains the thermal exponential $e^{-E_g/T}$, while D_{LL} does not. Again, the disorder average of $\langle D_{LL} \rangle$ diverges, as well as all higher moments, but as we will see in Sec. 9, it is the average of $\langle D_{LL} \rangle^{-1}$ that enters the final result, so the sum $\zeta_1^2 + \dots + \zeta_N^2$ can be effectively replaced by $(\text{const} \sim 1)^L$. Moreover, even keeping this factor along with τ^L, ρ^L would be beyond our precision, so we set $\zeta_1^2 + \dots + \zeta_N^2 \rightarrow 1$.

8.5. Migration of chaotic spots

The discussion of Sec. 8.2 regarded a segment of the chain containing one chaotic spot “living” on a given guiding resonance $(\underline{m}^g, \tilde{\omega}) = 0$. The system dynamics in the space of the actions $\{I_n\}$ corresponded to the diffusion on the hypersurface determined by the constraints

$$I_{tot} = \sum_n I_n = \text{const}, \quad (8.63a)$$

$$H_{tot} = \sum_n \left(\omega_n I_n + \frac{g}{2} I_n^2 \right) = \text{const}, \quad (8.63b)$$

$$(\underline{m}^g, \tilde{\omega}) = \sum_n m_n^g (\omega_n + g I_n) = 0. \quad (8.63c)$$

The last constraint is due to the fact that the system cannot leave the stochastic layer around the guiding resonance, and the variables p_k , introduced in Sec. 8.2 are simply

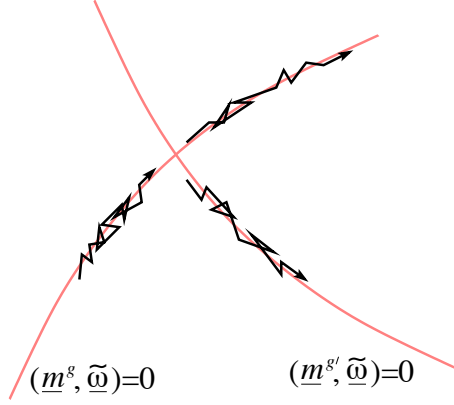


Figure 13: A schematic representation of an intersection between two resonant hypersurfaces $(\underline{m}^g, \tilde{\omega}) = 0$, $(\underline{m}^{g'}, \tilde{\omega}) = 0$, shown by the smooth curves (the plane of the figure corresponds to the curved manifold $I_{tot} = \text{const}$, $H_{tot} = \text{const}$). The wiggly trajectories represent the system diffusing along the resonances. First, the system diffuses along the g resonance and arrives at the intersection point. After some time it leaves the intersection point randomly choosing whether to continue along the g resonance or to switch to the g' resonance.

the coordinates on the corresponding hyperplane. In the course of diffusion the system may cross another hypersurface, determined by the same action and energy conservation constraints $I_{tot} = \text{const}$, $H_{tot} = \text{const}$, but with a different $(\underline{m}^{g'}, \tilde{\omega}) = 0$. The time required for this to happen can be estimated as $\sim (T/|\mu|)^2 \langle D_{LL} \rangle^{-1} e^{E_{g'}/T}$. The prefactor corresponds to the time needed to cross the typical thermal region of the action space, and D_{LL} is the diffusion coefficient of the most remote oscillator with $m_n^{g'} \neq 0$. This time coincides with the thermalization time of this oscillator, obtained in Sec. 8.3. The Arrhenius exponential corresponds to the number of attempts needed to overcome the activation barrier for the oscillators of the g' resonance. Thus estimate is valid for lengths $L \gg E_{g'}/T$; in the opposite limiting case the amount of action needed to put the system on the g' resonance is greater than the typical action, $\sim LT/|\mu|$, stored in a segment of the length L , so the activation time is determined by the diffusion coefficient at lengths $\sim E_g/T$.

Once the system variables fall in the stochastic layer of the second resonance, we have two chaotic spots not far from each other, each one acting as a stochastic pump.¹¹ Now nothing prevents either of them to leave its stochastic layer under the action of the other. Moreover, this happens in a relatively short time as the system only has to diffuse

¹¹ In connection with the problem of system sticking to various structures inside the stochastic layer, discussed in the end of Sec. 5.2, we note that when the system is changing the guiding resonance, sticking should be less probable than in the situation of the diffusion along a single guiding resonance. Indeed, when two chaotic spots are present relatively close to each other, each of them effectively represents an external source of noise for the other one, preventing it from sticking.

across the thin stochastic layer. Once this happens, one of the chaotic spots is turned off, the other one remaining alone, and thus confined to its own stochastic layer. If it is the g' resonance that is turned off, there is no overall effect on the system. However, if it is the original g resonance, the system has effectively switched from one resonance to the other, as shown schematically in Fig. 13. As the two resonances are, generally speaking, located in different regions of the chain, this process corresponds to migration of the chaotic spot along the chain.

In connection with migration of the chaotic spots it is worth mentioning a recent mathematical work [51]. For a one-dimensional chain of pendula with weak local coupling, energy above that of the unstable equilibrium was shown to be able to perform an arbitrary random walk along the chain.

9. Current through breaks

9.1. General remarks on the procedure

Global transport properties of random one-dimensional systems tend to be determined by rare strong obstacles [53]. The reason for this is that in one dimension such obstacles cannot be bypassed, in contrast to higher dimensions. Such rare obstacles were called “blockades” [64], “weak links” [65], or “breaks” [61, 66], and here the latter term will be used. In the present problem, a break is a region of the chain where the chaotic fraction w assumes anomalously small values on many consecutive sites, i. e., a region of the chain rarely visited by chaotic spots. Equilibration to the left and to the right of the break is assumed to be much faster than across the break, so the regions to the left and to the right can be assumed to be equilibrated with different values of the chemical potential and temperature, $\mu_L, T_L \equiv 1/\beta_L$ and $\mu_R, T_R \equiv 1/\beta_R$, respectively. The action and energy currents through the break, J^I, J^H , are defined as the amounts of action and energy transferred from left to right per unit time. In the linear response approximation they can be written as

$$\begin{bmatrix} J^I \\ J^H \end{bmatrix} = R_b^{-1} \begin{bmatrix} \beta_L \mu_L - \beta_R \mu_R \\ \beta_R - \beta_L \end{bmatrix}. \quad (9.1)$$

It is convenient to borrow the terminology from the electric circuit theory, as discussed in Sec. 4.4: the 2-column on the left-hand side will be simply called the current, the 2-column on the right-hand side will be called the voltage drop across the break. The 2×2 matrix R_b^{-1} corresponds to the break conductance, and its inverse, R_b , to the resistance. It is determined by the realization of disorder forming the break.

Quite generally, validity of the linear response theory and finiteness of the coefficient R_b^{-1} are immediate consequences of the diffusive character of the system dynamics in the space of actions. In the present work the origins of the linear response theory are most easily seen in Sec. 8.3, where a perturbation of the distribution function of an oscillator from its equilibrium value (say, putting it at a different temperature or chemical potential) is shown to correspond to an eigenfunction of the diffusion equation with a finite decay

rate. The analysis to be presented below corresponds to a more complicated situation, but the diffusion equation which was presented in Sec. 8 will lead to a definite expression for R_b^{-1} .

In a stationary situation the current is constant along the chain, while the voltage drop across a segment containing many breaks is the sum of the voltage drops across each break. Thus, the macroscopic conductivity σ entering Eq. (3.5) can be expressed as

$$\sigma = \left[\int R_b n_b db \right]^{-1}, \quad (9.2)$$

where $n_b db$ is the spatial density (or probability per unit length) of breaks of a given type b . Eq. (9.2) is nothing but the usual addition rule for resistors in series, as discussed in Sec. 4.4. Analogously to the problem of electronic hopping conduction in one-dimensional samples [53, 64, 65, 61, 66], there are two strong competing factors: breaks with very large resistances are extremely rare, while frequent breaks have too small resistance. As a result, the dominant contribution to the integral comes from breaks which are close to a certain optimal configuration. This also means that the macroscopic resistivity σ^{-1} is self-averaging on the length scale corresponding to the typical distance between such optimal breaks. This section is dedicated to finding such optimal breaks and to evaluation of Eq. (9.2) analogously to Ref. [61].

In Eq. (9.2), R_b is a random quantity, determined by the frequencies of all oscillators in the break region, while $n_b db$ is the probability measure in the space of these frequencies. However, evaluation of R_b directly in terms of the frequencies seems to be hopelessly complicated. Instead, a break will be characterized by the corresponding spatial profile of the chaotic fraction $\{w_n = e^{-\lambda_n}\}$, defined by Eq. (7.8). Its probability distribution on a given site is given by $p(\lambda) = d[1 - e^{-S(\lambda)}]/d\lambda$, where $S(\lambda)$ was calculated in Sec. 7. Assuming the chaotic fractions on different sites to be uncorrelated, one can write the probability measure per unit length as

$$\int n_b db \rightarrow \frac{1}{L} \int \prod_{|n| < L/2} d[1 - e^{-S(\lambda_n)}], \quad (9.3)$$

where $S(\lambda)$ is given by Eq. (7.51a), $S(\lambda) = C_1 \lambda^{p_1} \rho e^{\lambda/[C \ln^2(1/\tau^p \rho)]}$, and L is a length which is much larger than the size of a break, but much smaller than the distance between breaks. The fact that the integral in right-hand side of Eq. (9.3) is proportional to the length follows from the translational invariance of the probability distribution and is discussed in detail in Appendix G.

Strictly speaking, R_b is not a functional of $\{\lambda_n\}$ only, since λ is determined by the guiding and layer resonances, while R_b depends on the diffusion coefficients, which are determined by the same guiding resonance as λ , but also by the driving resonance which is different from the layer resonance. Still, it is quite strongly correlated with λ , as discussed in Sec. 8.4, Eq. (8.62). In the following, the relation between R_b and $\{\lambda_n\}$

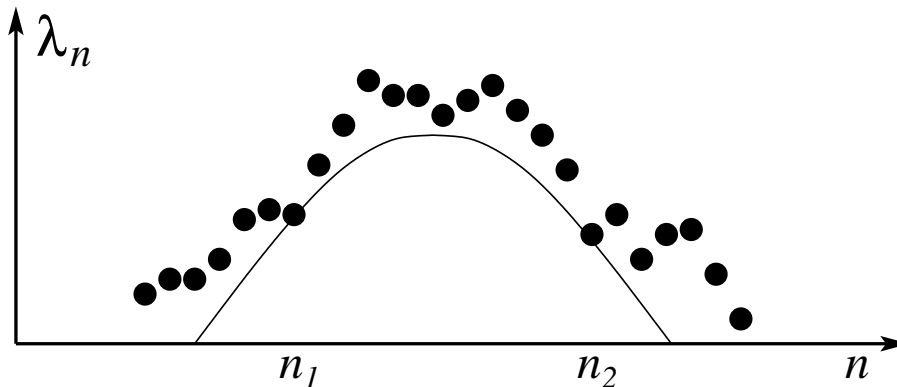


Figure 14: The profile $\{\lambda_n\}$ corresponding to some arbitrary break (shown by circles at integer positions). The solid curve shows the optimal break $b_\lambda(x)$, corresponding to this profile $\{\lambda_n\}$, which touches $\{\lambda_n\}$ at two points (denoted here by n_1 and n_2), and has the same resistance as the break with the profile $\{\lambda_n\}$, up to power-law prefactors.

will be approximated by a deterministic dependence $R_b = R(\{\lambda_n\})$, and then the integral in Eq. (9.2) will be written as an integral over $\{\lambda_n\}$. Determination of the dependence $R_b = R(\{\lambda_n\})$ is the main task of Secs. 9.2 and 9.3.

Obviously, the profile λ_n corresponding to the optimal break must be symmetric with respect to its center, which can be assumed to be either at $n = 0$, or half-way between $n = 0$ and $n = 1$, without loss of generality. Also, at the center the profile λ_n must have a maximum, $\lambda_0 \gg 1$. Two mechanisms for the current flow through the break can be identified, which require different treatment. First, a chaotic spot may find itself near the center of the break, at $|n| \sim L_\ell^{\max} \sim \lambda_0 / \ln(1/\tau^p \rho)$ (the typical size of the layer resonance at the center of the break, as estimated in Sec. 7), which occurs very rarely, once in a time $\propto e^{\lambda_0}$. Second, a chaotic spot may reside somewhere on the slope of the break, $|n| \gtrsim \lambda_0 / \ln(1/\tau^p \rho)$ which occurs more frequently. However, the current will still be determined by the diffusion of oscillators near the center of the break, $\sim D_{00}$, which has an additional smallness $\sim \tau^{-2|n|}$. For the optimal break all these contributions must have the same order; indeed, if one of the contributions to the current is too small, this means that in the corresponding region of the break λ_n can be decreased with no effect on the overall current, but with a gain in the probability.

Putting the abovesaid in more formal terms, we introduce a one-parametric family of functions $b_\lambda(x)$, concave and symmetric, $b_\lambda(x) = b_\lambda(-x)$, which we will call optimal breaks, parametrized by their value in the maximum, $b_\lambda(0) = \lambda$. The resistance of a break with an arbitrary profile $\{\lambda_n\}$ is the same (up to power-law prefactors) as that of a break from the optimal family, $\lambda_n^{\text{opt}} = b_\lambda(n)$, with the value of λ determined as the largest λ for which exists a shift x_0 such that $\lambda_n \geq b_\lambda(n - x_0)$ for all n . Indeed, this choice of λ implies that there are at least two sites, $n = n_1, n_2$, at which actually $\lambda_{n_1} = b_\lambda(n_1)$,

$\lambda_{n_2} = b_\lambda(n_2)$, and which lie on different sides of the break, as illustrated by Fig. 14. Then the transport through such a break will be dominated by the chaotic spot when it resides on the sites $n = n_1, n_2$. The resistance of the break becomes a function of a single number λ only, so that the integral in Eq. (9.2) can be written as

$$\sigma^{-1} = \int_0^\infty d\lambda R(\lambda) \mathcal{J}(\lambda) \prod_n e^{-S(b_\lambda(n))}, \quad (9.4)$$

where the Jacobian $\mathcal{J}(\lambda)$ is analyzed in Appendix G. The considerations of the previous paragraph already allow one to guess that the optimal breaks are likely to be triangular, $b_\lambda(x) \sim \lambda - 2|x| \ln(1/\tau)$, at least at large enough x , and thus the size of the break $L_b \sim \lambda / \ln(1/\tau)$.

9.2. Chaotic spot on the top of the break

The definition of the currents given in Sec. 9.1 leads to the following expression:

$$\begin{bmatrix} J^I \\ J^H \end{bmatrix} = \sum_{n>0} \begin{bmatrix} 1 \\ \omega_n \end{bmatrix} \frac{d\langle I_n \rangle_f}{dt} + \sum_{n>0} \begin{bmatrix} 0 \\ g/2 \end{bmatrix} \frac{d\langle I_n^2 \rangle_f}{dt} + \begin{bmatrix} 0 \\ O(\tau) \end{bmatrix}. \quad (9.5)$$

Here $\langle \dots \rangle_f$ denotes the average with respect to the distribution function f , whose time dependence is governed by the Arnold diffusion equation, Eq. (8.27). Integrating by parts and introducing the vectors \underline{u}^R such that $u_{n>0}^R = 1$, $u_{n\leq 0}^R = 0$, and $\underline{\tilde{\omega}}^R$ such that $\tilde{\omega}_{n>0}^R = \tilde{\omega}_n$, $\tilde{\omega}_{n\leq 0}^R = 0$, we can write the current as

$$\begin{bmatrix} J^I \\ J^H \end{bmatrix} = - \sum_{k,k'} \int \begin{bmatrix} (\underline{u}^R, \underline{u}_k) \\ (\underline{\tilde{\omega}}^R, \underline{u}_k) \end{bmatrix} D_{kk'} \frac{\partial f}{\partial p_k} W_s \prod_k dp_k. \quad (9.6)$$

where the diffusion coefficient $D_{kk'}$ is given by Eq. (8.28a), the distribution function f is defined in Eq. (8.26), and the stochastic layer width W_s is given by Eq. (7.10a). Note that it would not be correct to determine the distribution function itself from the stationary solution of Eq. (8.27). Indeed, the latter was written for a given fixed guiding resonance, while the position of the chaotic spot on the top of the break, considered here, is in fact very rarely occupied for short periods of time. The time required for the chaotic spot to jump off the top is of the same order as the equilibration time, so the distribution function on the left and on the right of the break is determined by a certain average over different guiding resonances [see Eq. (9.8) below].

Here we set $f \propto \exp[-\beta_{L/R}(\omega_n - \mu_{L/R})I_n - \beta_{L/R}gI_n^2/2]$ for the oscillators to the left/right of the top of the break which do not participate in the guiding resonance and for which $p_n = I_n$, while the contribution of the oscillators participating in the guiding resonance will be simply neglected. The relative error introduced by neglecting these oscillators is small, since the number of the oscillators in the guiding resonance, $2N_g$,

is much smaller than that for the layer resonance, $2N_\ell$, and other resonances driving the diffusion (for these we expect $N_r \sim N_\ell$). More important is the error introduced by setting the distribution function for other oscillators to its equilibrium value “by hands”: it is likely to overestimate the current by a factor ~ 1 , which is not so important as our main concern is about exponential factors. Using constraints (8.30), we express the currents as

$$\left[\begin{array}{c} J^I \\ J^H \end{array} \right] = \sum_{0 \leq n_1, n_2 \leq g} \left\langle \left[\begin{array}{c} 1 \\ \tilde{\omega}_{n_1} \end{array} \right] D_{n_1 n_2} [\beta_R(\tilde{\omega}_{n_2} - \mu_R) - \beta_L(\tilde{\omega}_{n_2} - \mu_L)] \right\rangle. \quad (9.7)$$

Here the thermal average $\langle \dots \rangle$ can already be performed over the equilibrium distribution where the difference between β_R, μ_R and β_L, μ_L is neglected, as we are working in the linear response regime. Moreover, the diffusion coefficient is always determined by the chaotic spot which has a specific position, so contributions from different possible positions n of the chaotic spots should be added with the corresponding weights, which we write as

$$D_{n_1 n_2} = \sum_n e^{-\lambda_n} D_{n_1 n_2}^{(n)}. \quad (9.8)$$

As discussed in Sec. 9.1, for the optimal break all terms of this sum should be of the same order. Since the dependence of $D_{n_1 n_2}^{(n)}$ on n is weak when $|n|, |n_1|, |n_2| \sim L_\ell$, the top of the break is smooth: $b_\lambda(x) = \lambda_0 + O(1)$ for $|x| \sim L_\ell^{\max} \sim \lambda_0 / \ln(1/\tau^p \rho)$.

As mentioned in Sec. 9.1, the diffusion coefficient $D_{n_1 n_2}^{(n)}$ is strongly correlated with the chaotic fraction w_n . Indeed, both are determined by the same guiding resonance. The difference is that w_n contains the thermal exponential $e^{-E_g/T}$, while $D_{n_1 n_2}^{(n)}$ does not. Another difference is that while the chaotic fraction is determined by the best separatrix-destroying resonance, the diffusion coefficient is determined by the second best one, the criteria for the optimization being exactly the same. Indeed, the power spectrum of the stochastic pump, Eq. (8.6) contains the same Melnikov-Arnold exponentials as the stochastic layer width, Eq. (7.10a). The difference between contributions of the best layer resonance and the second best resonance was discussed in Sec. 7.6, see Eq. (7.56). Thus, we adopt the following expression:

$$D_{n_1 n_2}^{(n)} \sim m_{n_1}^r m_{n_2}^r \frac{\Delta^3}{g^2} e^{-C_2 \lambda_n - C_3 \ln^2(1/\tau^p \rho)}. \quad (9.9)$$

with $0 < C_2 < 1, C_3 \sim 1$. Combining this with Eqs. (9.7), (9.8), we obtain

$$R^{-1} \Big|_{\text{top}} \sim \frac{\Delta^3}{g^2} \sum_n e^{-(1+C_2)\lambda_n - C_3 \ln^2(1/\tau^p \rho)} \left\langle \left[\begin{array}{c} (\underline{u}^R, \underline{m}^r) \\ (\underline{\tilde{\omega}}^R, \underline{m}^r) \end{array} \right] \left[\begin{array}{cc} (\underline{m}^r, \underline{u}^R) & (\underline{m}^r, \underline{\tilde{\omega}}^R) \end{array} \right] \right\rangle. \quad (9.10)$$

It will be seen in Sec. 9.4 that for a typical break, contributing to the integral in Eq. (9.2), the chaotic fractions w_n are of the same order as for the optimal break, $w_n \sim e^{-b_{\lambda_*}^{(n)}}$. This means that the sum in Eq. (9.10) contains many ($\sim L_\ell^{\max}$) terms. Since \underline{m}^r 's are different

for different n , the resulting matrix is not degenerate. Moreover, for each n the diagonal elements of the matrix can be estimated as $(\underline{u}^R, \underline{m}^r)^2 \sim L_\ell^{\max}$, $\langle (\underline{m}^r, \underline{\tilde{\omega}}^R) \rangle \sim L_\ell^{\max} \Delta^2$, and they are positive. The off-diagonal elements, $\langle (\underline{\tilde{\omega}}^R, \underline{m}^r)(\underline{m}^r, \underline{u}^R) \rangle \sim L_\ell^{\max} \Delta$, have random signs. Thus, the summation over n effectively multiplies the diagonal elements by the number of the terms in the sum, $\sim L_\ell^{\max}$, while the off-diagonal elements are multiplied by $\sim \sqrt{L_\ell^{\max}}$. As a result, we arrive at the following expression for the contribution from top of the break:

$$R^{-1}|_{\text{top}} \sim \frac{\Delta^3}{g^2} e^{-(1+C_2)\lambda - C_3 \ln^2(1/\tau^p \rho)} \begin{bmatrix} 1 & \sim (L_\ell^{\max})^{-1/2} \Delta \\ \sim (L_\ell^{\max})^{-1/2} \Delta & \sim \Delta^2 \end{bmatrix}, \quad (9.11)$$

where the overall prefactor $\sim (L_\ell^{\max})^2$ is omitted, as it is beyond our precision. In contrast, the factor $\sim (L_\ell^{\max})^{-1/2}$ determining the relative magnitude of different matrix elements, is kept.

9.3. Chaotic spot on the slopes of the break

When the chaotic spot resides on sites with $|n| \gtrsim L_\ell^{\max} \sim \lambda_0 / \ln(1/\tau^p \rho)$, its coupling to oscillators which are near the center of the break falls in the situation discussed in Sec. 8.4. The crucial point is that even for two neighboring oscillators the diffusion coefficient of the one which is closer to the chaotic spot is much larger than the diffusion coefficient of the more remote oscillator. This holds even if one takes into account that the diffusion coefficient is a strongly fluctuating random quantity whose moments are divergent.¹²

Let us first consider a break which is symmetric with respect to the bond between the sites $n = 0$ and $n = 1$. Then the oscillator at $n = 0$ is stronger coupled to the left part of the chain than to the right, while the oscillator at $n = 1$ is in the opposite situation. Then their distribution functions can be approximated by $f_0 \propto \exp[-\beta_L(\omega_0 - \mu_L)I_0 - \beta_L g I_0^2/2]$, $f_1 \propto \exp[-\beta_R(\omega_0 - \mu_R)I_1 - \beta_R g I_1^2/2]$, and calculation of the current according to Eq. (9.7) gives

$$R^{-1}|_{\text{slope}} = \sum_{n \lesssim -L_\ell^{\max}} e^{-\lambda_n} \left\langle \begin{bmatrix} 1 & \tilde{\omega}_1 \\ \tilde{\omega}_1 & \tilde{\omega}_1^2 \end{bmatrix} D_{11}^{(n)} \right\rangle + \sum_{n \gtrsim L_\ell^{\max}} e^{-\lambda_n} \left\langle \begin{bmatrix} 1 & \tilde{\omega}_0 \\ \tilde{\omega}_0 & \tilde{\omega}_0^2 \end{bmatrix} D_{00}^{(n)} \right\rangle. \quad (9.12)$$

We have neglected the off-diagonal components D_{10}, D_{01} of the diffusion coefficient, since the probability that an optimal driving resonance involves both these sites is low for $|n| \gg L_\ell^{\max}$.

¹²It is quite easy to check that for two independent random variables $1 < \zeta_1, \zeta_2 < \infty$, distributed according to a power law, $p(\zeta) = \alpha \theta(\zeta - 1)/\zeta^{1+\alpha}$, the probability of $\tau \zeta_2 > \zeta_1$ is given by $\tau^\alpha/2$.

Let us now consider a break which is symmetric with respect to the site $n = 0$. Then the oscillator at $n = 0$ is coupled equally well to the left and the right parts of the chain, so its distribution function $f_0(I_0)$ should be found from the diffusion equation which has the same form as Eq. (8.43), but with two terms on the right-hand side, corresponding to the contributions from the left and from the right. In contrast to Sec. 9.2, here this procedure is justified since the dynamics of the chaotic spots on the slopes of the break is faster than the dynamics of the oscillator in the center, so we can introduce the average diffusion coefficients

$$D_L = \sum_{n \lesssim -L_\ell^{\max}} e^{-\lambda_n} \langle D_{00}^{(n)} \rangle_L, \quad D_R = \sum_{n \gtrsim L_\ell^{\max}} e^{-\lambda_n} \langle D_{00}^{(n)} \rangle_R. \quad (9.13)$$

Here the thermal averaging is performed with respect to the variables of oscillators with $n < 0$ and $n > 0$, so that D_L and D_R depend on I_0 (namely, $D_{L,R} \propto I_0$). For the distribution function we obtain

$$f_0 \propto \exp \left[-\frac{D_L \beta_L + D_R \beta_R}{D_L + D_R} \left(\omega_0 I_0 + \frac{g}{2} I_0^2 \right) + \frac{D_L \beta_L \mu_L + D_R \beta_R \mu_R}{D_L + D_R} I_0 \right]. \quad (9.14)$$

Denoting the average with respect to this distribution function by $\langle \dots \rangle_0$, and calculating the current according to Eq. (9.6), we write the conductance as

$$\begin{aligned} R^{-1}|_{\text{slope}} &= \left\langle \left[\begin{array}{cc} 1 & \tilde{\omega}_0 \\ \tilde{\omega}_0 & \tilde{\omega}_0^2 \end{array} \right] \frac{D_L D_R}{D_L + D_R} \right\rangle_0 + \\ &+ \sum_{n \lesssim -L_\ell^{\max}} e^{-\lambda_n} \left\langle \left[\begin{array}{cc} 1 & \tilde{\omega}_1 \\ \tilde{\omega}_1 & \tilde{\omega}_1^2 \end{array} \right] D_{11}^{(n)} \right\rangle + \\ &+ \sum_{n \gtrsim L_\ell^{\max}} e^{-\lambda_n} \left\langle \left[\begin{array}{cc} 1 & \tilde{\omega}_{-1} \\ \tilde{\omega}_{-1} & \tilde{\omega}_{-1}^2 \end{array} \right] D_{-1,-1}^{(n)} \right\rangle. \end{aligned} \quad (9.15)$$

The two terms corresponding to the diffusion of the oscillators at $n = \pm 1$ are fully analogous to Eq. (9.12). They are of higher order in τ than the first term, but they are kept since the matrix appearing in the first term is almost degenerate. Indeed, for $D_{L,R} \propto I_0$ we can explicitly calculate the average:

$$\begin{aligned} \left\langle \left[\begin{array}{cc} 1 & \tilde{\omega}_0 \\ \tilde{\omega}_0 & \tilde{\omega}_0^2 \end{array} \right] I_0 \right\rangle_0 &= \left[\begin{array}{cc} 1 & \omega'_0 \\ \omega'_0 & (\omega'_0)^2 + 2g^2 T^2 / (\omega_0 - \mu)^2 + O(g^3) \end{array} \right] \langle I_0 \rangle_0, \\ \omega'_0 &= \omega_0 + \frac{2gT}{\omega_0 - \mu} - \frac{6g^2 T^2}{(\omega_0 - \mu)^2} + O(g^3). \end{aligned} \quad (9.16)$$

Note that the same kind of average actually appears in all terms in Eqs. (9.12), (9.15).

If the size of the slopes is of the same order as the size of the top, $\sim L_\ell^{\max}$, when the contribution from Eq. (9.12) or Eq. (9.15) is added to that from Eq. (9.11), they are of

the same order, so the resulting matrix is not degenerate, and can be inverted without problem to obtain R . In the opposite case, when the contribution from Eq. (9.12) or Eq. (9.15) dominates, matrix inversion should be done with care.

Let us first consider Eq. (9.12). The determinant of the resulting matrix is

$$\langle D_{00} \rangle \langle D_{11} \rangle (\omega'_0 - \omega'_1)^2 + 2g^2 T^2 (\langle D_{00} \rangle + \langle D_{11} \rangle) \left[\frac{\langle D_{00} \rangle}{(\omega_0 - \mu)^2} + \frac{\langle D_{11} \rangle}{(\omega_1 - \mu)^2} \right],$$

where we denoted

$$\langle D_{00} \rangle = \sum_{n \gtrsim L_t^{\max}} e^{-\lambda_n} \langle D_{00}^{(n)} \rangle, \quad \langle D_{11} \rangle = \sum_{n \lesssim -L_t^{\max}} e^{-\lambda_n} \langle D_{11}^{(n)} \rangle. \quad (9.17)$$

At first glance, the determinant can become small when $\omega_0 \approx \omega_1$. Note, however, that both $\langle D_{00} \rangle$ and $\langle D_{11} \rangle$ contain factors $1/(\omega_1 - \omega_0)^2$, since coupling of the oscillator at $n = 1$ to the oscillators on the left slope necessarily involves tunneling through the oscillator at $n = 0$, and vice versa. Thus, already the first term in the determinant is regular, so the second one, which is small as $O(\rho^2)$, can be safely neglected.

For Eq. (9.15) the situation is somewhat different. The determinant is given by

$$\langle D_{00} \rangle \langle D_{11} \rangle (\omega'_0 - \omega'_1)^2 + \langle D_{00} \rangle \langle D_{-1,-1} \rangle (\omega'_0 - \omega'_{-1})^2 + \langle D_{00} \rangle^2 \frac{2g^2 T^2}{(\omega_0 - \mu)^2},$$

where we defined $\langle D_{00} \rangle = \langle D_L D_R / (D_L + D_R) \rangle_0$, and $\langle D_{11} \rangle, \langle D_{-1,-1} \rangle$ are defined analogously to Eq. (9.17). The first two terms have a smallness $O(\tau^2)$ coming from $\langle D_{11} \rangle, \langle D_{-1,-1} \rangle$, while the last term has a smallness $O(\rho^2)$. Still, the smallness of the determinant amounts to an overall power-law prefactor which is beyond our accuracy.

9.4. Optimization

For the moment, let us ignore the matrix structure of the break conductance R^{-1} . Indeed, as we have seen in Secs. 9.2, 9.3, the matrix elements differ by a factor which is at most a power of τ, ρ , or λ , and possible problems with the matrix inversion amount to the same kind of factors. The optimization of the break shape involves exponentials, so it can be performed without paying attention to the matrix structure.

From the discussion of Secs. 9.2 and 9.3 and the estimate (8.62) one can conclude that the optimal break functions $b_\lambda(x)$, defined in the end of Sec. 9.1, should have the form, shown in Fig. 15:

$$b_\lambda(x) = \begin{cases} \lambda + O(1), & |x| \sim \lambda / \ln(1/\tau^p \rho), \\ \lambda - 2|x| \ln(1/\tau), & |x| \gg \lambda / \ln(1/\tau^p \rho). \end{cases} \quad (9.18)$$

Then the product in Eq. (9.4) is expressed in terms of [see Eq. (7.51a)]

$$\sum_n S(b_\lambda(n)) = C_1 \rho \sum_n [b_\lambda(n)]^{p_1} \exp \left[\frac{b_\lambda(n)}{C \ln^2(1/\tau^p \rho)} \right] = C'_1 \rho \lambda^{p_1} \exp \left[\frac{\lambda}{C \ln^2(1/\tau^p \rho)} \right], \quad (9.19)$$

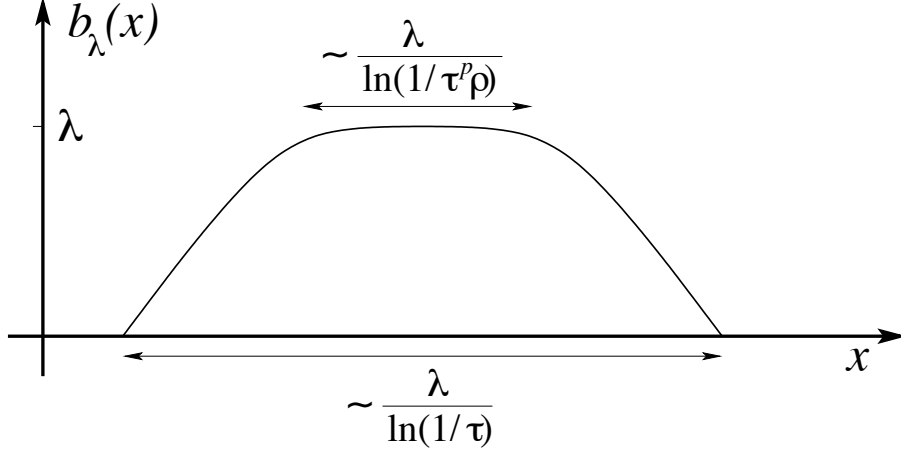


Figure 15: The optimal break $b_\lambda(x)$ at $\lambda \gg 1$. $b_\lambda(x)$ is defined as the family of functions, parametrized by λ , such that the resistance of a break with an arbitrary profile $\{\lambda_n\}$ is the same (up to power-law prefactors) as that of an optimal break, $\lambda_n^{p_1} = b_\lambda(n)$, with the value of λ determined as the largest λ for which exists a shift x_0 such that $\lambda_n \geq b_\lambda(n - x_0)$ for all n (see Sec. 9.1 of the main text for details).

where C'_1 is another logarithmic function of τ and ρ . The main dependence of R on λ is exponential, $R(\lambda) \propto e^{C'_2 \lambda}$, $1 < C'_2 < 2$ [see Eqs. (8.62) and (9.11)], so the integral in Eq. (9.4) takes the form

$$\sigma^{-1} \propto \int_0^\infty d\lambda \exp \left\{ C'_2 \lambda + \ln \mathcal{J}(\lambda) - C'_1 \rho \lambda^{p_1} \exp \left[\frac{\lambda}{C \ln^2(1/\tau^p \rho)} \right] \right\}. \quad (9.20)$$

The Jacobian is calculated in Appendix G, and it turns out that

$$\ln \mathcal{J}(\lambda) \sim \ln S(\lambda) \sim \frac{\lambda}{C \ln^2(1/\tau^p \rho)}, \quad (9.21)$$

so it can be neglected in comparison with $C'_2 \lambda$. Then the optimal value λ_* , maximizing the argument of the exponential, is found from the equation

$$C'_2 = \left(\frac{p_1}{\lambda_*} + \frac{1}{C \ln^2(1/\tau^p \rho)} \right) C'_1 \rho \lambda_*^{p_1} \exp \left[\frac{\lambda_*}{C \ln^2(1/\tau^p \rho)} \right], \quad (9.22)$$

so that with logarithmic precision

$$\lambda_* = C \ln^2 \frac{1}{\tau^p \rho} \ln \frac{1}{\rho}. \quad (9.23)$$

This determines the leading exponential in the macroscopic conductivity,

$$\ln \sigma_*^{-1} = C'_2 \lambda_* - \frac{C'_2 C \ln^2(1/\tau^p \rho)}{1 + (p_1/\lambda_*) C \ln^2(1/\tau^p \rho)} \approx C'_2 C \ln^2 \frac{1}{\tau^p \rho} \ln \frac{1}{\rho}, \quad (9.24)$$

as well as the typical distance between such breaks,

$$\ln L_* = \frac{C'_2 C \ln^2(1/\tau^p \rho)}{1 + (p_1/\lambda_*) C \ln^2(1/\tau^p \rho)} \approx C'_2 C \ln^2 \frac{1}{\tau^p \rho}. \quad (9.25)$$

This distance diverges as $\tau \rightarrow 0$ or $\rho \rightarrow 0$. Segments of the chain shorter than L_* cannot be characterized by a conductivity, and the macroscopic equations given in Sec. 3 are not valid. For such segments only the total conductance of the segment can be defined as the response of the currents to the difference of potentials μ/T , $1/T$, applied at the ends of the segment. This conductance is determined by the strongest break on the segment, and thus is strongly dependent on the realization of disorder on the segment. Its probability distribution can be calculated analogously to Ref. [61], but is beyond the scope of the present work.

The integration over λ around the optimal value λ_* can be performed in the Gaussian approximation, and the values of λ effectively contributing to the integral are

$$|\lambda - \lambda_*| \sim \ln \frac{1}{\tau^p \rho}. \quad (9.26)$$

It is easy to check that the cubic terms in the expansion of the argument of the exponential in $\lambda - \lambda_*$ are small as $1/\ln(1/\tau^p \rho)$, so the Gaussian approximation is valid. Going back to the integrals over each individual λ_n , we find that the integral converges at

$$|\lambda_n - b_{\lambda_*}(n)| \sim 1. \quad (9.27)$$

This means that for a typical break, contributing to the integral in Eq. (9.2), the chaotic fractions w_n are of the same order as for the optimal break, $w_n \sim e^{-b_{\lambda_*}(n)}$. Hence, the conductance of such a break is contributed by many possible positions of the chaotic spot.

Now one can turn to the study of the matrix structure of the macroscopic conductivity σ . It also becomes clear when each of the two situation mentioned in the end of Sec. 9.3 is realized: the size of the top of the break, $\sim \lambda_*/\ln(1/\tau^p \rho)$, and the size of the slopes, $\sim \lambda_*/\ln(1/\tau)$, are of the same order unless $\ln(1/\rho) \gg \ln(1/\tau)$, in which case the slopes are much longer. The inverse of a linear combination of matrices appearing in Secs. 9.2 and 9.3 always has positive quantities on the diagonal ($\sim \Delta^2$ and ~ 1), while the off-diagonal elements contain terms proportional to ω_n plus a thermal correction, $O(gT/(\omega_n - \mu))$. This inverse should be averaged over the frequencies, as the macroscopic conductivity is determined by many breaks. As a result, the diagonal elements remain of the same order of magnitude as before the averaging, while in the off-diagonal ones, ω_n , which has a random sign, averages to zero, and only the thermal correction survives. Thus, the matrix structure of the conductivity is

$$\sigma \propto \begin{bmatrix} 1 & O(gT/|\mu|) \\ O(gT/|\mu|) & O(\Delta^2) \end{bmatrix}. \quad (9.28)$$

We remind the reader that the matrix elements of σ have the following meaning [see Eq. (3.5)]: σ_{11} determines the response of the action current to the gradient of μ/T when T is constant, σ_{12} determines the response of the action current to the gradient of $1/T$ when μ/T is constant, while σ_{21} and σ_{22} correspond to the same for the energy current.

Acknowledgements

The author is grateful to I. L. Aleiner, B. L. Altshuler, S. Flach, and O. M. Yevtushenko for helpful discussions.

Appendix A. Thermodynamics of a strongly disordered nonlinear Schrödinger chain

Consider a chain of a long but finite length L . Any microscopic state of the chain (a set of complex numbers $\{\psi_n\}$) can be characterized by definite values of the total energy H , given by Eq. (2.3), and the total action (norm) $I_{tot} = \sum_n |\psi_n|^2$ (or their densities, $\mathcal{H} \equiv H/L$ and $\mathcal{I} \equiv I_{tot}/L$, as introduced in Sec. 3). In a thermal state, characterized by two parameters, $\beta \equiv 1/T$ and μ , the microscopic variables are distributed according to the grand canonical distribution $\mathcal{P}(\{I_n, \phi_n\}) \propto e^{-\beta(H - \mu I_{tot})}$. The temperature T and the chemical potential μ determine the average action and energy per oscillator:

$$\mathcal{I}(T, \mu) = \frac{T}{L} \frac{\partial}{\partial \mu} \ln \int \exp \left[-\beta H(\{I_n, \phi_n\}) + \beta \mu \sum_{n=1}^L I_n \right] \prod_{n=1}^L \frac{dI_n d\phi_n}{2\pi}, \quad (\text{A.1a})$$

$$\mathcal{H}(T, \mu) = \mu \mathcal{I}(T, \mu) - \frac{1}{L} \frac{\partial}{\partial \beta} \ln \int \exp \left[-\beta H(\{I_n, \phi_n\}) + \beta \mu \sum_{n=1}^L I_n \right] \prod_{n=1}^L \frac{dI_n d\phi_n}{2\pi}. \quad (\text{A.1b})$$

Here the integration limits are $0 \leq I_n < \infty$, $0 \leq \phi_n < 2\pi$. In the limit of small τ (strong disorder), Eqs. (A.1a), (A.1b) simplify:

$$\mathcal{I}(T, \mu) = \frac{1}{L} \sum_{n=1}^L \int_0^{\infty} I_n e^{-\beta(\omega_n - \mu)I_n - \beta g I_n^2/2} \frac{dI_n}{Z_n(T, \mu)} + O(\tau), \quad (\text{A.2a})$$

$$\mathcal{H}(T, \mu) = \frac{1}{L} \sum_{n=1}^L \int_0^{\infty} \left(\omega_n I_n + \frac{g}{2} I_n^2 \right) e^{-\beta(\omega_n - \mu)I_n - \beta g I_n^2/2} \frac{dI_n}{Z_n(T, \mu)} + O(\tau), \quad (\text{A.2b})$$

$$Z_n(T, \mu) \equiv \int_0^{\infty} e^{-\beta(\omega_n - \mu)I_n - \beta g I_n^2/2} dI_n \approx \begin{cases} T/(\omega_n - \mu), & \omega_n - \mu \gg gT \\ \sqrt{2\pi T/g} e^{(\mu - \omega_n)^2/(2gT)}, & \mu - \omega_n \gg gT. \end{cases} \quad (\text{A.2c})$$

As usual, thermal fluctuations in the total energy and action are proportional to \sqrt{L} , and are smaller than the average values themselves, $L\mathcal{I}$ and $L\mathcal{H}$, for a sufficiently large L . Moreover, even though each term in the sum is still a random quantity due to the randomness of ω_n , summation over a large number of sites performs the effective disorder average. Thus, in the above equations one can replace

$$\frac{1}{L} \sum_{n=1}^L \rightarrow \int_{-\Delta/2}^{\Delta/2} \frac{d\omega_n}{\Delta}. \quad (\text{A.3})$$

In other words, the total action and energy are self-averaging, and one does not have to invoke many disorder realizations.

Performing the integrations, and keeping only the leading and subleading terms in the small parameter $gT/(|\mu|\Delta)$ (i. e., expanding the exponential in g), we obtain

$$\mathcal{I} = \frac{T}{\Delta} \ln \frac{\Delta/2 - \mu}{-\Delta/2 - \mu} - \frac{2(-\mu)gT^2}{(\mu^2 - \Delta^2/4)^2} + O(g^2) + O(\tau), \quad (\text{A.4a})$$

$$\mathcal{H} = T \left(1 + \frac{\mu}{\Delta} \ln \frac{\Delta/2 - \mu}{-\Delta/2 - \mu} \right) + \frac{gT^2(\mu^2 + \Delta^2/4)}{(\mu^2 - \Delta^2/4)^2} + O(g^2) + O(\tau). \quad (\text{A.4b})$$

These expressions work only for $\mu < -\Delta/2$, $|\mu + \Delta/2| \gg \sqrt{gT}$ (this is the condition for smallness of the subleading term with respect to the leading one). The assumption $|\mathcal{H}| \lesssim (\Delta/2)\mathcal{I}$ corresponds to μ not being too close to $-\Delta/2$, and the strong inequality $|\mathcal{H}| \ll \mathcal{I}\Delta$, Eq. (2.14), translates into $|\mu| \gg \Delta$. Expanding Eqs. (A.4a), (A.4b) in the small parameter $\Delta/|\mu|$, we obtain

$$\mathcal{I} = \frac{T}{|\mu|} \left(1 + \frac{\Delta^2}{12\mu^2} - \frac{2gT}{\mu^2} \right) + O(g^2T^2/\mu^2\Delta^2) + O(\Delta^4/\mu^4) + O(\tau), \quad (\text{A.5a})$$

$$\mathcal{H} = T \frac{12gT - \Delta^2}{12\mu^2} + O(g^2/\mu^2\Delta^2) + O(\Delta^4/\mu^4) + O(\tau), \quad (\text{A.5b})$$

which leads to Eq. (3.3). For $\mu > -\Delta/2$ it is essential to keep $gI_n^2/2$ in the exponential. In this case instead of Eqs. (A.4a), (A.4b) one obtains

$$\mathcal{I} = \begin{cases} (\mu + \Delta/2)^2/(2g\Delta), & -\Delta/2 < \mu \leq \Delta/2, \\ \mu/g, & \mu \geq \Delta/2, \end{cases} \quad (\text{A.6a})$$

$$\mathcal{H} = \begin{cases} (2\mu^3 + 3\mu^2\Delta/2 - \Delta^3/8)^2/(6g\Delta), & -\Delta/2 < \mu \leq \Delta/2, \\ (\mu^2 - \Delta^2/12)/2g, & \mu \geq \Delta/2. \end{cases} \quad (\text{A.6b})$$

So far we were concerned the mapping $(T, \mu) \rightarrow (\mathcal{I}, \mathcal{H})$. It turns out that the inverse correspondence, $(\mathcal{I}, \mathcal{H}) \rightarrow (T, \mu)$, is not always well-defined, as was noted in Ref. [58] for the case without disorder. Below we study this problem for the strongly disordered case.

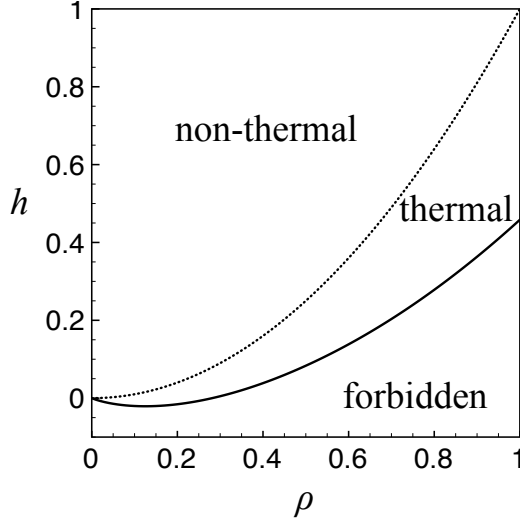


Figure A.16: The $(I > 0, \mathcal{H})$ half-plane in the dimensionless variables $\rho = gI/\Delta$, $h = g\mathcal{H}/\Delta^2$. The solid line corresponds to $T = 0$; the region below this line is forbidden. The dashed parabola corresponds to $T \rightarrow \infty$; the region above the parabola corresponds to non-thermal states which cannot be described by the grand canonical distribution.

First, let us determine the allowed values of I and \mathcal{H} . For each $I > 0$ the Hamiltonian H has a minimum. Minimization of H under the constraint $\sum I_n = IL$ is performed by introducing the Lagrange multiplier μ , and is equivalent to elimination of μ from Eqs. (A.6a), (A.6b):

$$\mathcal{H} \geq \begin{cases} (I/6)(\sqrt{32gI\Delta} - 3\Delta), & 0 \leq I \leq \Delta/(2g), \\ gI^2/2 - \Delta^2(24g), & I \geq \Delta/(2g). \end{cases} \quad (\text{A.7})$$

Clearly, there is no upper bound on \mathcal{H} for a given I . Indeed, one can consider a state $I_1 = IL$, $I_2 = \dots = I_L = 0$, for which $H = gI^2L^2/2 + O(L)$, that is for $L \rightarrow \infty$ the average energy density \mathcal{H} can be made arbitrarily large.

However, for thermal states the largest value of \mathcal{H} is obtained when $T \rightarrow \infty$. In order for the partition function to remain finite one should keep $\beta\mu = \text{const} < 0$, then all $I_n = I = -1/(\beta\mu)$, and we obtain the $T \rightarrow \infty$ line to be $\mathcal{H} = gI^2$ (in fact, it is the same as in Ref. [58]; indeed, $\beta = 0$ effectively removes the disorder from the partition function). Thus, the whole region $\mathcal{H} > gI^2$ of the right (I, \mathcal{H}) half-plane corresponds to non-thermal states (i. e., no T and μ corresponding to given I, \mathcal{H} can be found in this region); see the discussion in Ref. [58] for details and Fig. A.16 for the graphical representation of the right (I, \mathcal{H}) half-plane. The assumptions Eqs. (2.14), (2.15) ensure the fact that the considerations of the present work are restricted to thermal states only.

Appendix B. On the spreading of a finite-norm wave packet

Here we are going to see what the macroscopic equations of Sec. 3 predict when an initial condition in the form of a finite-size wave packet is taken for $\mathcal{I}(x)$, $\mathcal{H}(x)$. Let us use the variables ρ, h , introduced in Eq. (3.2), and assume

$$h < 0, \quad \rho^2 \ll |h| \ll \rho. \quad (\text{B.1})$$

Then we can rewrite the transport equations in a closed compact form:

$$\frac{\partial}{\partial(t\Delta)} \begin{bmatrix} \rho \\ h \end{bmatrix} = \frac{\partial}{\partial x} e^{-C' \ln^2(1/\tau^p \rho) \ln(1/\rho)} \begin{bmatrix} 1 & C_1 \rho \\ C_1 \rho & C_2 \end{bmatrix} \frac{\partial}{\partial x} \begin{bmatrix} -1/\rho \\ h/(12\rho^2) \end{bmatrix}, \quad C_1, C_2 \sim 1. \quad (\text{B.2})$$

Now one can estimate the growth of the typical size of the cloud, $L(t)$, by writing $\rho \sim \rho_0 L_0 / L(t)$ and approximating the spatial derivatives as $\partial_x \rightarrow 1/L(t) \rightarrow \rho / (\rho_0 L_0)$. Let us also assume $\ln(1/\tau) \ll \ln(1/\rho)$. Then one obtains the following estimate:

$$\frac{d\rho^{-1}}{d\tilde{t}} \sim e^{-C' \ln^3 \rho^{-1}} \Rightarrow L(t) \sim e^{[(C')^{-1} \ln t]^{1/3}}, \quad (\text{B.3})$$

which is Eq. (3.8). Here we rescaled the time as $\tilde{t} \sim t\Delta / (\rho_0^2 L_0^2)$ and approximated the integral

$$\int e^{C' \ln^3 \rho^{-1}} d\rho^{-1} \sim e^{C' \ln^3 \rho^{-1}},$$

as power-law prefactors are beyond our precision.

It is important to check that if inequalities (B.1) are satisfied at the initial moment, they remain satisfied for all times. This is certainly the case if the ρ cloud and the h cloud have the same length scale $L(t)$ during the expansion: $\rho \sim \rho_0 L_0 / L(t)$, $h \sim h_0 L_0 / L(t)$. Let us check that in the course of the expansion the two length scales L_ρ, L_h do not separate. Clearly, $L_h \gg L_\rho$ is impossible since the expansion of the h cloud outside the ρ cloud is blocked by the exponential. To see that $L_h \ll L_\rho$ is also impossible, let us write the currents as (the terms proportional to C_1 are small and can be neglected)

$$\begin{bmatrix} J^\rho \\ J^h \end{bmatrix} \propto \begin{bmatrix} \partial_x \rho \\ (C_2/12)\partial_x h - (C_2/6)(h/\rho)\partial_x \rho \end{bmatrix}. \quad (\text{B.4})$$

Thus, the ρ cloud expands on its own, so one can study the expansion focusing on ρ only. If at some instant $L_h \ll L_\rho$, then $\partial h / \partial t$ will be larger than $\partial \rho / \partial t$ by a factor L_ρ^2 / L_h^2 , so the expansion of the h cloud will be faster, and it will eventually catch up.

Note that the length scale L_* , Eq. (3.7), determining the validity of the macroscopic transport equations, diverges much faster than L . This means that, strictly speaking, the spreading of a wave packet cannot be described by macroscopic equations. Still, as discussed in Sec. 4.5.5, the effect of the fluctuations at short length scales is just to modify the factor C' , so the functional form of the dependence $L(t)$, Eq. (B.3), should

not be affected. However, the spreading of the wave packet is subject to strong sample-dependent fluctuations.

For not sufficiently large L another point is worth checking. One of the key assumptions of the present work is that the system can overcome an arbitrarily high activation barrier E , in a sufficient time, $\propto e^{E/T}$, i. e., an arbitrarily large amount of action and energy can be concentrated at a given point at some instant of time. However, the wave packet contains only a fixed finite amount of action and energy, so sufficiently large fluctuations are forbidden. The condition for applicability of the Gibbs distribution can be written as

$$\frac{H - \mu I_{tot}}{T} \gg C' \ln^2 \frac{1}{\tau^p \rho} \ln \frac{1}{\rho}. \quad (\text{B.5})$$

The right-hand side of this inequality represents the typical value of the activation barrier corresponding to the optimal break, as discussed in Sec. 9.4. The left-hand side is just the size of the cloud, L . Since $\rho \propto 1/L$, this inequality is satisfied after a sufficiently long time of the expansion.

Appendix C. Probability distribution of a product of denominators

Here we study the properties of the probability distribution

$$p_n(\zeta) = \int_0^1 \delta\left(\zeta - \frac{1}{x_1 \dots x_n}\right) dx_1 \dots dx_n = \frac{\theta(\zeta - 1)}{\zeta^2} \frac{\ln^{n-1} \zeta}{(n-1)!}. \quad (\text{C.1})$$

If one adopts Stirling's formula for $(n-1)!$, Eq. (C.1) can be rewritten as

$$p_n(\zeta) = \frac{\theta(\zeta - 1)}{\zeta \sqrt{2\pi(n-1)}} \exp\left[-\frac{\ln^2(\zeta/e^{n-1})}{2(n-1)} + \frac{\ln^3(\zeta/e^{n-1})}{3(n-1)^2} - \dots\right]. \quad (\text{C.2})$$

When all terms in the exponent except the first one are much smaller than unity, which is the case if

$$\left|\ln \frac{\zeta}{e^{n-1}}\right| \ll 3^{1/3}(n-1)^{2/3}, \quad (\text{C.3})$$

they can be neglected, and Eq. (C.2) corresponds to the log-normal distribution. The total probability contained in the log-normal region is determined by the error function $\text{erf}([(9/8)(n-1)]^{1/6})$. Thus, the rest of the probability decays as $e^{-n^{1/3}}$, i. e., slower than exponentially. The average of ζ^2 , which diverges for the actual distribution, for the log-normal one is finite and equal to $e^{4(n-1)}$.

Another interesting region is the tail of the distribution, where the probability integral can be calculated by the steepest descent:

$$\int_{\zeta}^{\infty} p_n(\zeta') d\zeta' = \int_{\ln \zeta}^{\infty} e^{-l+(n-1)\ln l} \frac{dl}{(n-1)!} = \frac{1}{\zeta (n-1)! \ln(\zeta/e^{n-1})} \left[1 - \frac{n-1}{\ln^2(\zeta/e^{n-1})} + \dots\right], \quad (\text{C.4})$$

where we have linearized the argument of the exponential with respect to l . The correction is small when

$$\left| \ln \frac{\zeta}{e^{n-1}} \right| \gg \sqrt{n-1}. \quad (\text{C.5})$$

Comparing this with Eq. (C.3), we see that the two regions actually overlap. The approximate form of the distribution $p_n(\zeta)$ in the tail region can be obtained by differentiating Eq. (C.4) with respect to ζ .

Let us now study the sum of \mathcal{N} independent random variables ζ with random signs, $z = |\pm \zeta_1 \pm \dots \pm \zeta_{\mathcal{N}}|$. As all moments of the distribution $p_n(\zeta)$ diverge, the central limit theorem is not valid and the distribution of z , $p_z(z)$, does not tend to a Gaussian. In the tail region (large z), $p_z(z)$ coincides with the distribution of $\max\{\zeta_1, \dots, \zeta_{\mathcal{N}}\}$, so the sum is simply determined by its largest term. The maximum of $p_z(z)$ is at $z = 0$, due to the possibility of the cancellation between different terms in the sum, even though each individual term is bounded from below [$p_n(\zeta)$ vanishes for $\zeta < 1$]. These properties will be discussed in more detail in the end of this appendix. Here we note that the random variable $\max\{\zeta_1, \dots, \zeta_{\mathcal{N}}\}$ represents an upper bound on z since their distributions coincide at large z , while the probability of small values of $\max\{\zeta_1, \dots, \zeta_{\mathcal{N}}\}$ is suppressed, in contrast to small values of z , as discussed above.

The probability for $\max\{\zeta_1, \dots, \zeta_{\mathcal{N}}\}$ to be smaller than some value z is given by the product of the probabilities,

$$\mathcal{P}\{\zeta_1, \dots, \zeta_{\mathcal{N}} < z\} \approx \left(1 - \int_z^\infty p_n(\zeta) d\zeta \right)^{\mathcal{N}} \approx \exp \left[-\frac{\mathcal{N}}{z(n-1)!} \frac{\ln^n z}{\ln(z/e^{n-1})} \right]. \quad (\text{C.6})$$

Most of the probability is contained in the region of z where the argument of the exponential is of the order of unity, i. e.

$$\frac{1}{z(n-1)!} \frac{\ln^n z}{\ln(z/e^{n-1})} = \frac{1}{\mathcal{N}}. \quad (\text{C.7})$$

At large n the solution of this equation is given by

$$z = \left[\sqrt{2\pi n} \ln f(\mathcal{N}^{1/n}) \right]^{-1-1/\ln f(\mathcal{N}^{1/n})} \left[e f(\mathcal{N}^{1/n}) \right]^n, \quad (\text{C.8})$$

where the function $f(x)$ is defined as the solution of the equation

$$\frac{f}{1 + \ln f} = x. \quad (\text{C.9})$$

In particular, if $\mathcal{N} \sim c^n$, then $z \sim (ef(c))^n$. To give an idea of the behavior of $f(x)$, we note that $f(1) = 1$, and $x \ln(ex) \leq f(x) < 2x \ln(ex)$ for $x > 1$. In the region around the solution of Eq. (C.7) the probability (C.6) can be approximated by linearizing the

logarithm of the argument of the exponential in Eq. (C.6) with respect to $\ln z$, as in Eq. (C.4):

$$\mathcal{P}\{\zeta_1, \dots, \zeta_N < e^{-\lambda}\} = \exp \left[- \exp \left[\frac{\ln f}{1 + \ln f} (\lambda + n \ln(e f)) \right] \right]. \quad (\text{C.10})$$

A lower bound on z can be obtained if one replaces $p_z(z)$ by a box distribution $p_z(0) \theta(1/p_z(0) - z)$ thus suppressing the probability of large z . Unable to calculate $p_z(0)$ explicitly, we obtain the lower bound in three steps: (i) replace $p_n(\zeta)$ by the corresponding log-normal distribution, which already suppresses the probability of large z ; (ii) apply the central limit theorem to the sum of log-normally distributed random variables; (iii) replace the resulting Gaussian by a box of the same height. This procedure results in a box distribution with a height larger than $p_z(0)$. To account for random signs of ζ_k , we redistribute the log-normal symmetrically between the positive and negative ζ , then the second moment of this distribution is given by the average of ζ^2 over the log-normal, $e^{4(n-1)}$, so the central limit theorem immediately gives

$$p_z(0) < \frac{2}{\sqrt{2\pi N} e^{2(n-1)}}. \quad (\text{C.11})$$

To conclude this appendix, let us return to the distribution of the sum of random variables not satisfying the central limit theorem. Consider a random variable ζ whose probability distribution $p_\zeta(\zeta)$ is symmetric, $p_\zeta(\zeta) = p_\zeta(-\zeta)$, and for $|\zeta| \gtrsim \zeta_\infty$ can be approximated by

$$p_\zeta(\zeta) \approx \frac{1}{2} \frac{\zeta_0^{\alpha-1}}{|\zeta|^\alpha}, \quad |\zeta| \gtrsim \zeta_\infty, \quad (\text{C.12})$$

where $\zeta_0 \lesssim \zeta_\infty$ so that the total probability contained in the region $|x| \gtrsim \zeta_\infty$ does not exceed unity. Let $1 < \alpha \leq 3$ so that the total probability converges, but the second moment diverges. Then the central limit theorem is not applicable for the sum $z = \zeta_1 + \dots + \zeta_N$. The probability distribution for this sum can be expressed as

$$p_z(z) = \int_{-\infty}^{\infty} \frac{dk}{2\pi} e^{ikz} \left[\int_{-\infty}^{\infty} e^{-ik\zeta} p_\zeta(\zeta) d\zeta \right]^N \approx \int_{-\infty}^{\infty} \frac{dk}{2\pi} e^{ikz} \exp \left[-N \int_{-\infty}^{\infty} (1 - e^{-ik\zeta}) p_\zeta(\zeta) d\zeta \right]. \quad (\text{C.13})$$

At small $k \ll 1/\zeta_\infty$ the ζ integral can be approximated as

$$\begin{aligned} \int_{-\infty}^{\infty} e^{-ik\zeta} p_\zeta(\zeta) d\zeta &= 1 - \zeta_0^{\alpha-1} \int_{\zeta_\infty}^{\infty} \frac{1 - \cos k\zeta}{\zeta^\alpha} d\zeta + O(k^2 \zeta_\infty^2) = \\ &= 1 - (k\zeta_0)^{\alpha-1} \left[\int_0^{\infty} \frac{1 - \cos u}{u^\alpha} du + O(k^{3-\alpha} \zeta_\infty^{3-\alpha}) \right] + O(k^2 \zeta_\infty^2). \end{aligned} \quad (\text{C.14})$$

The integral over u is equal to $-\Gamma(1-\alpha)\sin(\pi\alpha/2)$. The $O(k^2\zeta_\infty^2)$ term can be neglected when $\mathcal{N} \gg (\zeta_\infty/\zeta_0)^{(3-\alpha)/(\alpha-1)}$, so we can write

$$p_z(z) \approx \int_{-\infty}^{\infty} \frac{dk}{2\pi} e^{ikz - |kz_N|^{\alpha-1}} = \begin{cases} [\pi(\alpha-1)z_N]^{-1} \Gamma\left(\frac{1}{\alpha-1}\right), & |z| \ll z_N, \\ (\mathcal{N}/2)\zeta_0^{\alpha-1}/z^\alpha, & |z| \gg z_N, \end{cases} \quad (\text{C.15})$$

where z_N represents the typical value of $|z|$:

$$z_N = \zeta_0 \left[-\mathcal{N} \Gamma(1-\alpha) \sin \frac{\pi\alpha}{2} \right]^{1/(\alpha-1)}. \quad (\text{C.16})$$

The expression for $p_z(z)$ at large $|z| \gg z_N$ was obtained by expanding the exponential as $e^{-|kz_N|^{\alpha-1}} = 1 - |kz_N|^{\alpha-1} + \dots$, performing analytical continuation from the positive imaginary semiaxis of z , and using the relation $\Gamma(\alpha)\Gamma(1-\alpha)\sin\pi\alpha = \pi$. It turns out to coincide with the tail of the probability distribution of $\max\{|\zeta_1|, \dots, |\zeta_N|\}$ (up to a factor of 2, which accounts for the difference between the distributions of z and $|z|$):

$$\frac{d}{dz} (\mathcal{P}\{|\zeta| < z\})^\mathcal{N} \approx \frac{d}{dz} \exp\left(-\frac{\mathcal{N}}{\alpha-1} \frac{\zeta_0^{\alpha-1}}{z^{\alpha-1}}\right) \approx \frac{\mathcal{N}\zeta_0^{\alpha-1}}{z^{\alpha-1}}. \quad (\text{C.17})$$

Let us now consider the sum of positive random variables, assuming $p_\zeta(\zeta)$ to vanish at $\zeta < 0$ and to have the form (C.12) without the factor 1/2 at large ζ . For $1 < \alpha < 2$ the integration is analogous to Eq. (C.14), but the result must be analytical in the lower complex half-plane of k . Then, instead of Eq. (C.15) we obtain

$$p_z(z) \approx \int_{-\infty}^{\infty} \frac{dk}{2\pi} e^{ikz + \mathcal{N}\Gamma(1-\alpha)(ik\zeta_0)^{\alpha-1}} = - \int_0^{\infty} \frac{d\kappa}{\pi} e^{-\kappa z} \text{Im} \exp\left[-\mathcal{N}\Gamma(1-\alpha)(\kappa\zeta_0)^{\alpha-1} e^{i\pi\alpha}\right], \quad (\text{C.18})$$

which at large z again gives $\mathcal{N}\zeta_0^{\alpha-1}/z^\alpha$. For $2 < \alpha < 3$ the first moment, $\bar{\zeta}$, of $p_\zeta(\zeta)$, is finite, so it should be subtracted, and at large z we obtain $\mathcal{N}\zeta_0^{\alpha-1}/(z - \mathcal{N}\bar{\zeta})^\alpha$.

Appendix D. Change of variables in the vicinity of a resonance

Consider N oscillators, $n = 1, \dots, N$, and suppose that the condition

$$\sum_{n=1}^N m_n \frac{\partial H(I_1, \dots, I_N)}{\partial I_n} \equiv (\underline{m}, \underline{\tilde{\omega}}) = 0. \quad (\text{D.1})$$

is satisfied for some values of the actions $\underline{I} = \underline{I}'$. Then the slow phase is introduced as

$$\check{\phi} = \sum_{n=1}^N m_n \phi_n. \quad (\text{D.2a})$$

To complete the transformation to new phases ϕ'_k , we write

$$\phi'_1 = \check{\phi}, \quad \phi'_{k>1} = \sum_{n=1}^N u_{kn} \phi_n, \quad (\text{D.2b})$$

where the matrix u_{kn} is chosen so that the vectors $\underline{u}_k \equiv (u_{k1}, \dots, u_{kN})$ satisfy the orthogonality relations

$$(\underline{u}_{k>1}, \underline{u}_{k'>1}) = \delta_{kk'}, \quad (\underline{u}_{k>1}, \underline{m}) = 0. \quad (\text{D.3})$$

Then, defining $\underline{u}_1 = \underline{m}$, we can easily invert the matrix:

$$(u^{-1})_{nk} = \begin{cases} m_n/|\underline{m}|^2, & k = 1, \\ u_{kn}, & k > 1, \end{cases} \quad |\underline{m}|^2 \equiv (\underline{u}_1, \underline{u}_1) = \sum_{n=1}^N m_n^2, \quad (\text{D.4})$$

and write the completeness relation as

$$\frac{m_n m'_n}{|\underline{m}|^2} + \sum_{k=2}^N u_{kn} u_{kn'} = \delta_{nn'}. \quad (\text{D.5})$$

The transformation for phases fixes the transformation to the new actions p_k in the vicinity of the resonance point (so that the whole transformation is canonical):

$$\underline{I} = \sum_{k=1}^N p_k \underline{u}_k. \quad (\text{D.6})$$

This gives

$$\frac{\partial H}{\partial p_k} = \sum_{n=1}^N \frac{\partial H}{\partial I_n} \frac{\partial I_n}{\partial p_k} = \sum_{n=1}^N u_{kn} \frac{\partial H}{\partial I_n}, \quad (\text{D.7})$$

so that $\partial H / \partial p_1 = 0$, and p_1 is the effective pendulum momentum. The kinetic part of the pendulum Hamiltonian is then determined by $\partial^2 H / \partial p_1^2 = g|\underline{m}|^2$, and this is what appears in Eq. (7.5).

Let us now approximate

$$\phi'_k(t) = \frac{\partial H}{\partial p_k} t + \left(\frac{\partial^2 H}{\partial p_1^2} \right)^{-1} \left(\frac{\partial^2 H}{\partial p_k \partial p_1} \right) \phi'_1(t), \quad (\text{D.8})$$

where the derivatives are taken at the point \underline{I}' . The second term appears when the equations of motion are written to the first order in p_1 which gives $d\phi'_1/dt = (\partial^2 H / \partial p_1^2) p_1$. Inverting Eqs. (D.2a), (D.2b), we obtain

$$\phi_n(t) = \sum_{k=1}^N \phi'_k(t) u_{kn} = \frac{\partial H}{\partial I_n} t + \left(\underline{m}, \frac{\partial^2 H}{\partial \underline{I} \partial \underline{I}}, \underline{m} \right)^{-1} \frac{\partial(\underline{m}, \tilde{\omega})}{\partial I_n} \check{\phi}(t), \quad (\text{D.9})$$

which is Eq. (8.2).

Let us now see how the stochastic layer thickness translates into an effective integration measure on the resonant manifold. Namely, we consider the integral of a function $F(I_1, \dots, I_n)$, smooth on the scale of the stochastic layer width:

$$\int \prod_{k=2}^N \frac{dp_k d\phi'_k}{2\pi} \int_{\text{layer}} \frac{dp_1 d\phi'_1}{2\pi} F = \int F \mathcal{M} \delta(m_1 \tilde{\omega}_1 + \dots + m_N \tilde{\omega}_N) \prod_{n=1}^N dI_n, \quad (\text{D.10})$$

where \mathcal{M} is the measure to be determined. Since the transformation is canonical,

$$\prod_{k=1}^N \frac{dp_k d\phi'_k}{2\pi} = \prod_{n=1}^N \frac{dI_n d\phi_n}{2\pi}, \quad (\text{D.11})$$

\mathcal{M} is determined from the condition

$$W_s \equiv \int_{\text{layer}} \frac{dp_1 d\phi'_1}{2\pi} = \int dp_1 \mathcal{M} \delta(m_1 \tilde{\omega}_1 + \dots + m_N \tilde{\omega}_N), \quad (\text{D.12})$$

where W_s is the volume of the stochastic layer in the pendulum phase space. In order to resolve the δ -function we write

$$d(\underline{m}, \underline{\tilde{\omega}}) = \sum_{n, n'=1}^N m_n \frac{\partial^2 H}{\partial I_n \partial I_{n'}} dI_{n'} = \left(\underline{m}, \frac{\partial^2 H}{\partial \underline{I} \partial \underline{I}}, \underline{m} \right) dp_1 + \sum_{k=2}^N \left(u_k, \frac{\partial^2 H}{\partial \underline{I} \partial \underline{I}}, \underline{m} \right) dp_k \quad (\text{D.13})$$

The last term vanishes, and the integration over p_1 gives

$$\mathcal{M} = W_s \sum_{n, n'=1}^N m_n \frac{\partial^2 H}{\partial I_n \partial I_{n'}} m_{n'} = g[\underline{m}]^2 W_s. \quad (\text{D.14})$$

It is this measure that appears in Eq. (7.8).

Appendix E. Integrals used in thermal averaging

Let us consider the following integral:

$$J_{\alpha_1 \dots \alpha_n}(A) = \int_0^\infty \exp\left(-x_1 - \dots - x_n - \frac{A}{x_1^{\alpha_1} \dots x_n^{\alpha_n}}\right) dx_1 \dots dx_n. \quad (\text{E.1})$$

At $A \gg 1$ the leading exponential asymptotics is easily found by noticing that the maximum of the exponent in the integrand is reached at

$$x_k^{\max} = \alpha_k \left(\frac{A}{\alpha_1^{\alpha_1} \dots \alpha_n^{\alpha_n}} \right)^{1/(\alpha_1 + \dots + \alpha_n + 1)}, \quad (\text{E.2})$$

so we obtain

$$\ln J_{\alpha_1 \dots \alpha_n}(A \gg 1) = -(\alpha_1 + \dots + \alpha_n + 1) \left(\frac{A}{\alpha_1^{\alpha_1} \dots \alpha_n^{\alpha_n}} \right)^{1/(\alpha_1 + \dots + \alpha_n + 1)}. \quad (\text{E.3})$$

Let us note that

$$(\alpha_1 + \dots + \alpha_n) \ln \frac{\alpha_1 + \dots + \alpha_n}{n} \leq \sum_{k=1}^n \alpha_k \ln \alpha_k \leq (\alpha_1 + \dots + \alpha_n) \ln(\alpha_1 + \dots + \alpha_n). \quad (\text{E.4})$$

The left inequality is the Jensen's inequality following from the convexity of the function $x \ln x$ (the equality holds when all $\alpha_k = \alpha$), while the right inequality obviously follows from the monotony of $\ln x$ (the equality holds when all α_k except one are zero). Denoting $\alpha_1 + \dots + \alpha_n = n\alpha$, we obtain an estimate

$$\exp \left[-\frac{n\alpha + 1}{\alpha^{n\alpha/(n\alpha+1)}} A^{1/(n\alpha+1)} \right] \leq J_{\alpha_1 \dots \alpha_n}(A \gg 1) \leq \exp \left[-\frac{n\alpha + 1}{(n\alpha)^{n\alpha/(n\alpha+1)}} A^{1/(n\alpha+1)} \right]. \quad (\text{E.5})$$

Even though the saddle point approximation is not supposed to be valid when some of the α_k 's are zero, the right inequality is still correct since the integration over the corresponding $n - 1$ coordinates simply gives $\int e^{-x_k} dx_k = 1$, while the integration over the remaining coordinate in the saddle point approximation gives the same result, as can be checked directly.

Let us now focus on the case when all $\alpha_k = \alpha$,

$$J_\alpha(A) = \int_0^\infty \exp \left[-x_1 - \dots - x_n - \frac{A}{(x_1 \dots x_n)^\alpha} \right] dx_1 \dots dx_n, \quad (\text{E.6})$$

and improve this estimate by calculating the prefactors in front of the exponentials in the Gaussian approximation: Let us perform an orthogonal change of variables

$$x_k = \frac{y_{\parallel}}{\sqrt{n}} + \sum_{m=1}^{n-1} e_k^m y_m, \quad (\text{E.7})$$

where the unit basis vectors e^m are orthogonal between themselves, as well as to the direction of y_{\parallel} :

$$\sum_{k=1}^n e_k^m e_k^{m'} = \delta_{mm'}, \quad \sum_{k=1}^n e_k^m = 0 \quad (\text{E.8})$$

To the second order in the perpendicular deviations,

$$\begin{aligned} x_1 \dots x_n &= \left(\frac{y_{\parallel}}{\sqrt{n}} \right)^n + \frac{1}{2} \left(\frac{y_{\parallel}}{\sqrt{n}} \right)^{n-2} \sum_{m, m'=1}^{n-1} \left(\sum_{k \neq k'} e_k^m e_{k'}^{m'} \right) y_m y_{m'} = \\ &= \left(\frac{y_{\parallel}}{\sqrt{n}} \right)^n - \frac{1}{2} \left(\frac{y_{\parallel}}{\sqrt{n}} \right)^{n-2} \sum_{m=1}^{n-1} y_m^2, \end{aligned} \quad (\text{E.9})$$

where we took advantage of the orthogonality:

$$\sum_{k \neq k'} e_k^m e_{k'}^{m'} = \left(\sum_{k=1}^m e_k^m \right) \left(\sum_{k'=1}^m e_{k'}^{m'} \right) - \sum_{k=1}^m e_k^m e_k^{m'} = -\delta_{mm'}$$

Then the integral is easily calculated as ($Y = y_{\parallel} / \sqrt{n}$)

$$\begin{aligned} J_{\alpha}(A \gg 1) &= \int_0^{\infty} \sqrt{n} dY \int d^{n-1} \vec{y}_{\perp} \exp \left[-nY - \frac{A}{Y^{n\alpha}} - \frac{\alpha}{2} \frac{A}{Y^{n\alpha}} \frac{|\vec{y}_{\perp}|^2}{Y^2} \right] = \\ &= \sqrt{\frac{(2\pi)^{n-1} n}{(\alpha A)^{n-1}}} \int_0^{\infty} e^{-nY - A/Y^{n\alpha}} Y^{(n\alpha+2)(n-1)/2} dY = \\ &= \frac{n(\alpha n + 2 - \alpha)}{2} \sqrt{\frac{(2\pi)^n}{n\alpha + 1}} (\alpha A)^{n/(n\alpha+1)} \exp \left[-\frac{n\alpha + 1}{\alpha} (\alpha A)^{1/(n\alpha+1)} \right]. \end{aligned} \quad (\text{E.10})$$

The third line is obtained from the second one by denoting $u = Y^{(n\alpha+2)(n-1)/2+1}$, and integrating over u in the Gaussian approximation. The prefactor is large, so to obtain a lower bound we can simply omit it. Then, setting $n = 2N_g - m_{n_*}^g$ and $\alpha = 1/4$, we arrive at Eq. (7.15).

To obtain the upper bound, we note that $x^{n/2} e^{-nx/2} \leq e^{-n/2}$, which gives

$$J_{\alpha}(A \gg 1) \leq n(n\alpha + 2)(2\pi/e)^{n/2} \exp \left[-\frac{n}{2} (\alpha A)^{1/(n\alpha+1)} \right]. \quad (\text{E.11a})$$

Note that the integral over \vec{y}_{\perp} can be calculated in the Gaussian approximation only when $\alpha A / Y^{n\alpha} \gg 1$, otherwise it is of the order of unity. Thus, to obtain an upper bound, we just set the factor $(Y^{n\alpha} / \alpha A)^{n-1}$ in the second line of Eq. (E.10) to unity and integrate over $Y^n = u$ in the Gaussian approximation:

$$\begin{aligned} J_{\alpha}(A \gg 1) &\leq \sqrt{\frac{(2\pi)^n n^2}{n\alpha + 1}} (\alpha A)^{(2n-1)/(n\alpha+1)} \exp \left[-\frac{n\alpha + 1}{\alpha} (\alpha A)^{1/(n\alpha+1)} \right] \leq \\ &\leq n(8\pi/e^2)^{n/2} \exp \left[-\frac{n}{2} (\alpha A)^{1/(n\alpha+1)} \right], \end{aligned} \quad (\text{E.11b})$$

where the last inequality was written using $(xe^{-x/2})^n \leq (2/e)^n$. Since $8\pi/e^2 = 3.4 \dots > 2\pi/e = 2.3 \dots$, we adopt the latter estimate. This is precisely Eq. (7.20).

Appendix F. Effective diffusion coefficient along a thin layer

Consider the diffusion equation for the distribution function $\hat{f}(W, p_2, \dots, p_N) \equiv f(W, \vec{p})$ in a flat space (the volume element being $dW dp_2 \dots dp_N$):

$$\frac{\partial \hat{f}}{\partial t} = -\partial_W J_W - \partial_k J_k, \quad J_W = -\hat{D}_{WW} \partial_W \hat{f} - \hat{D}_{Wk} \partial_k \hat{f}, \quad J_k = -\hat{D}_{kW} \partial_W \hat{f} - \hat{D}_{kk'} \partial_{k'} \hat{f}. \quad (\text{F.1a})$$

Here $\partial_W = \partial/\partial W$, $\partial_k = \partial/\partial p_k$, and the summation over repeating indices $k = 2, \dots, N$ is assumed. The diffusion is confined to a thin layer $W_1(\vec{p}) < W < W_2(\vec{p})$, $W_2(\vec{p}) - W_1(\vec{p}) \equiv W_s(\vec{p})$, so that the normal component of the current vanishes at the boundaries:

$$\left(J_W - \frac{\partial W_{1,2}}{\partial p_k} J_k \right) \Big|_{W=W_{1,2}} = 0. \quad (\text{F.1b})$$

All dependencies on p_k are assumed to be slow on the scale W_s : $W_s \partial_k \hat{f} \ll \hat{f}$. Thus, one can seek the distribution function in the form

$$\hat{f}(W, \vec{p}) = f(\vec{p}) + \tilde{f}(W, \vec{p}), \quad \int_{W_1(\vec{p})}^{W_2(\vec{p})} \tilde{f}(W, \vec{p}) dW = 0. \quad (\text{F.2})$$

Then our goal is to eliminate \tilde{f} and find the effective equation for $f(\vec{p})$.

Integrating Eq. (F.1a) over W and using the boundary conditions, we obtain

$$W_s(\vec{p}) \frac{\partial f(\vec{p})}{\partial t} = -\partial_k \int_{W_1(\vec{p})}^{W_2(\vec{p})} J_k(W, \vec{p}) dW. \quad (\text{F.3})$$

Let us perform the gradient expansion, $\tilde{f} = \tilde{f}^{(1)} + \tilde{f}^{(2)} + O(\partial_k^3)$. To deal with the diffusion equation and the boundary condition we need J_k to $O(\partial_k)$ and J_W to $O(\partial_k^2)$:

$$-J_k = \hat{D}_{kk'} \partial_{k'} f + \hat{D}_{kW} \partial_W \tilde{f}^{(1)} + O(\partial_k^2), \quad (\text{F.4a})$$

$$-J_W = \hat{D}_{Wk} \partial_k f + \hat{D}_{WW} \partial_W \tilde{f}^{(1)} + \hat{D}_{Wk} \partial_k \tilde{f}^{(1)} + \hat{D}_{WW} \partial_W \tilde{f}^{(2)} + O(\partial_k^3). \quad (\text{F.4b})$$

Let us multiply Eq. (F.1a) by W_s and subtract from it Eq. (F.3). Since $\partial_t = O(\partial_k^2)$, we can neglect $\partial_t \tilde{f}$ and write

$$\begin{aligned} 0 = & W_s \partial_W \left[\hat{D}_{Wk} \partial_k f + \hat{D}_{Wk} \partial_k \tilde{f} + \hat{D}_{WW} \partial_W \tilde{f} \right] + \\ & + W_s \partial_k \hat{D}_{kk'} \partial_{k'} f - \partial_k \left(\int_{W_1}^{W_2} \hat{D}_{kk'} dW \right) \partial_{k'} f + \\ & + W_s \partial_k \hat{D}_{kW} \partial_W \tilde{f} - \partial_k \int_{W_1}^{W_2} \hat{D}_{kW} \partial_W \tilde{f} dW + O(\partial_k^3). \end{aligned} \quad (\text{F.5})$$

There are only two terms of the order $O(\partial_k)$, from which we obtain

$$\tilde{f}^{(1)} = - \left(\int \frac{\hat{D}_{Wk}}{\hat{D}_{WW}} dW \right) \partial_k f, \quad -J_k = \left(D_{kk'} - \frac{D_{kW} D_{Wk'}}{D_{WW}} \right) \partial_{k'} f \equiv D_{kk'}^{\parallel} \partial_{k'} f. \quad (\text{F.6})$$

Substituting J_k into Eq. (F.3), we obtain the desired effective equation for $f(\vec{p})$:

$$\frac{\partial f(\vec{p})}{\partial t} = \frac{1}{W_s(\vec{p})} \frac{\partial}{\partial p_k} \int_{W_1(\vec{p})}^{W_2(\vec{p})} dW \left[\hat{D}_{kk'}(W, \vec{p}) - \frac{\hat{D}_{kW}(W, \vec{p}) \hat{D}_{Wk'}(W, \vec{p})}{\hat{D}_{WW}(W, \vec{p})} \right] \frac{\partial f(\vec{p})}{\partial p_{k'}}. \quad (\text{F.7})$$

Finally, we have to make sure that the correction $\tilde{f}^{(2)}$ is regular (its explicit form is not even needed). Collecting the $O(\partial_k^2)$ terms in Eq. (F.5), we obtain

$$\begin{aligned} \partial_W \hat{D}_{WW} \partial_W \tilde{f}^{(2)} = & \partial_W \hat{D}_{Wk} \partial_k \left(\int \frac{\hat{D}_{Wk'}}{\hat{D}_{WW}} dW \right) \partial_{k'} f - \partial_k D_{kk'}^{\parallel} \partial_{k'} f + \\ & + \frac{1}{W_s} \partial_k \left(\int_{W_1}^{W_2} D_{kk'}^{\parallel} dW \right) \partial_{k'} f. \end{aligned} \quad (\text{F.8})$$

The boundary conditions translate into

$$\hat{D}_{WW} \partial_W \tilde{f}^{(2)} \Big|_{W=W_{1,2}} = \hat{D}_{Wk} \partial_k \left(\int_{W_1,2}^{W_{1,2}} \frac{\hat{D}_{Wk'}}{\hat{D}_{WW}} dW \right) \partial_{k'} f + \frac{\partial W_{1,2}}{\partial p_k} D_{kk'}^{\parallel} \partial_{k'} f. \quad (\text{F.9})$$

Eq. (F.8) is compatible with these boundary conditions and can be straightforwardly integrated, indeed giving $\tilde{f}^{(2)}$ of the second order of smallness.

Appendix G. Jacobian for integration over breaks

Our goal is to find the Jacobian $\mathcal{J}(\lambda)$ in the transformation

$$\int \prod_n p(\lambda_n) d\lambda_n \rightarrow \int d\lambda \mathcal{J}(\lambda) \prod_n e^{-S(b_\lambda(n))}, \quad (\text{G.1})$$

where the probability distribution $p(\lambda_n)$ is represented as

$$p(\lambda_n) = \frac{d[1 - e^{-S(\lambda_n)}]}{d\lambda_n} \equiv S'(\lambda_n) e^{-S(\lambda_n)}. \quad (\text{G.2})$$

The calculation is based on three main observations.

First, as discussed in Sec. 9.1, for each break profile $\{\lambda_n\}$ one can specify the two sites, n_1, n_2 , where it touches the corresponding optimal break, $\lambda_{n_{1,2}} = b_\lambda(n_{1,2} - x_0)$, for some values of λ, x_0 , which are determined by the profile $\{\lambda_n\}$. Thus, the whole integration manifold of $\{\lambda_n\}$ can be split into submanifolds corresponding to given values of n_1, n_2 :

$$\int d\vec{\lambda} \equiv \int \prod_n d\lambda_n \rightarrow \sum_{n_1 \leq n_2} \int d\vec{\lambda}^{(n_1, n_2)} \quad (\text{G.3})$$

Second, at fixed n_1, n_2 there is one-to-one correspondence between $\lambda_{n_1}, \lambda_{n_2}$ and the parameters λ, x_0 of the optimal break $b_\lambda(n - x_0)$. That is, for an arbitrary profile $\{\lambda_n\}$ the parameters λ, x_0 are in fact determined by four numbers $n_1, n_2, \lambda_{n_1}, \lambda_{n_2}$. The transformation $(\lambda_{n_1}, \lambda_{n_2}) \leftrightarrow (\lambda, x_0)$ is determined by

$$d\lambda_{n_{1,2}} = \partial_\lambda b_\lambda(n_{1,2} - x_0) d\lambda - b'_\lambda(n_{1,2} - x_0) dx_0, \quad (\text{G.4})$$

where we denoted $b'_\lambda(x) \equiv \partial b_\lambda(x)/\partial x$. The integration measure transforms as

$$d\lambda_{n_1} d\lambda_{n_2} = \left[b'_\lambda(n_1 - x_0) \partial_\lambda b_\lambda(n_2 - x_0) - b'_\lambda(n_2 - x_0) \partial_\lambda b_\lambda(n_1 - x_0) \right] dx_0 d\lambda. \quad (\text{G.5})$$

Third, at fixed $n_1, n_2, \lambda_{n_1}, \lambda_{n_2}$, or, equivalently, at fixed n_1, n_2, λ, x_0 , the integration range for λ_n with $n \neq n_1, n_2$ is simply $b_\lambda(n - x_0) < \lambda_n < \infty$, so the integration is straightforward. Thus, one can write

$$\begin{aligned} \int d\vec{\lambda} \prod_n p(\lambda_n) &= \sum_{n_1 \leq n_2} \int d\lambda_{n_1} d\lambda_{n_2} p(\lambda_{n_1}) p(\lambda_{n_2}) \prod_{n \neq n_1, n_2} \exp[-S(b_\lambda(n - x_0))] = \\ &= \sum_{n_1 \leq n_2} \int d\lambda_{n_1} d\lambda_{n_2} S'(\lambda_{n_1}) S'(\lambda_{n_2}) e^{-\Xi(\lambda)}. \end{aligned} \quad (\text{G.6})$$

Here we introduced

$$e^{-\Xi(\lambda)} = \prod_n \exp[-S(b_\lambda(n - x_0))], \quad (\text{G.7})$$

assuming it to be independent of x_0 . This is not strictly true, since n is integer and x_0 is continuous, so it is actually a periodic function of x_0 with unit period, but we neglect this modulation.

Let us now pass from $\lambda_{n_1}, \lambda_{n_2}$ to λ, x_0 keeping λ fixed, and change the summation variables as $n_1 = n, n_2 = n + l$ as well as the integration variable as $x_0 = n + l - x$:

$$\begin{aligned} &\sum_{n_1 \leq n_2} \int_{n_1}^{n_2} dx_0 S'(b_\lambda(n_1 - x_0)) S'(b_\lambda(n_2 - x_0)) \times \\ &\quad \times \left[b'_\lambda(n_1 - x_0) \partial_\lambda b_\lambda(n_2 - x_0) - b'_\lambda(n_2 - x_0) \partial_\lambda b_\lambda(n_1 - x_0) \right] = \\ &= \sum_{n=-\infty}^{\infty} \sum_{l=0}^{l_{max}} \int_{x_{min}}^{x_{max}} dx \left[\frac{\partial S(b_\lambda(x - l))}{\partial x} \frac{\partial S(b_\lambda(x))}{\partial \lambda} - \frac{\partial S(b_\lambda(x))}{\partial x} \frac{\partial S(b_\lambda(x - l))}{\partial \lambda} \right] = \\ &= L \mathcal{J}(\lambda), \end{aligned} \quad (\text{G.8})$$

which gives precisely the sought Jacobian. Due to translational invariance, the sum over n produces the total length L , which appears in Eq. (9.3). The value of $l_{max} = l_{max}(\lambda)$ is determined from the equation $b_\lambda(l_{max}/2) = 0$, and the range of x integration is given by

$$\begin{aligned} 0 \leq x \leq l, \quad 0 \leq l \leq \frac{l_{max}}{2}, \\ l - \frac{l_{max}}{2} \leq x \leq l_{max}, \quad \frac{l_{max}}{2} \leq l \leq l_{max}. \end{aligned} \quad (\text{G.9})$$

Replacing the summation over l by integration, we can rewrite the Jacobian as

$$\begin{aligned} \mathcal{J}(\lambda) &= - \int_0^{l_{\max}/2} dx dy \left[\frac{\partial S(b_\lambda(-y))}{\partial y} \frac{\partial S(b_\lambda(x))}{\partial \lambda} + \frac{\partial S(b_\lambda(x))}{\partial x} \frac{\partial S(b_\lambda(-y))}{\partial \lambda} \right] = \\ &= S(\lambda) \int_{-l_{\max}/2}^{l_{\max}/2} \frac{\partial S(b_\lambda(x))}{\partial \lambda} dx. \end{aligned} \quad (\text{G.10})$$

References

- [1] P. W. Anderson, Absence of diffusion in certain random lattices, *Phys. Rev.* 109 (1958) 1492.
- [2] A. Lagendijk, B. van Tiggelen, D. A. Wiersma, *Phys. Today* 62 (2009) 24.
- [3] M. E. Gertsenshtein, V. B. Vasil'ev, *Theory of Probability and its Applications* 4 (1959) 391.
- [4] N. F. Mott, W. D. Twose, *Adv. Phys.* 10 (1961) 107.
- [5] J. Fröhlich, T. Spencer, C. E. Wayne, *J. Stat. Phys.* 42 (1986) 247.
- [6] S. A. Gredeskul, Y. S. Kivshar, *Phys. Rep.* 216 (1992) 1.
- [7] D. L. Shepelyansky, *Phys. Rev. Lett.* 70 (1993) 1787.
- [8] M. I. Molina, G. P. Tsironis, *Phys. Rev. Lett.* 73 (1994) 464–467.
- [9] M. I. Molina, *Phys. Rev. B* 58 (1998) 12547–12550.
- [10] T. Paul, P. Leboeuf, N. Pavloff, K. Richter, P. Schlagheck, *Phys. Rev. A* 72 (2005) 063621.
- [11] T. Paul, P. Schlagheck, P. Leboeuf, N. Pavloff, *Phys. Rev. Lett* 98 (2007) 210602.
- [12] A. Iomin, S. Fishman, *Phys. Rev. E* 76 (2007) 056607.
- [13] J. Bourgain, W.-M. Wang, *J. Eur. Math. Soc.* 10 (2008) 1–45.
- [14] S. Fishman, A. Iomin, K. Mallick, *Phys. Rev. E* 78 (2008) 066605.
- [15] G. Kopidakis, S. Komineas, S. Flach, S. Aubry, *Phys. Rev. Lett.* 100 (2008) 084103.
- [16] A. S. Pikovsky, D. L. Shepelyansky, *Phys. Rev. Lett.* 100 (2008) 094101.
- [17] S. Fishman, Y. Krivolapov, A. Soffer, *J. Stat. Phys.* 131 (2008) 843.
- [18] M. Albert, T. Paul, P. Leboeuf, N. Pavloff, *Phys. Rev. Lett.* 100 (2008) 250405.
- [19] S. Tietsche, A. Pikovsky, *Europhys. Lett.* 84 (2008) 10006.
- [20] S. Flach, D. O. Krimer, C. Skokos, *Phys. Rev. Lett.* 102 (2009) 024101.
- [21] C. Skokos, D. O. Krimer, S. Komineas, S. Flach, *Phys. Rev. E* 79 (2009) 056211.
- [22] S. Fishman, Y. Krivolapov, A. Soffer, *Nonlinearity* 22 (2009) 2861.
- [23] A. Iomin, *Phys. Rev. E* 80 (2010) 037601.
- [24] H. Veksler, Y. Krivolapov, S. Fishman, *Phys. Rev. E* 80 (2009) 037201.
- [25] T. Paul, M. Albert, P. Schlagheck, P. Leboeuf, N. Pavloff, *Phys. Rev. A* 80 (2009) 033615.
- [26] M. Mulansky, K. Ahnert, A. Pikovsky, D. L. Shepelyansky, *Phys. Rev. E* 80 (2009) 056212.
- [27] M. Albert, T. Paul, N. Pavloff, P. Leboeuf, *Phys. Rev. A* 82 (2010) 011602(R).
- [28] J. D. Bodyfelt, T. Kottos, B. Shapiro, *Phys. Rev. Lett.* 104 (2010) 164102.
- [29] H. Veksler, Y. Krivolapov, S. Fishman, *Phys. Rev. E* 81 (2010) 017201.
- [30] Y. Krivolapov, S. Fishman, A. Soffer, *New J. Phys.* 12 (2010) 063035.
- [31] A. Iomin, *Phys. Rev. E* 81 (2010) 017601.
- [32] C. Skokos, S. Flach, *Phys. Rev. E* 82 (2010) 016208.
- [33] S. Flach, *Chem. Phys.* 375 (2010) 548.
- [34] M. Mulansky, A. Pikovsky, *Europhys. Lett.* 90 (2010) 10015.
- [35] T. V. Lapyeva, J. D. Bodyfelt, D. O. Krimer, C. Skokos, S. Flach, *Europhys. Lett.* 91 (2010) 30001.
- [36] A. Pikovsky, S. Fishman, *Phys. Rev. E* 83 (2011) 025201.
- [37] M. Johansson, G. Kopidakis, S. Aubry, *Europhys. Lett.* 91 (2010) 50001.

- [38] T. Schwartz, G. Bartal, S. Fishman, M. Segev, *Nature* 446 (2007) 52.
- [39] Y. Lahini *et al.*, *Phys. Rev. Lett.* 100 (2008) 013906.
- [40] Y. Lahini *et al.*, *Phys. Rev. Lett.* 103 (2009) 013901.
- [41] J. Billy *et al.*, *Nature* 453 (2008) 891.
- [42] G. Roati *et al.*, *Nature* 453 (2008) 895.
- [43] B. Deissler *et al.*, *Nature Physics* 6 (2010) 354.
- [44] A. Dhar, J. L. Lebowitz, *Phys. Rev. Lett.* 100 (2008) 134301.
- [45] A. Dhar, K. Saito, *Phys. Rev. E* 78 (2008) 061136.
- [46] M. Mulansky, K. Ahnert, A. Pikovsky, *Phys. Rev. E* 83 (2011) 026205.
- [47] V. Oganessian, A. Pal, D. A. Huse, *Phys. Rev. B* 80 (2009) 115104.
- [48] I. García-Mata, D. L. Shepelyansky, *Eur. Phys. J. B* 71 (2009) 121.
- [49] D. O. Krimer, R. Khomeriki, S. Flach, *Phys. Rev. E* 80 (2009) 036201.
- [50] W.-M. Wang, Z. Zhang, *J. Stat. Phys.* 134 (2009) 953–968.
- [51] V. Kaloshin, M. Levi, M. Saprykina, (to be published).
- [52] N. F. Mott, *Philos. Mag.* 19 (1969) 835.
- [53] J. Kurkijarvi, *Phys. Rev. B* 8 (1973) 922.
- [54] B. V. Chirikov, *Phys. Rep.* 52 (1979) 263.
- [55] A. J. Lichtenberg, M. A. Leiberman, *Regular and Stochastic Motion*, Springer-Verlag, New York, 1983.
- [56] D. J. Thouless, *J. Phys. C* 5 (1972) 77.
- [57] N. Bilas, N. Pavloff, *Eur. Phys. J. D* 40 (2006) 387.
- [58] K. O. Rasmussen, T. Cretegnny, P. G. Kevredikis, N. Grønbech-Jensen, *Phys. Rev. Lett.* 84 (2000) 3740.
- [59] G. M. Zaslavsky, *Chaos in dynamic systems*, Harwood Academic Publishers, Newark, 1985.
- [60] B. V. Chirikov, V. V. Vecheslavov, *J. Stat. Phys.* 71 (1993) 243.
- [61] M. E. Raikh, I. M. Ruzin, *Sov. Phys. JETP* 68 (1989) 642.
- [62] V. K. Melnikov, *Soviet Mathematics-Doklady* 3 (1962) 109.
- [63] V. I. Arnold, *Soviet Mathematics-Doklady* 5 (1964) 581.
- [64] V. K. S. Shante, C. M. Varma, A. N. Bloch, *Phys. Rev. B* 8 (1973) 4885.
- [65] P. A. Lee, *Phys. Rev. Lett.* 53 (1984) 2042.
- [66] A. S. Rodin, M. M. Fogler, *Phys. Rev. B* 80 (2009) 155435.
- [67] M. Khodas, S. Fishman, O. Agam, *Phys. Rev. E* 62 (2000) 4769.
- [68] A. N. Kolmogorov, *Dokl. Akad. Nauk SSSR* 98 (1954) 525.
- [69] J. Moser, *Nachr. Akad. Wiss. Göttingen, Math.-Phys. Kl.* 1 (1962) 1.
- [70] V. I. Arnold, *Uspehy Math. Nauk* 18 (1963) 13.
- [71] C. Froeschlé, J.-P. Scheidecker, *Phys. Rev. A* 12 (1975) 2137.
- [72] E. Diana, L. Galgani, M. Casartelli, G. Casati, A. Scotti, *Theor. Math. Phys.* 29 (1976) 1022.
- [73] M. Casartelli, E. Diana, L. Galgani, A. Scotti, *Phys. Rev. A* 13 (1976) 1921.
- [74] J. Pöschel, *Commun. Math. Phys.* 127 (1990) 351.
- [75] D. M. Leitner, P. G. Wolynes, *Phys. Rev. Lett.* 79 (1997) 55.
- [76] V. Y. Demikhovskii, F. M. Izrailev, A. I. Malyshev, *Phys. Rev. Lett.* 88 (2002) 154101.
- [77] I. L. Aleiner, D. L. Altshuler, G. V. Shlyapnikov, *Nature Physics* 6 (2010) 900.
- [78] J. D. Bodyfelt, T. V. Laptyeva, C. Skokos, D. O. Krimer, S. Flach, *Phys. Rev. E* 84 (2011) 016205.
- [79] G. Czycholl, B. Kramer, A. MacKinnon, *Z. Phys. B* 43 (1981) 5.
- [80] M. Kappus, F. Wegner, *Z. Phys. B* 45 (1981) 15.
- [81] A. B. Rechester, R. B. White, *Phys. Rev. Lett.* 45 (1980) 851.
- [82] L. D. Landau, E. M. Lifshitz, *Statistical Physics, Part 1*, Pergamon Press, Oxford, 1959.
- [83] H. B. Callen, T. A. Welton, *Phys. Rev.* 81 (1951) 34.